People's Democratic Republic of Algeria
Ministry of Higher Education and Scientific Research
Ibn Khaldoun University –Tiaret

Department of Civil engineering
Master - Structures specialty

Graduation Project

Free Vibration Analysis of Multi-directional Porous Functionally Graded Sandwich Plates

Submitted by ::
TARFAYA Sanaa Bent elarab
BELKHARROUBI Djazia

Board of Examiners

President	ABDELAZIZ Hadj Henni	MCA
Examiner	REBAHI Abderazak	MCA
Examiner	AIT AMAR MEZIANE MED	Pr
Supervisor	HADJI Lazreg	Pr

Academic year: 2023– 2024

Acknowledgements

First and foremost, we thank Allah for making all things possible for us, for giving us strength and wisdom to undertake this study.

Our heartfelt gratitude goes to our esteem supervisor**, Pr. HADJI Lazreg**, for his endless support and guidance, as well as the members of the jury; Chairman **Mr.ABDELAZIZ Hadj Henni** and the examiner **Mr.RABAHI Abderazak** and **Pr..AIT AMAR Meziane Mohamed** who have taken time to read, discuss, and correct our dissertation.

Special thanks to Mr. Daham for his help.

We would like to thank the respondents, as well as everyone who has stood by us and supported us in difficult times.

Dedication

To my beloved family. To my best friends with whom I spent the best moments at university.

Sanaa

Dedication

I dedicate this work to my family for their support and encouragement.

To my closest friends, who have supported and encouraged me throughout this process.

Djazia

Abstract

The present study focuses on the analysis and modeling of the mechanical behavior of multidirectional porous sandwich plates made of FGM composite material. Two cases namely of sandwich plates have been considered in this study: Sandwich with FGM skins and homogeneous core and sandwich with FGM core and homogeneous skins. In this context, a new displacement field including both cross-sectional and transverse shear deformations was used, the material properties of the sandwich plate are assumed to vary in both the longitudinal and transversal directions. The equations of motion will be determined using Hamilton's theory. The objective of this research is firstly to propose a new theory of shear deformation. Then, the research is focused on the determination of exact solutions of the mechanical response (vibration) of multidirectional porous sandwich plates made of FGM materials. Consequently, the analysis of the effect of porosity on the response of these structures and the effect of the material index will be highlighted. Finally, the numerical validation of the proposed high order shear deformation theory will be presented by confronting the obtained results with those of other known models in the literature.

Keywords : Sandwich plate, FGM material, Porosity effect, Multidirectional, Navier's solution, Hamilton's principle, Free vibration.

Résumé

La présente mémoire traite essentiellement l'analyse et la modélisation du comportement mécanique des plaques sandwiches poreuses multidirectionnelles en matériau FGM. Deux types de plaque sandwiches ont été considérés dans cette étude : Sandwich avec peaux en FGM et cœur homogène et sandwich avec cœur en FGM et peaux homogènes. Dans ce contexte, on a utilisé un nouveau champ de déplacement incluant à la fois le gauchissement de la section transversale et les déformations de cisaillement transverse, les propriétés matérielles de la plaque sandwich sont supposées variées dans les deux directions longitudinale et transversale. Les équations de mouvement seront déterminées en utilisant le principe d'Hamilton. L'objectif de cette mémoire consiste en premier lieu en proposition d'une nouvelle théorie de déformation de cisaillement. Ensuite, la recherche est focalisée sur la détermination des solutions exactes de la réponse mécanique (vibration) des plaques sandwiches poreuses multidirectionnelles en matériaux FGM. En conséquence, l'analyse de l'effet de la porosité sur la réponse de ces structures et l'effet de l'indice matériel sera mise en évidence. Enfin, la validation numérique de la théorie de déformation de cisaillement d'ordre élevé proposée sera présentée en confrontant les résultats obtenus avec ceux d'autres modèles connus dans la littérature.

Mots clés : Plaque sandwich, Matériau FGM, Effet de porosité, Multidirectionnel, Solution de Navier, Principe d'Hamilton, Vibration libre.

الملخص

في هذه الأطروحة قمنا بدراسة معمقة لتأثير المسامية على الترددات الاهتزاز للهياكل المتمثلة في الصفائح المختلطة (الساندويش) متعددة الأبعاد والمتدرجة وظيفيًا باستعمال نظرية تشوه القص المكرر بدرجة عليا مع مراعاة تأثير إجهاد القص العرضي.

هذه المسامات تولد وتنتج داخل المواد المتدرجة وظيفيا أثناء التصنيع والتركيب (التعدين) لدينا نوعين من صفائح الساندويش التي نستعملها في هذه النظرية ذات أربعة مجاهيل فقط، ولكنها تلبي شروط انعدام اجهادات القص على مستوى الجهة العليا والجهة السفلى لصفائح الساندويش التي تم استخدامها تقتصر دراستنا على نوعين من الصفائح.

- النوع الأول عبارة عن ساندويش ذي طبقتين في الجهة العليا والسفلى من مواد متدرجة ولب متجانس في الوسط.

أما النوع الثاني عبارة عن ساندويش ذي طبقتين متجانستين في الجهة العليا والسفلى ولب متدرج وظيفيا في الوسط.

نفرض أن الخصائص الميكانيكية للهياكل متدرجة باستمرار في اتجاه السُمك وفق قانون أسي بسيط من أجل دراسة دقيقة لتحقيق الاستجابة للاهتزاز الحر،يتم تحديد معادلات الحركة للتحليل الديناميكي من خلال مبدأ هاملتون. وتم اعتماد تقنية حل نافي لاشتقاق حلول تحليلية للهياكل السندويشة متعددة الأبعاد ذات المساند البسيطة حيث يتم التحقق من دقة الحلول وفعالية النموذج المقترح من خلال المقارنة مع الأبحاث السابقة.

الكلمات المفتاحية : الهياكل السندويشة؛ المواد المتدرجة وظيفيا؛ تأثير المسامية؛ متعددة الأبعاد؛ حل نافي؛ مبدأ هاملتون؛ الاهتزاز الحر

List of notations

[ ]	Matrix.
{ }	Column vector.
E	Young's modulus
E_c	Young's modulus of ceramic
E_m	Young's modulus of metal
E_1	Young's modulus of the top surface
E_2	Young's modulus of the bottom surface
$E(z)$	Module de Young en fonction de « z »
v	Poisson coefficient
$v(z)$	Coefficient de Poisson en fonction de « z »
$V(z)$	Volume fraction
n_x, n_z	Material index in x and z directions
b	Width of the plate
h	Thickness of plate
L	Length of plate
u, v, w	Displacements in the x, y and z directions
u_0, v_0, w_0	Components of the displacement field of the middle plane of the plate
ϕ_x, ϕ_y, ϕ_z	Rotations around x, y and z axes
$f(z)$	Warping function (Transverse shear function)
ρ	Mass density
σ_x, σ_y	Normal stresses
$\tau_{xy}, \tau_{xz}, \tau_{yz}$	Shear stresses
$\varepsilon_x, \varepsilon_y, \varepsilon_z$	Déformations in x, y and z directions
$\gamma_{xy}, \gamma_{xz}, \gamma_{yz}$	Angular deformations
δ	Variation operator
$\delta u, \delta v, \delta w_b, \delta w_s$	Virtual field of displacements

δU	Variation of plate deformation energy
δT	Variation of the kinetic deformation energy of the plate.
w_b	Component of deflection due to bending
w_s	Component of deflection due to shear
N	Normal membrane stresses
M^b	Pure bending moments
M^s	Additional bending moments due to transverse shear
S	Pure shear force
m, n	Mode number
A_{ij}	Stiffness coefficients
B_{ij}	Coupling stiffness terms
D_{ij}	Bending stiffness terms
A_{ij}^s	Shear stiffness terms
B_{ij}^s	Shear stiffness terms
D_{ij}^s	Shear stiffness terms
H_{ij}^s	Shear stiffness terms
$I_{0,}\ I_{1,,}\ J_{1,,}\ K_2$	Inertias
Q_{ij}	Stiffness coefficients
∂	Partial derivative
a_{ij}	Components of Stiffness matrix
i, j	Natural numbers
[K]	Stiffness matrix
[M]	Masse Matrix
{Δ}	Column vector
$\overline{w}$	Dimensionless frequencies
ω	Natural frequency of the plate
γ_α^0	Shear strain measured of the middle plane
k_x^b	Bending curvature in the X direction
k_x^s	Shear curvature in the X direction
U_{mn}, V_{mn}, W_{bmn}, et W_{smn}	Arbitrary parameters.

List of figures

Chapter I : Sandwich materials

Chapter II : Introduction on Functionally Graded Materials FGM

Chapter III : Reminder on plate theories

Chapter IV : Free Vibration Analysis of Multi-directional Porous Functionally Graded Sandwich Plates

Chapter V : Results and discussions

List of tables

Chapter III : Reminder on plate theories

Chapter V: Results and discussions

Tabel of content

CHAPTER II

Introduction on Functionally Graded Materials FGM

CHAPTER III

Reminder on plate theories

CHAPTER IV

Free Vibration Analysis of Multi-directional Porous Functionally Graded Sandwich Plates

CHAPTER V

Results and discussions

General introduction

Lightweight composite materials with high strength-to-weight and thickness-to-weight ratios have been successfully utilized in the aerospace industry and other technological applications. However, traditional composite materials are unusable in high-temperature environments. Metals have been commonly used in technology for many years due to their excellent mechanical strength and hardness. However, under high-temperature conditions, the mechanical strength of metal becomes low, similar to traditional composite materials.

Ceramic materials exhibit excellent thermal resistance characteristics. However, ceramic applications are typically limited due to their low hardness. Laminated composite materials offer the design flexibility necessary to achieve desired stiffness and strength through the choice of laminate scheme. The anisotropic nature of laminated composite structures often results in stress concentrations near material interfaces and geometric discontinuities, which can lead to damage such as matrix delamination, cracking, and adhesive bond separation (Reddy, 2004).

The advancement of composite materials has made it possible to combine specific properties of various materials within a single component. The local optimization of these properties, achieved by, for example, associating a material with high hardness on the surface of a tough material, poses the challenge of the interface. The abrupt transition of material properties across this interface between distinct materials can lead to significant inter-laminar stresses or a high concentration of stresses, potentially causing plastic deformation or crack formation. To address these adverse effects, a technique used is that of Functionally Graded Materials (FGM).

During the production of functionally graded materials (FGMs), micro-voids and porosities can occur due to manufacturing errors or technical issues. The presence of porosity significantly alters the mechanical behavior of these materials. Therefore, the impact of porosity on functionally graded materials is a major concern that must be studied to safely design these composites.

Numerous researchers have studied the behavior of functionally graded material (FGM) plates and have defined the volume fraction using various mixing laws, such as the power law (P-FGM), the exponential law (E-FGM), and the sigmoidal law (S-FGM), in order to ensure a harmonious distribution of stresses across all interfaces.

Due to the significance of these materials and their numerous applications, many researchers have conducted static, vibrational, thermomechanical, and buckling analyses on FGM structures.

The present work focuses on the study of the dynamic behavior of multidirectional porous sandwich plates in FGMs. Two models of porous FGM sandwich plates are considered: one with porous FGM faces and a homogeneous core, and the other with a porous FGM core and homogeneous faces.

Three porosity distribution models are proposed. Therefore, our thesis is composed of five chapters.

In the first chapter, we attempt to define sandwich materials in general and provide an overview in the second chapter of functionally graded materials (FGMs), their concept, as well as their manufacturing and application domains.

The third chapter is dedicated to presenting the various theories of sandwich plates. The fourth chapter involves the implementation of an analytical method for the vibration analysis of multidirectional rectangular porous sandwich plates in FGMs, taking into account the presence of porosities during the manufacturing process of these FGMs.

In the final chapter, we focus on studying the dynamic response of porous FGM sandwich plates with simply supported boundary conditions. Several curves are presented to study the dynamic behavior of FGM sandwich plates with porosities either in the faces or in the core of the sandwich plate.

A calculation program has been developed for this numerical application of a case study to validate and compare the developed theory with results from the literature. The effect of varying certain parameters on the results is discussed. Finally, flexural and free vibration analyses are performed, and the results are analyzed and discussed.

This work concludes with a general summary of the research conducted, including perspectives for future work.

Problem Statement

How can the mechanical behavior be analytically resolved to determine the free vibration frequencies of multidirectional porous FGM sandwich plates?

Chapter I

Sandwich materials

I.1. Introduction

Composite materials have revolutionized industries ranging from aerospace to consumer goods, offering an innovative solution to the complex demands of modern engineering. These materials, composed of two or more distinct constituents, exploit the unique properties of each component to create a synergistic whole that exceeds the sum of its parts. By carefully selecting and combining materials such as fibers, resins, and additives, composites can be engineered to deliver exceptional strength, stiffness, and durability while remaining lightweight and versatile. This versatility has made composites indispensable in a multitude of applications, from high-performance aircraft and automotive components to everyday products like sporting goods and infrastructure. In this introduction, we will explore the underlying principles, manufacturing processes, properties, and wide-ranging applications of composite materials, highlighting their pivotal role in driving innovation and advancing technology across various industries.

Sandwich structures, a subset of composite materials, exemplify this versatility by combining the principles of composite materials with a unique layered design , These are the first historically lightweight and high-performance composite structures. The first chapter is dedicated to understanding the issues of sandwich materials and their properties.

I.2. Definition of sandwich materials

Sandwich construction has been widely utilized in the structures of aircraft, missiles, and spacecraft due to its high strength-to-weight ratio. This construction method typically involves thin, rigid, and robust sheets made of metallic or fiber composite materials, which are separated by a thick layer of low-density material, as illustrated in (Figure I.1). The thick layer of low-density material is commonly referred to as the core material.

While the core material normally has high compressive and shear strengths, the skin material is usually very stiff. This combination provides a high flexural modulus to the sandwich structure when they are glued together.

In a sandwich structure, we must not overlook a third component: the adhesive. It is the adhesive that ensures proper assembly of the structure and also facilitates effective transmission of stresses from one medium to another. Its main characteristic should be good shear strength. In the case of composite material skins, the inclusion of this third phase can be avoided by using a self-adhesive resin.

The choice of constituents depends mainly on the specific application and the design criteria set up by it. The design of a structural sandwich will not be one of geometry only but an integrated process of sizing and materials selection.(Dan, Z 1995)

In addition to their good flexural rigidity, buckling resistance, and lightweight nature, sandwich materials also possess excellent thermal and acoustic insulation properties. This explains their increasingly frequent use as partitions. These materials are increasingly employed in aerospace or transportation industries as primary or secondary structures, such as in the hulls of fast boats, aircraft flooring, and other applications.

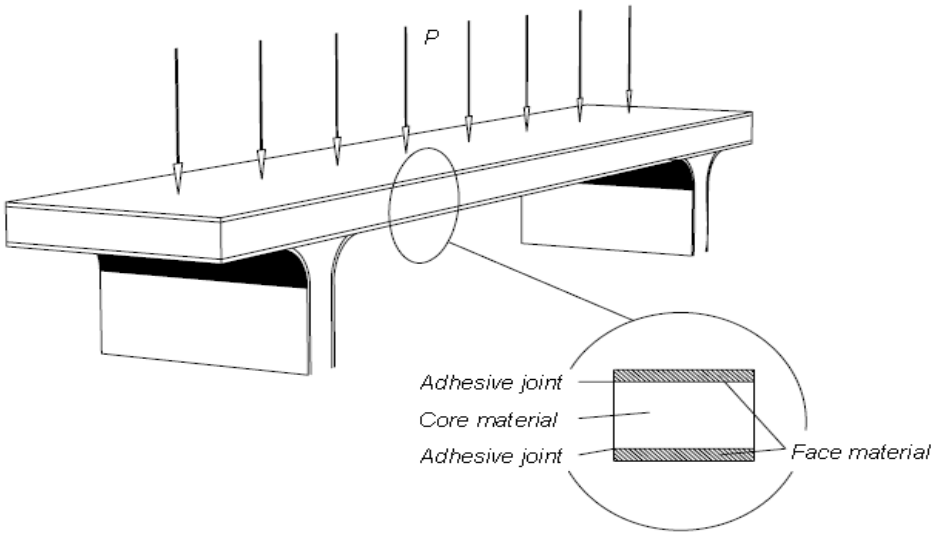

Figure I.1. Schematic of a structural sandwich panel (Dan Z, 1995).

I.3. The constituent elements of sandwich materials

A sandwich construction offers a compromise that allows for both rigidification and alignment of a structure. Generally speaking, it is composed of three fundamental components with distinct yet complementary properties: the heart, the petal, and the interface (adhesive) .

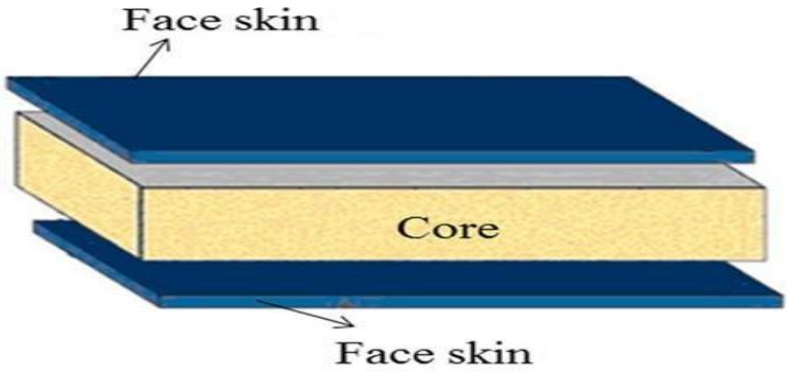

Figure I.2. Typical sandwich composite

I.3.1. The skins

The skins are usually thin and can be constructed of any material that can be layered. Wood, metal, or composite materials can be used to make them. The application of the composite materials will determine the kind and arrangement of layers. The goal of the skins is to absorb normal stresses, which are described as bending forces (tension or compression).

I.3.2. The core

Lightweight, the core generally has very low bending resistance. The essential function of the sandwich core is to transmit, through transverse shear, the mechanical actions from one skin to the other. It can be made from the following materials

Foams: inexpensive and lightweight, these materials are easy to machine but have very low mechanical properties

Balsa: It is a type of wood known for its various uses, and one of its main characteristics is its lightweight nature. It boasts a high capacity for both acoustic and thermal insulation and does not deform with temperature variations.

Honeycomb: This structure is typically made from thin sheet material (aluminum alloy, polyamide paper). Strips of adhesive are arranged in regular bands on the sheets, which are then glued together to form a block. This block is then cut into slices, which are in turn transformed into a honeycomb panel through expansion.

There are two types of cores:

a) Solid cores (Berthelot and al., 1996) in which we find:

Balsa wood or cellular woods (Figure I.3)

Various cellular foams .

Resins loaded with hollow glass microspheres called syntactic foams.

This cellular or solid core is assumed to be isotropic (material properties identical in all directions).

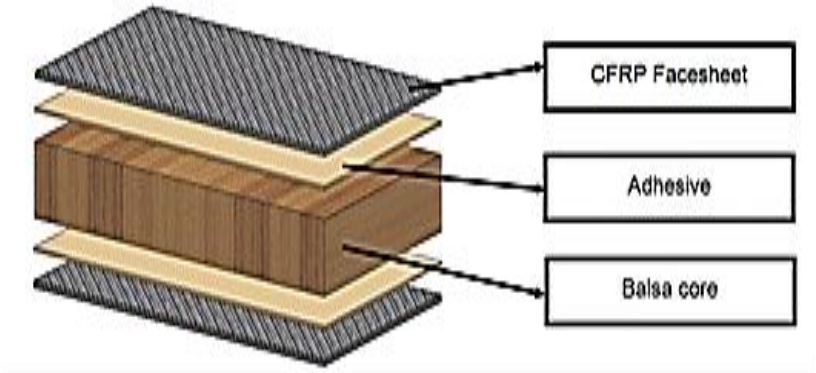

Figure I. 3. Sandwich materials with solid cores (Balsa wood)

a) Hollow cores (Berthelot and al., 1996), primarily of honeycomb type (Figure I.4) they are:

Lightweight metallic alloys;

Kraft papers;

Polyamide paper, such as Nomex paper.

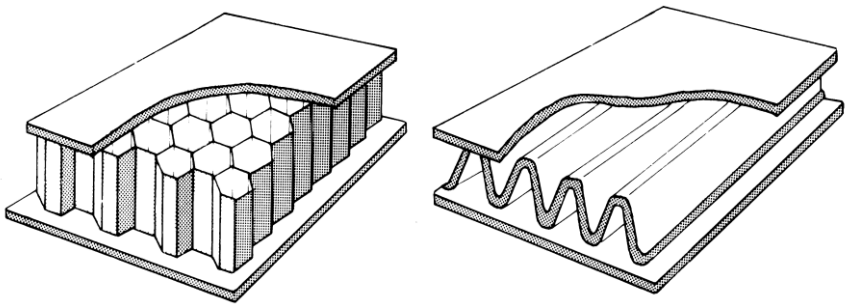

(a) Honeycomb (b) Corrugated core

Figure I.4. Sandwich materials with hollow cores

I.3.3. The interface

Sandwich materials are created through welding, bonding, or brazing. During numerical simulations, it is assumed that regardless of the assembly method, the different layers are perfectly bonded.

Sandwich structures are characterized by:

Great lightness, for example, the surface mass of the dome of the Basilica of Saint Peter (45 meters in length) is γs= 2600 Kg/m2 (constructed in stone). The surface mass of the same dome made of steel/polyurethane foam sandwich is γs =33 kg/m2 (Chatin and al.,2000).

• High bending stiffness due to the spacing of the skins.

• Very good thermal insulation. However, sandwich materials do not dampen vibrations, and their fire resistance is not good for certain types of cores, and their susceptibility to buckling is greater than that of classical materials.

I.4. Design of sandwich structures

Sandwich structures are light multifunctional composite structures, constructed by embedding a low-density core between two thin stiff facings.

The facing–core interface is the weakest part of the sandwich structure. Adhesives are usually used in this interface to bond up and bottom facings with inner core.

The multifunctional performance of sandwich structure greatly depends on the structure configuration and the choice of sandwich materials. The advantages of sandwich structures include enhanced energy absorption properties, great stiffness to weight ratios, excellent ballistic resistance performance, and good thermal and acoustic isolation properties.These benefits of sandwich structures lead to wide .

Typiquement, sandwich theory (beam or plate theory) and material selection serve as the foundation for the design.

1.4.1. Material Selection – Core

The primary objective of the core located within the sandwich panel is to maximize the distance between the two outer layers, thereby enhancing the panel's stiffness, while minimizing added weight. Additionally, it serves to withstand the forces generated when the structure is under load.

I.4.1.1. Bending Strength

Sandwich structures are typically more rigid than regular beams. This is made possible by the skins' ability to support forces and the effective geometric distribution, which results in a larger stiffness factor <EI>. Since the ultimate mechanical behavior of the sandwich structure is directly related to the skins' adherence to the core, it is imperative that they do so as closely as possible.

I.4.1.2. Shock Resistance

The impact resistance of sandwich constructions is significantly influenced by the core's ability to absorb energy. The absorption capacity of the core material is improved by increasing its density. A foam core exhibits different behavior during an impact than a honeycomb core.

The impact energy within the sandwich will be dispersed by a foam core, which will absorb it into its cellular structure. For this reason, thermoplastic PVC foams and flexible thermosetting foams both have superior shock-absorbing qualities.

The walls of honeycomb cores carry energy perpendicularly from one skin to the other, which may cause the skin on the other side to rip.

I.4.1.3. Compression Strength

The sandwich structure's core absorbs the compressive pressures. When it comes to the panels, honeycomb constructions can withstand severe compressive pressures. However, its anisotropy raises the failure risk when subjected to multidirectional stresses like hydrostatic forces. As a result, a foam and honeycomb combination solution is selected.

I.4.1.4. Peel Strength

Inadequate adhesive strength may rupture sandwich constructions by causing the skins to delaminate. The adhesive strength between the core and the skins in sandwich constructions with foam cores needs to be higher than the core's shear strength. More adhesive forces are available from PVC foams than from balsa or polymethacrylimide (PMI). However, the brittle nature of polyurethane (PU) foams complicates the bonding process.

Regarding honeycomb cores, obtaining high peel strength is challenging due to their smaller contact surface.

I.4.1.5. Insulation

In many applications, mass reduction, vibration damping, and thermal and acoustic insulation are critical. Many foams provide superior acoustic and thermal insulation due to their cellular structure, but honeycomb sandwich constructions provide less definitive and more constrained performance.

Consequently, the usage of foam-cored sandwich structures is advised where good thermal and acoustic insulation qualities are needed. It is better to use sandwich structures with honeycomb cores while trying to lose weight.

I.4.1.6. Water Absorption

Moisture and water absorption can cause a significant deterioration in the mechanical characteristics. The usage of moisture-sensitive or water-sensitive cores raises the danger of delamination much more in situations where the sandwich skins are defective or damaged. The evaporation of water absorbed internally can result in skin delamination even with regular use. Before putting the sandwich construction into service, the core must undergo extra heat treatment in order to resolve this problem.

I.5. Solicitations and Modes of Degradation of Sandwich Structures

Bending loads are the primary loads sustained by these structures, including compression, torsion, or tension (Figure I.5). A sandwich structure is thus subjected to:

Bending moment,

Torsional moment,

Normal force,

Shear force.

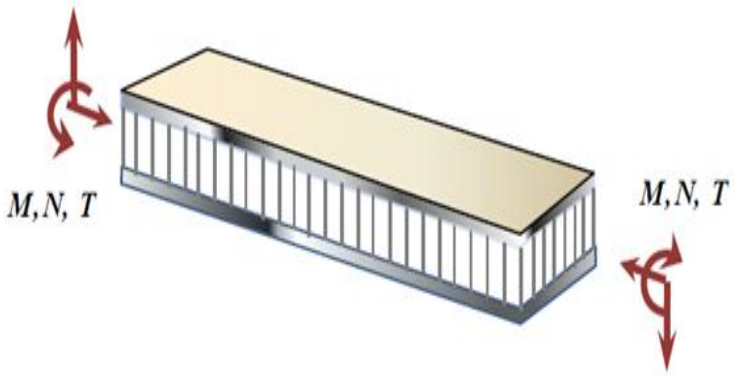

Figure I.5. Different loads (M, N, T) applied to a sandwich.

The various modes of failure are illustrated here for a sandwich structure subjected to bending, to better understand the mechanical behavior of these structures.

(Jin and al.,2003), (Avila and al.,2007), (Yoshi and al.,1992), (Thomesen and al., 1995), (Belouettar and al.,2009).

I.5.1. General buckling of the skins

A sandwich beam subjected to compression can fail due to instability conditions affecting the entire beam (Fig. 1.6). Buckling can also occur when the stresses in the skins and core are below their respective rupture strengths. The load causing the sandwich to buckle depends on parameters such as the dimensions of the sandwich, the type of sandwich, bending stiffness, skin thickness, core thickness, and the shear modulus of the core. (Arbaoui J, 2009)

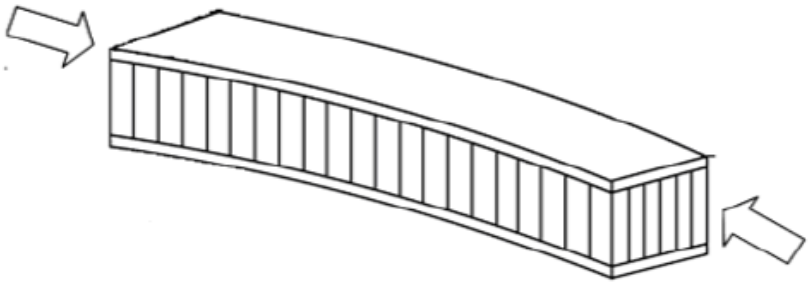

Figure I.6. General buckling of the sandwich skins(Gognard and al.,2000).

I.5.2. Failure of the skins in tension or compression

In this case, the stresses in the skins exceed the allowable stresses of the material constituting the skins (Figure I.7). To avoid this phenomenon, it is necessary to use materials with higher rupture stresses, or increase the thickness of the skins (which reduces the applied stresses). Alternatively, increasing the thickness of the core also helps reduce stresses in the skins. (Laggoun O. 2020)

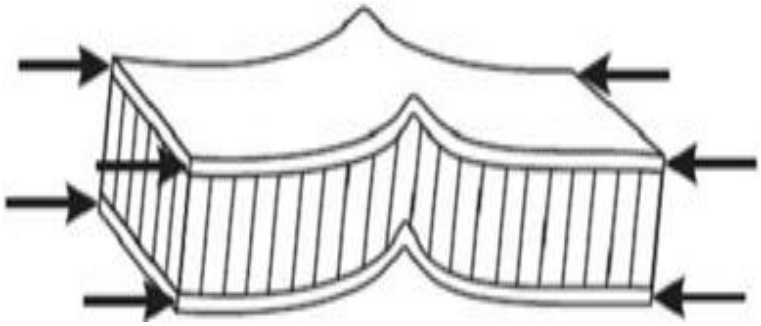

Figure I.7. Failure of the skins in tension or compression(Gognard and al., 2000).

I.5.3. Local failure modes

Localized indentation occurs when stress becomes concentrated, leading to a specific mode of failure. This concentration of stress can arise from either the application of a localized load or the placement of a point or linear support.

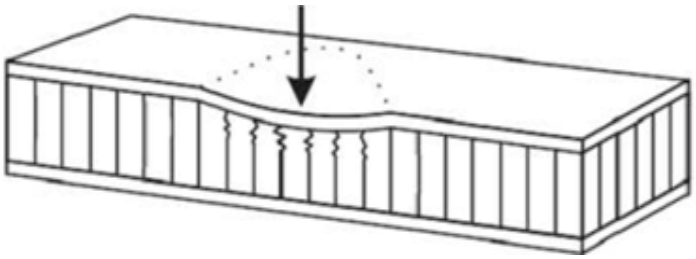

Figure I.8. Local modes of failure by indentation (Gognard and al., 2000).

I.5.4. Shear core failure

Core failure will occur if the shear strength of the core material is less than the shear stress (Figure I.9). This can be fixed by using a core material with a higher shear strength or by increasing the core's thickness. On the other hand, altering the skins' thickness or composition will have no effect.

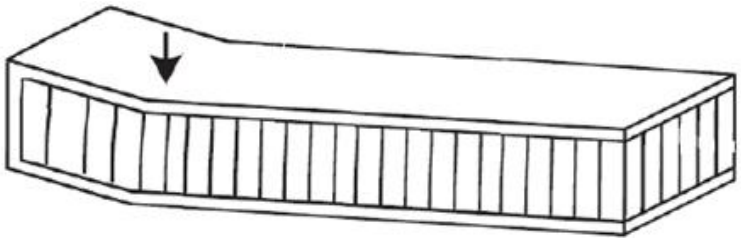

Figure I.9. Shear core failure (Hexcel and al., 2004).

I.5.5. General buckling of the core

When the length-to-thickness ratio is low and the shear stiffness is negligible compared to the bending stiffness, global buckling takes the form of core buckling. This type of buckling is almost independent of the skin properties but depends linearly on the core thickness and shear modulus. To increase the resistance to this critical load, it is therefore necessary to either increase the core thickness or use a core material with a higher shear modulus.

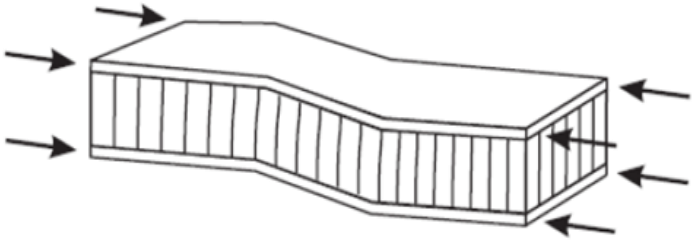

Figure I.10. General buckling of the core (Hexcel and al.,2004).

I.5.6. Localized buckling "wrinkling" or "dimpling."

The skins, considered by themselves, without connection to the soul, easily buckle due to their thinness. It is the soul that prevents their buckling. However, if the ultimate stress is reached, the soul may no longer be able to prevent buckling.

In this case, localized buckling of the skins, or "wrinkling" (Figure I.11), occurs. Unlike general buckling, localized buckling can take different configurations that do not depend on the geometry of the structure. However, it is influenced by the elastic moduli of the skins and the core, and the shear modulus of the core. If localized skin buckling is a concern, one can either use a material with a higher elastic modulus for the skins, or use a material for the core with higher elastic properties. (Laggoun O. 2020)

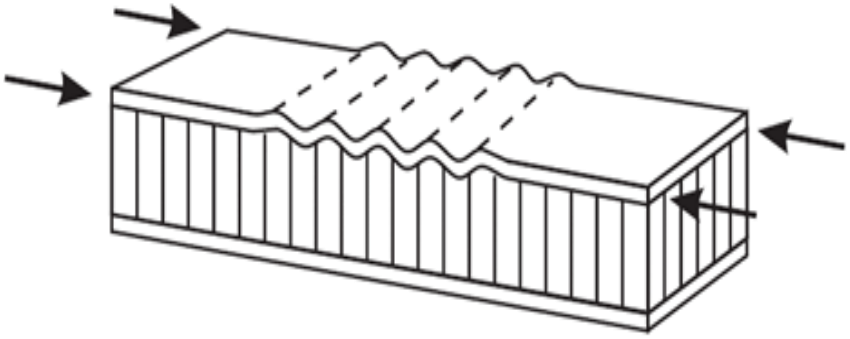

Figure I.11. Localized buckling « wrinkling» (Hexcel and al., 2004).

In the case of a honeycomb core, aside from failures due to "wrinkling," another mode of failure due to localized skin buckling in dimples, called "dimpling," may also occur

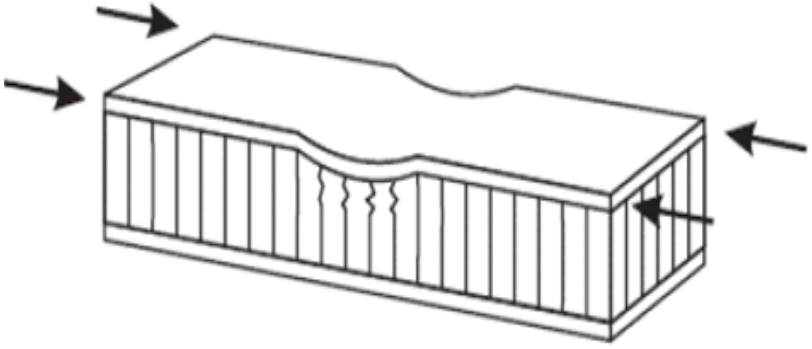

Figure I.12. Localized buckling "dampling" (Hexcel and al.,2004).

I.5.7. Degradation of the adhesive

The degradation of the adhesive between the skins and the honeycomb core typically occurs in three types:

- Degradation of the adhesive between the skins and the core,
- Degradation of the attachment of the core cells,
- Degradation of the attachment of the node of the core cells.

(Figure I.1 3) illustrates the modes of adhesive degradation. Exposure to moisture causes significant degradation of the adhesive strength, which can alter the degradation mode and lead to advanced failure of the sandwich panel.

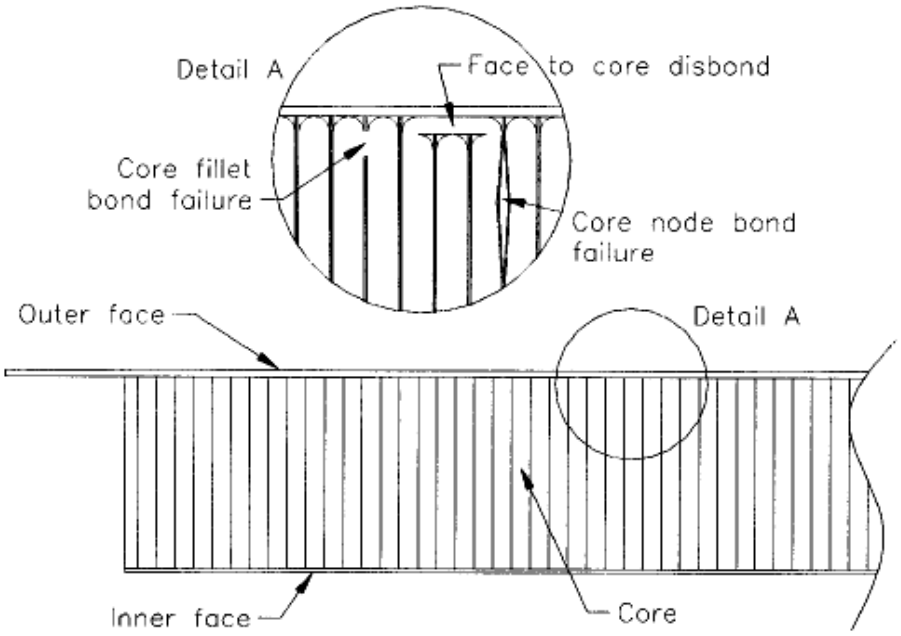

Figure I.13. Failure of adhesive bonds in sandwich panels after degradation.

I.6. The theory of sandwich plates

A sandwich structure consists of a low-density core material sandwiched between two high-stiffness and high-strength face sheets (skins) that are bonded to the core. The core's main function is to transmit the shear forces acting between the skins caused by external loads. These skins can be made from laminates (layered composites) or metallic materials. The thickness of the lower and upper skins are denoted by h1 and h2, respectively. The core thickness is represented by hc, and the total thickness of the sandwich structure is H (H = h1 + hc + h2). At any point within the structure, the mid-plane is chosen as the reference plane for the (x, y) coordinate system.

I.6.1. Assumptions of the sandwich materials theory

Sandwich plate theory is a branch of engineering mechanics that deals with the analysis of sandwich structures, which are composed of two thin face sheets (skins) separated by a thicker core. The core material is typically low-density and low-stiffness, while the face sheets are high-strength and high-stiffness materials. The primary function of the core is to provide separation between the face sheets and to transfer shear loads between them. The face sheets, on the other hand, primarily carry the bending and in-plane loads.

Sandwich plate theory is based on several simplifying assumptions that allow for a tractable mathematical analysis. These assumptions are:

Thick core relative to face sheets: The thickness of the core is significantly greater than the thickness of the face sheets. This assumption simplifies the analysis of bending and shear deformation in the sandwich structure.

Linear in-plane displacements of the core: The in-plane displacements (u and v) of the core along the x and y directions are assumed to be linear functions of the z-coordinate. This assumption allows for the use of Kirchhoff-Love plate theory, which simplifies the analysis of bending in thin plates.

Constant in-plane displacements in the face sheets: The in-plane displacements (u and v) in the face sheets are assumed to be constant through the thickness of the face sheets. This assumption is valid for thin face sheets, as the bending deformation is dominant over the in-plane deformation.

Negligible transverse normal strain: The transverse normal strain (εz) is assumed to be negligible compared to the other strain components. This assumption is valid for most sandwich structures, as the core is primarily responsible for carrying shear loads.

Core transmits only transverse shear stresses: The core is assumed to transmit only transverse shear stresses (τxz and τyz). The normal stresses (σxx, σyy, and σzz) in the core are neglected. This assumption is valid for low-density core materials that are primarily responsible for transmitting shear loads.

Negligible transverse shear stresses in face sheets: The transverse shear stresses (τxz and τyz) in the face sheets are neglected. This assumption is valid for thin face sheets, as the bending stresses are dominant over the shear stresses.

Small deformation theory: The theory is based on the assumption of small deformations, meaning that the strains are small compared to unity. This allows for the use of linear elasticity theory, which simplifies the stress-strain relationships.

I.7. The assembly of sandwich materials

I.7.1. Bonding of skins to the core in sandwich structures

Perfect bonding for optimal performance of sandwich structures Achieving a perfect bond between the core and skins is crucial for maximizing the performance of sandwich structures. This ensures that the loads are evenly distributed between these components.

Bonding remains a widely employed method for joining sandwich structures. This process involves applying an adhesive to unite the preformed core and skins. As depicted in (Figure 1.14, a,b) the bonding is accomplished using resins compatible with the materials employed.

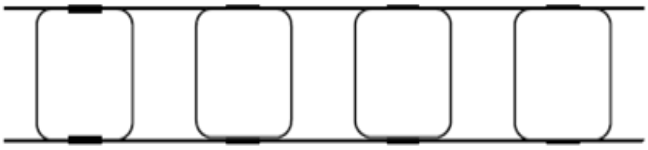

(a) : Panels made with square tubes.

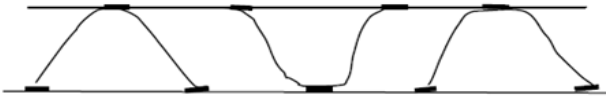

Figure I.14. Panels made by collaging various profiles.

I.7.2. Folding technique

Sandwich panels, after their fabrication, can be shaped by folding using the technique illustrated in (Figure 1.15) This method involves the following steps:

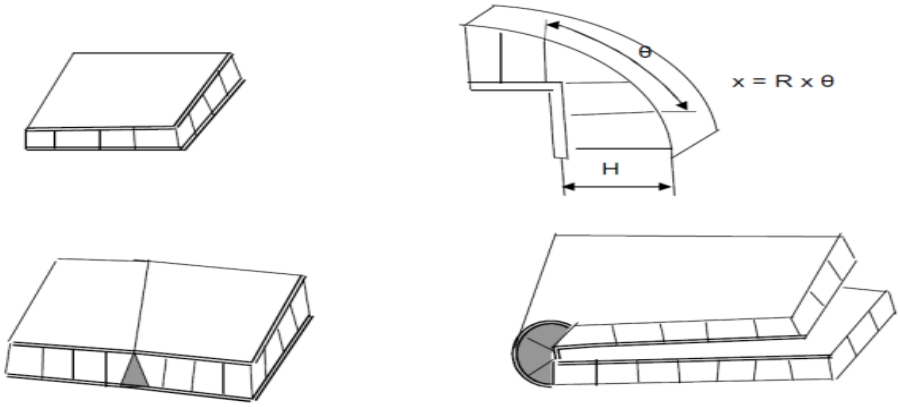

Figure I.15. Folding of sandwich panels

Removal of a skin strip: The first step involves removing a strip of width x from one of the skins of the sandwich panel. This removed strip exposes the core of the panel.

Application of adhesive: An appropriate adhesive is then applied to the exposed core due to the removal of the skin strip. The choice of adhesive depends on the specific materials used for the sandwich panel and the required performance criteria.

Clamping and polymerization: The piece, with the applied adhesive, is then clamped into a folded position according to the desired shape. This clamping holds the panel in place while the adhesive fully polymerizes. Complete polymerization ensures a strong and durable bond between the skins and the core in the folded area.

Filling of angles (optional): For the fold angles, an epoxy-type filling resin can be used. This resin may optionally be lightened by incorporating microballoons, tiny hollow particles, to

reduce the total weight of the sandwich panel. The filling resin reinforces and stiffens the fold angles, ensuring better mechanical strength and structural stability.

I.8. The interest in sandwich structures

The main advantage of sandwich structures, as opposed to traditional monolithic composites, lies in their very high specific stiffness. The core density is typically around 100 kg m-3. By modifying the nature and thickness of the skin and/or core, the structure can be tailored to the most suitable material. Thus, improving stiffness, which reflects the material's bending behavior, is achieved by either increasing the core thickness, leading to an increase in its moment of inertia, or by increasing the modulus of elasticity of the skins. Since the sandwich core has low density, the mass of the composite does not significantly increase.

Sandwich composite materials have significant advantages over traditional materials. They bring numerous functional benefits: lightweight, mechanical and chemical resistance, reduced maintenance, freedom of shapes. They can increase the lifespan of certain equipment due to their mechanical and chemical properties. They contribute to enhancing safety through better impact and fire resistance. They provide better thermal or acoustic insulation and, for some, good electrical insulation. They also enrich design possibilities by allowing structures to be lightened and complex shapes to be achieved, capable of fulfilling multiple functions. In each application market (automotive, construction, electrical, industrial equipment, etc.), these remarkable performances are the origin of innovative technological solutions. (Arbaoui J . 2009)

I.9. Applications of sandwich materials

Sandwich materials are widely used across various industries due to their remarkable properties like high stiffness-to-weight ratio, strong mechanical resistance, thermal and acoustic insulation, and design flexibility. Here are some concrete examples of their applications:

I.9.1. Aerospace construction

The trap doors of landing gear, various fairings (between wing and fuselage, engine pylons, flap tracks) are secondary parts built with sandwich panels and by cocuring composite laminates (carbon/epoxy, kevlar/epoxy) onto Nomex honeycomb or aluminum bonded with epoxy film adhesives.

Engine cowlings are largely constructed with sandwich materials, with (carbon/epoxy) skins bonded to aluminum Nomex cores (Belouettar and al., 2009). To achieve the required thermal resistance, phenolic or polyamide epoxy adhesives are used.

Acoustic panels are sandwich structures with the inner skin, facing the engine, made of a perforated skin onto which a microporous fabric is bonded.

A significant number of helicopter parts are constructed from monolithic pieces or sandwiches with composite skins bonded to Nomex (Hexcel and al., 2004).

I.9.2. Automobiles

In the automotive industry, sandwich materials find extensive use in car body panels, roofs, floors, and interior components. Their incorporation enhances vehicle safety, improves fuel efficiency, and reduces noise levels, leading to a more comfortable and secure driving experience. Sandwich materials are revolutionizing automotive design, contributing to the development of lighter, safer, and more fuel-efficient vehicles.

I.9.3. Other application areas of sandwich materials

Civil Engineering: Box girder bridges, chimneys, elastic foundations (these plate structures can be found in various industrial applications such as raft foundations), storage tanks, swimming pools.

Aeronautics: Rocket engine components, spacecraft fuselages.

Chemical Engineering: Heat exchangers, heat pipes, reaction vessels.

Engineering: Cutting tools, engine components (Keddouri Ahmed and al., 2021).

I.10. Conclusion

This chapter is dedicated to defining and presenting the concepts of sandwichstructures. Firstly, the main mechanical properties of sandwich materials are outlined, along with the types of damage they can incur. The second chapter will focus on introducing functionally graded materials (FGM), defining their concept and characteristics. We will then examine the laws governing these materials, as well as the research conducted and the analysis of the mechanical behavior of FGM structures. Numerous works have been devoted to the study of FGM structures, presenting a wide variety of research in the literature. These studies have addressed various issues related to the mechanical behavior of FGM structures, such as stability, buckling, and vibrations, including elements such as beams, plates, shells, and other FGM materials.

Chapter II

Introduction on Functionally Graded Materials FGM

II.1. Introduction

In the progress of science and technology, materials have played a crucial role. Thescientific application of base materials into diverse inorganic and organic compounds has paved the way for developing the advanced polymers, engineering alloys, structural ceramics, etc. The structure of enhancement of advanced material is illustrated in Figure II.1. Functionally graded materials (FGMs) are heterogeneous advanced composite materials consisting of two or more constituent phases with a continuously variable distribution . The variations in the phase distribution may be reflected in their volume or weight fraction, orientation, and shape. In the vast majority of studies of FGMs in engineering, the researchers aim to achieve their goals with only one of these factors, i.e. the volume fraction being a typical variable.

The variation of the volume fractions may be exclusively through the thickness of the structure and/or in any other direction, such as coordinates of a plate or shell. The mechanical properties such as Young's modulus of elasticity, Poisson's ratio .(shear Behnam S, 2014)

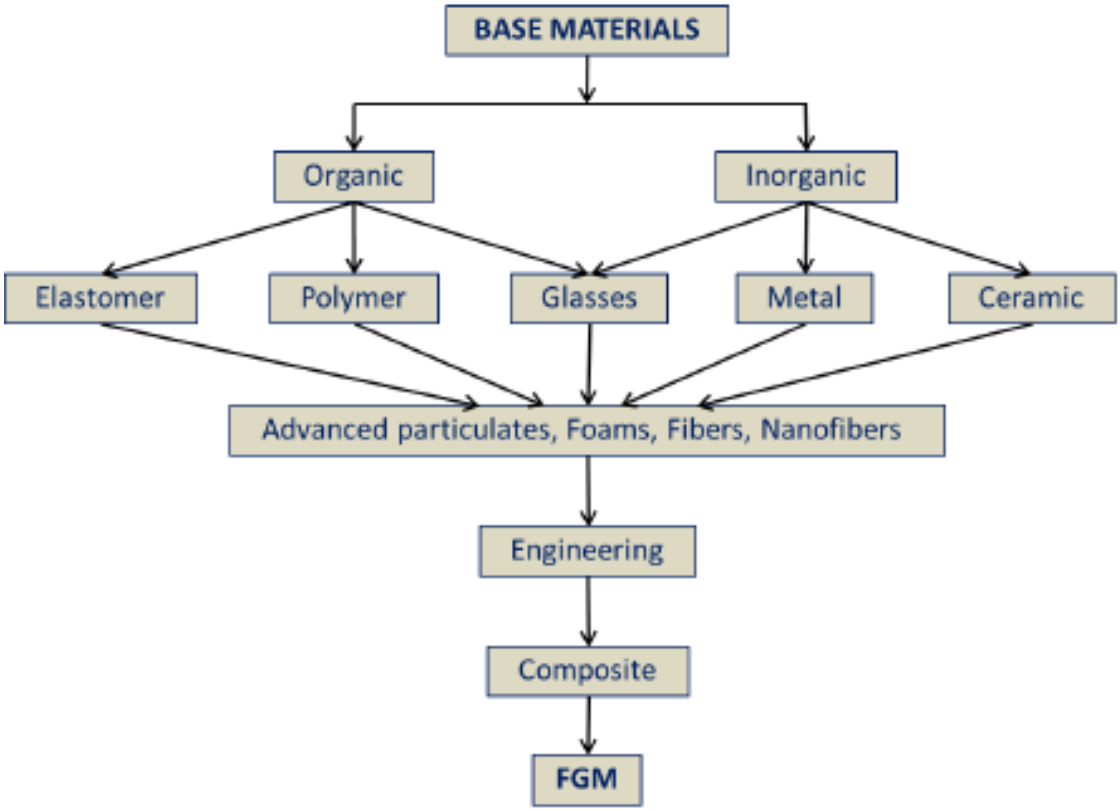

Figure II.1. Representation of advance material hierarchy . (Vinh Loc Tran, 2016)

II.2. Brief Background of Functionally Graded Materials

The concept of Functionally Graded Materials (FGMs) was initiated in the early 1980s in Japan, where this material concept was first proposed. This type of composite material was suggested to reduce thermal stresses in conventional laminate composite materials developed for reusable rocket engines. Functionally graded materials are characterized by a gradual change in material composition or structure, with the intention of inducing a variation in material properties along side the change in composition and structural direction.

Functionally graded materials, characterized by gradually modified microstructures, can be obtained in monolithic materials by adjusting the microstructural composition. This approach allows for obtaining exceptional properties that reduce concentrated thermal stresses in such materials. Additionally, these materials can be designed to be selectively reinforced in areas requiring specific properties. Gradual variations in composition and microstructure, including chemical composition, physical state, and geometric configuration, throughout the volume of composite materials result in corresponding modifications to the material properties.

The concept of functionally graded materials emerged during the space shuttle project in Japan, aiming to create a thermal barrier capable of with standing surface temperatures of 2000 K and temperature gradients of 1000 K across cross-sections less than 10 mm thick. The recurring issues observed in traditional laminated composite materials at that time stemmed from inadequate adhesion between the two materials and a sharp interface with incompatible properties. This challenge was addressed by replacing the sharp interface with a progressive one, thereby eliminating areas of high stress concentration.

The gradual transition from one composition to another led to the development of functionally graded materials. Initially intended for thermal barrier applications in aerospace and fusion reactors, these materials have since been expanded to other areas, such as environments subject to extreme wear. Functionally graded materials, reinforced by metal-ceramic composites, can withstand high temperatures by combining the best properties of both materials. This approach improves performance and reduces the risk of delamination. By making the composition transition between materials gradual, the sharp interface between the matrix and reinforcement is eliminated, thus reducing thermal stress concentrations. The concept of functionally graded materials has thus facilitated the development of materials offering special characteristics such as improved Young's modulus, increased tensile strength, and enhanced wear resistance.

Functionally graded materials, reinforced with both metals and ceramics, are capable of withstanding high-temperature environments by combining the best properties of these two materials. Ceramics withstand high temperatures, while metals provide the necessary mechanical properties to support ceramics, thereby enhancing performance and reducing the risk of delamination. The gradual transition of material content from one to another causes the matrix to perceive the reinforced material as a uniformly distributed impurity, eliminating a clear boundary between the matrix and

reinforcement. As a result, the sharp interface is eliminated, significantly reducing thermal stress concentrations. The concept of functionally graded materials has enabled the development of materials with special characteristics such as improved Young's modulus, increased tensile strength, and enhanced wear resistance.

Functionally graded materials, with their array of unique mechanical properties, offer several advantages over conventional composite materials when exposed to extreme working environments. This field of research has garnered attention from researchers over the past few decades, with its scope continually expanding. The ability to continuously control a material's microstructure to modify its properties and functionality is a constant goal of the scientific community. Drawing inspiration from nature's functionally graded materials has been a consistent driving force behind the development of these artificial materials. For instance, wood serves as a natural example of FGM composed of cellulose in a lignin matrix, much like bones and teeth. These natural materials were designed to meet specific needs, a philosophy adopted in engineering material design. The distinctive characteristics of functionally graded materials lie in their ability to tailor their properties for specialized applications, making them suitable for various intended and potential uses. Appropriately designed FGMs at the microstructural level can lead to significant improvements in material properties, including enhanced wear resistance and increased toughness. Functionally graded materials existed before the work of Japanese researchers in 1972 on graded polymer materials, but the first systematic description of these materials appeared in 1995 in the research of Koizumi and Niino. Natural functionally graded materials are discussed in the following section.

II.3. Definition and concept of Functionally Graded Materials

Functionally graded material is an advanced engineering material that is able to survive in a harsh working environment, without losing its properties, and without failing during service. Functionally graded material (FGM) is characterized by a compositional gradient of one material into another, which is totally different from the conventional composite materials, which are either homogeneous mixtures that involve a compromise between the properties of the component materials, or two different materials joined together as in the case of laminate composite materials. Functionally graded materials are materials that are designed to meet varying functionalities . Engineering is constantly turning to nature to seek answers to a number of questions when trying to solve engineering problems. Functionally graded materials are one of such cases. Functionally graded materials exist in materials from nature, such as bones, teeth, wood, and bamboo . Nature has designed these materials because of the service conditions to which these materials are subjected. The high wear-resistant performance that is required from the outside of a human tooth is the reason why nature had to design teeth as a functionally graded material. The outer part of the teeth is made with high wear-resistant material that is referred to as enamel. The inner structure of the teeth is made ductile, because it is needed as a shock absorber, and to improve the fatigue life of the teeth. Human bone is also designed by God in a similar fashion, because of the service requirement expected from the bone.(Rasheedat M, 2017)

a b

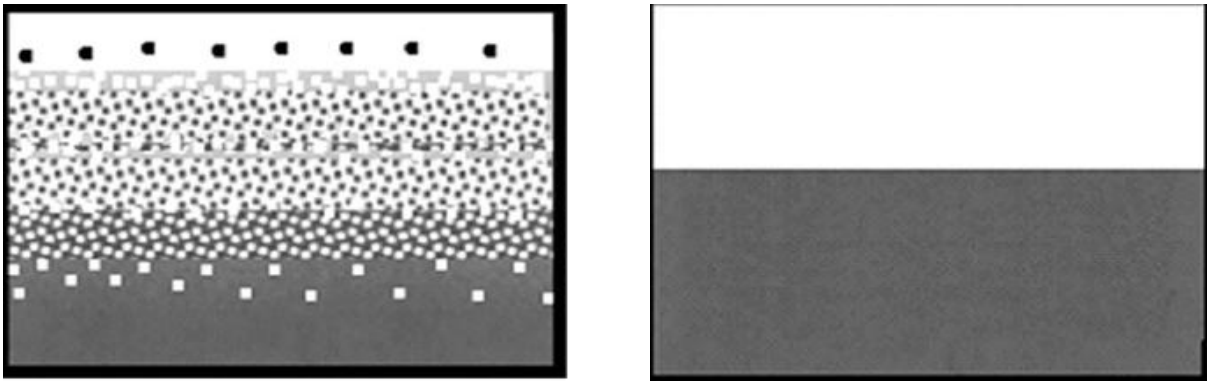

Figure II.2. Schematic diagram of a functionally graded composite material and b traditional laminate composite material .

II.3.1. Comparison between Functionally Graded Materials (FGMs) and traditional composite materials

There is a distinct interface between metals and ceramics in an ordinary composite material, but not in an FGM. This difference corresponds to the distribution of properties such as thermal expansion coefficient, thermal conductivity, and thermal resistance. An ordinary composite material contains a sudden change in properties at the interface, while an FGM presents a gradual change inside it. The difference in thermal expansion coefficients at the interface causes internal thermal stress at elevated temperatures, sometimes leading to the destruction of the interfaces. As shown in Figure II.3, an FGM reduces thermal stress by almost 30% and can prevent destruction of the interface. Figure II.3 shows the difference in compositions and properties between an ordinary composite material and FGM

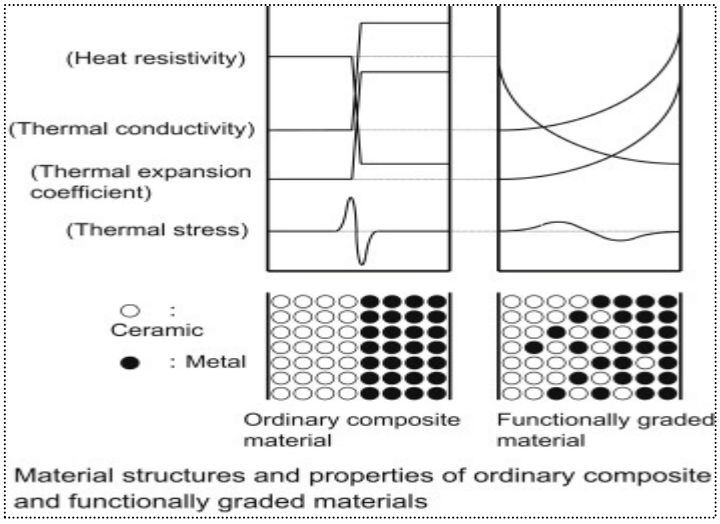

Figure II.3 . Material structures and properties of ordinary composites and functionally graded materials.(Yoshikazu S, 2013)

1. Interface:

- Traditional composite materials have distinct interfaces between different materials (e.g., metals and ceramics).

"FGMs do not have clear interfaces; rather, they demonstrate a gradual transition in composition and properties."

2 Property Variation:

- In traditional composites, properties such as thermal expansion coefficient, thermal conductivity, and thermal resistance can vary abruptly at interfaces.
- FGMs demonstrate a more continuous variation of properties, allowing for improved structural integrity and performance.

3. Design Flexibility:

- FGMs provide greater flexibility in adapting material properties to specific application requirements compared to traditional composites.
- Traditional composites may have limitations in achieving desired property gradients due to their layered structure.

II.4. Processing techniques of functionally graded materials (FGM)

Functionally graded materials (FGMs) are obtained through the diffusion and bonding between atoms of different materials, ensuring a permanent bond and quality performance. Currently, there are numerous methods to prepare FGMs, and among these, the most important techniques used in the FGM manufacturing industry will be presented below.

II.4.1. Vapour Deposition Technique

There are different types of vapour deposition techniques,they include: sputter deposition, Chemical Vapour Deposition (CVD) and Physical Vapour Deposition (PVD).These vapour deposition methods are used to deposit functionally graded surface coatings and they give excellent microstructure, but they can only be used for depositing thin surface coating. They are energy intensive and produce poisonous gases as their by products .

All the above mentioned processes cannot be used to produce bulk FGM because they are generally slow and energy intensive, therefore they are uneconomical to be used in producing bulk FGM. Some of the fabrication methods for producing bulk functionally graded materials are as follows : (Rasheedat M and al., 2012).

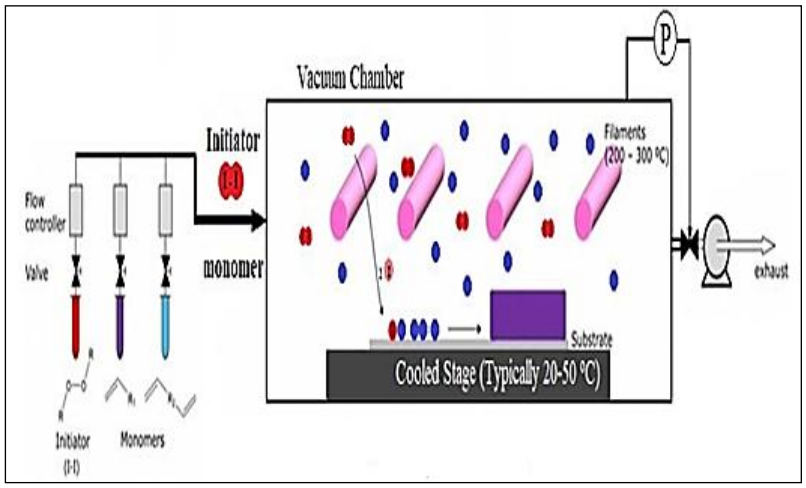

Figure II.4. Chemical Vapour Deposition (CVD). (Ansari and al., 2010).

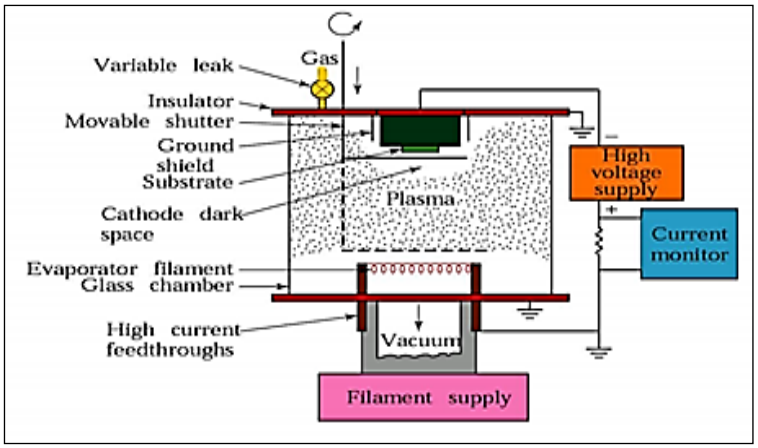

Figure. II.5. Physical Vapour Deposition (PVD). (Seol and al., 2012).

Other methods used in producing functionally graded coating include: plasma spraying, electrodeposition, electrophoretic, Ion Beam Assisted Deposition (IBAD), Self-Propagating High-temperature Synthesis (SHS), etc

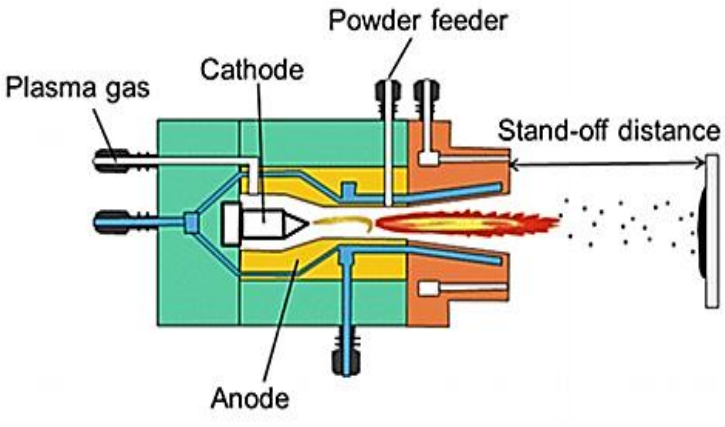

Figure II.6. Plasma projection deposit (PPD) (Malandrino and al., 2009).

II.4.2. Powder Metallurgy (PM)

A functionally graded material can be produced using powder metallurgy (PM) in three basic steps: first, the powder is weighed and mixed in accordance with a predetermined spatial distribution specified by the functional requirements; second, the pre-mixed powders are stacked and compacted; and third, sintering . A multi-step structure is formed as a result of this procedure. The centrifugal approach is employed if a continuous structure is desired.

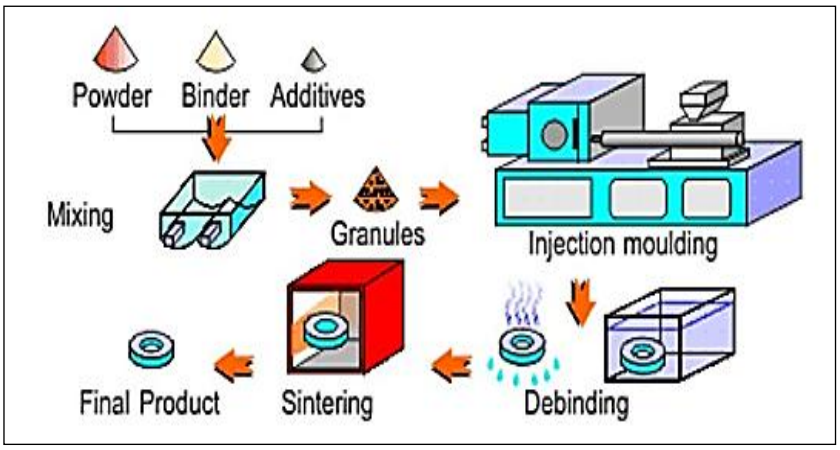

Figure II.7. Powder Metallurgy (PM) (Popoola and al., 2016).

II.4.3. Centrifugal method

The centrifugal casting method is performed by pouring a molten material containing another reinforcing material, either in a molten state or solid, into a mold inside a rotating die to produce a functionally graded material . A centrifugal force is created by rotating the die which helps to draw the molten material towards the mold and create separation in the suspended solid powder material and the melting of the two materials, as a result of the different densities of the two materials, and hence the creation of a FGM . The graded distribution of the FGM formed by the centrifugal casting method would be significantly influenced by the processing parameters, such as the difference in density between the reinforcing powder particles and the molten material, the particle size and the particle size distribution of the powder, the viscosity of the molten material, and the solidification time. The apparatus for the centrifugal method and motion of solid particles under the centrifugal force are shown in Figure II.8.

The main advantage of using the centrifugal casting method for the production of FGMs is that a continuous gradient can be produced. The main disadvantages of the centrifugal casting method include the following:

It can only be used to produce a cylindrical section, such as a tube, bushing, and cylindrical or tubular castings that are simple in shape.

The gradation is limited by the centrifugal force and the density difference of the constituent materials.

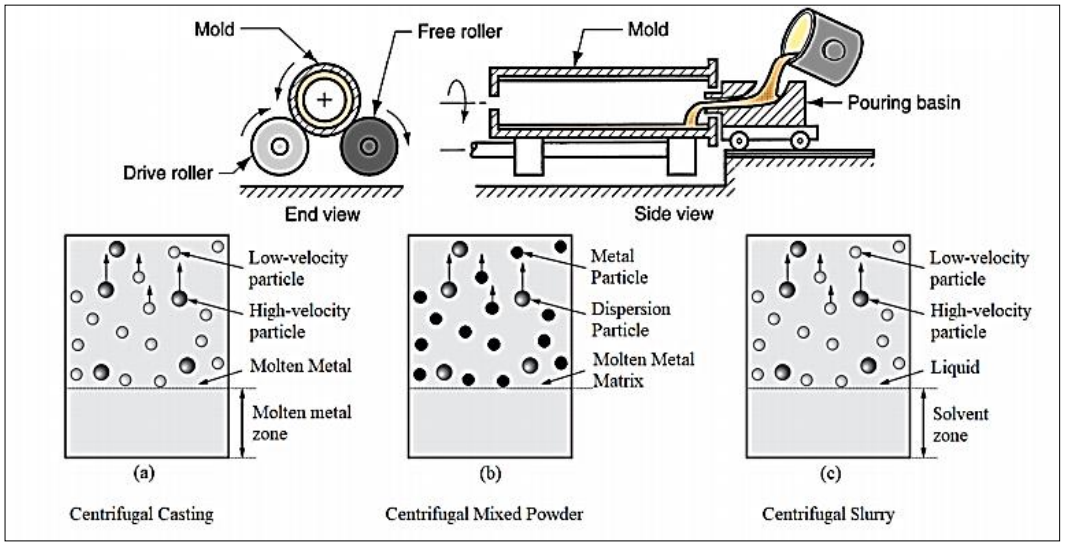

Figure II.8. Centrifugal casting method (MCC). (Watanabe and al., 2011).

II.4.4. Solid Freeform (SFF) Fabrication Method

Solid freeform is an additive manufacturing process that offers lots of advantages that include: higher speed of production, less energy intensive, maximum material utilization, ability to produce complex shapes and design freedom as parts are produced directly from CAD (e.g. AutoCAD) data . SFF involves five basic steps : generation of CAD data from the software like AutoCAD, Solid edge etc, conversion of the CAD data to Standard

Triangulation Language (STL) file, slicing of the STL into two dimensional cross-section profiles, building of thencomponent layer by layer, and lastly removal and finishing.There are various types of SFF technologies, laser based processes are mostly employed in fabrication of functionally graded materials . Laser based SFF process for FGM include: laser cladding based method , Selective Laser Sintering (SLS) , 3-D

Printing (3-DP) , and Selective Laser Melting (SLM) . Laser cladding based system and selective laser melting are capable of producing fully dense components. Solid freeform provide manufacturing flexibility amongst other advantages but the technology is characterized by poor surface finish making it necessary to carry out a secondary finishing operation. There are lots of Proceedings of the World Congress on Engineering 2012 Vol III WCE 2012, July 4 - 6, 2012, London, U.K .(Rasheedat M and al., 2012)

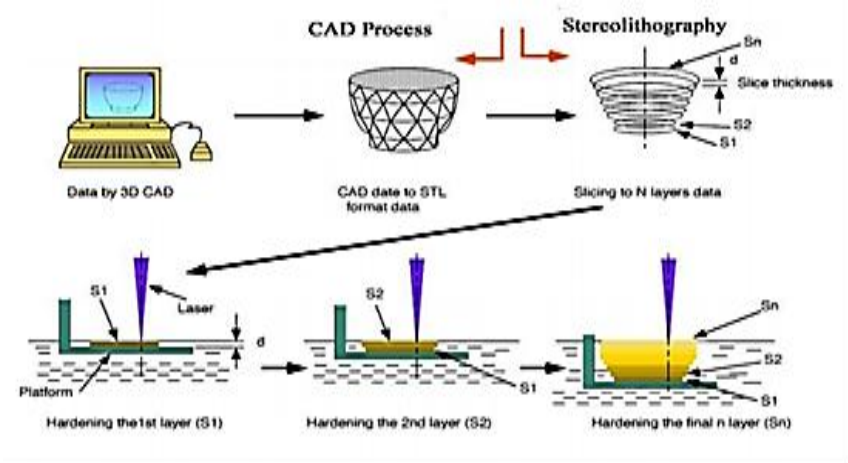

Figure II.9. Solid Freeform (SFF) Fabrication Method (Chen and al., 2019).

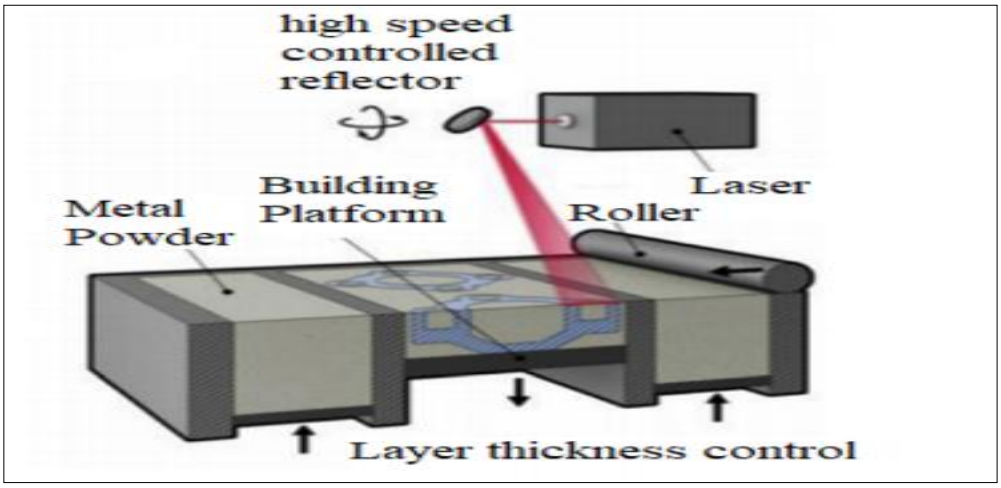

Figure II.10. Selective Laser Sintering (SLS) / Selective Laser Fusion (SLF)(Leu and al., 2012).

II.5. Effective material properties of FGM

In general, functionally graded materials (FGMs) are produced from two material phases with different properties, classified by their variable microstructure in space. This

technique is designed to optimize the performance of structural elements by distributing corresponding properties.

A detailed description of the actual graded microstructure is generally not available unless information on the distribution of volumetric fraction is provided. While the volumetric fraction of each phase gradually varies in the direction of grading, the effective properties of functionally graded materials (FGMs) change along this direction. Thus, there are two possible approaches to model graded materials. In the first approach, a piecewise variation of the ceramic or metal volumetric fraction is assumed, and the FGM is considered to be composed of quasi-homogeneous layers of ceramic-metal with the same volumetric fraction in each region, as shown in Figure II.11a. In the second approach, a continuous variation of the ceramic or metal volumetric fraction is assumed, where the metal volumetric fraction can be represented as a coordinate function following the thickness (z), as illustrated in Figure II.11.b.

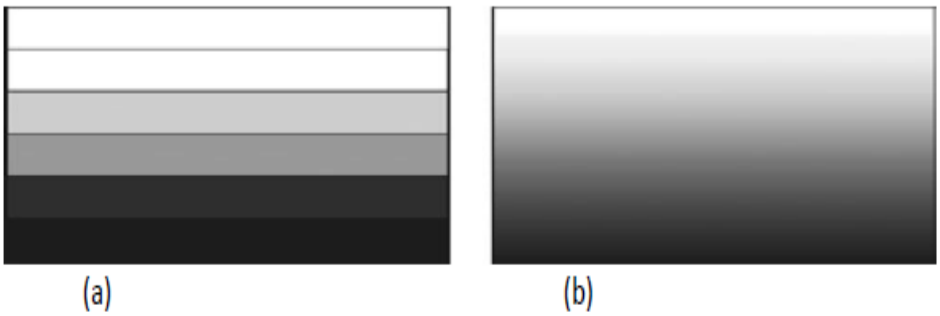

Figure II.11. Analytical models for an FGM layer.

II.5.1. Physical and Mechanical Properties of Functionally Graded Materials (FGMs)

Physical and mechanical properties of Ceramic and Metal

Ceramics:

Physical Properties: Ceramics typically exhibit high hardness, low density, and excellent thermal and electrical insulation properties. Their crystal structure often contributes to these properties. Additionally, ceramics can have low thermal expansion coefficients, making them resistant to thermal shock.

Mechanical Properties: Ceramics are brittle materials with high compressive strength but low tensile strength. Their fracture toughness, a measure of resistance to crack propagation, is typically lower compared to metals. However, ceramics can withstand high temperatures and harsh environments better than most metals, making them suitable for applications such as refractories, cutting tools, and thermal barriers.

Metals:

Physical Properties: Metals are known for their ductility, malleability, and high electrical and thermal conductivity. They usually have high density and a metallic luster due to their metallic bonding structure, which involves delocalized electrons. Metals also exhibit good thermal expansion properties.

Mechanical Properties: Metals have high ductility and toughness, making them capable of withstanding significant deformation before failure. They typically have both high compressive and tensile strengths, although their strength can vary depending on factors such as alloy composition, heat treatment, and microstructure. Metals are widely used in structural applications, machinery, electrical wiring, and many other fields due to their versatile mechanical properties.

Understanding the physical and mechanical properties of ceramics and metals is crucial for selecting the most appropriate material for specific engineering applications. While ceramics excel in high-temperature and corrosive environments, metals offer superior ductility and toughness, making them suitable for applications requiring deformation resistance and structural integrity.

II.6. Behavior laws of FGM materials

Voigt model, originally introduced by Voigt in 1889, is a well-known model of homogenization and usually used to predict the effective elastic properties for the different kinds of composite materials. The Voigt idea was to define such properties by averaging stresses over all phases with the strain uniformity assumption . For the sake of simplification, Voigt scheme is the most popular and most commonly used model for estimating the properties of FGM.

According to this rule, an arbitrary material property P of the FGM is assumed to vary smoothly along a direction (usually thickness direction), as a function of the volume fractions and properties of the constituent materials. This property can be expressed as

$$P_F = \sum_{i=1}^{n} P_i * V_{Fi} \qquad \textbf{(II.1)}$$

P can represent, for example, the young's modulus (E), the Poisson's ratio (ν) and the mass density (ρ) etc. Pi and Vi are respectively the material property and volume fraction of the constituent i of FGM. The volume fractions of all the constituent materials should add up to unity, such that **. (Sadgui A, 2022)**

$$\sum_{i=1}^{n} V_{Fi} = 1 \qquad \textbf{(II.2)}$$

The most distinctive features of an FGM are the microstructures with smoothly graded macro-properties. An FGM can be defined by the variation in volume fractions.

Most researchers utilize power law function, exponential function, or sigmoid function to describe the volume fractions. The bonds between particles must be sufficiently strong internally to resist rupture, and also externally to prevent wear. The material properties, including Young's modulus and Poisson's ratio, on the top and bottom surfaces are different but are determined based on performance requirements. However, the Young's modulus and Poisson's ratio vary continuously through the thickness, along the z-axis, i.e., E = E(z), v = v(z). The Young's modulus through the thickness of the plate in gradient material properties varies according to the power law "P-FGM," or with the sigmoid function "S-FGM," or alternatively, the exponential function "E-FGM."

II.6.1. Power law function (P-FGM)

The volume fraction of the P-FGM is assumed to obey a power-law function

$$V_c(z) = \left(\frac{z + h/2}{h} \right)^P \qquad \textbf{(II.3)}$$

where p is the material parameter that dictates the material variation profile through the thickness and h is the thickness of the plate.

Once the local volume fraction « v_c (z) » has been defined, the material properties of a P-FGM can be determined by the rule of mixture .

$$E(z) = E_m + (E_c - E_m) V_c(z) \qquad \textbf{(II.4)}$$

where Em and Ec are the Young modulus of the lowest (z =- h/2) and top surfaces (z =h⁄2) of the FGM structure, respectively. The variation of Young’s modulus in the thickness direction of the P-FGM beam is depicted in Fig(II.12) , which shows that the Young’s modulus changes rapidly near the lowest surface for p > 1, and increases quickly near the top surface for p < 1. (Sallai B and al, 2022)

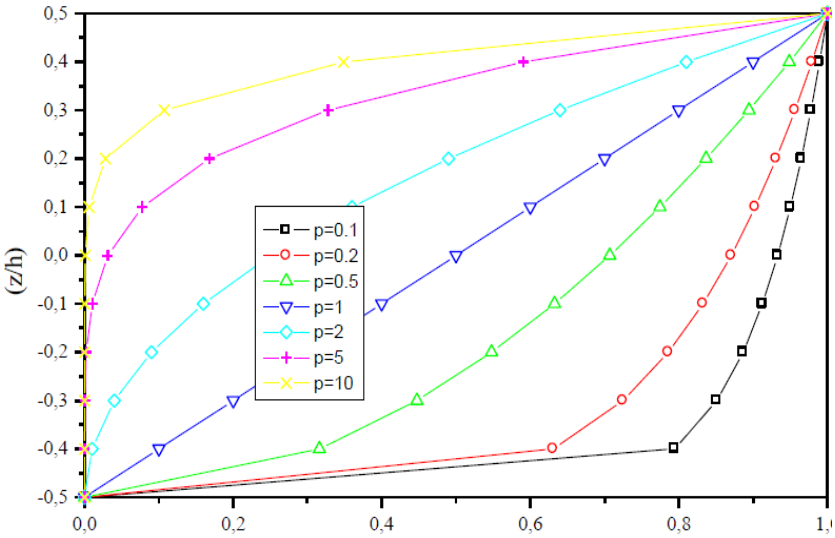

Figure II.12. Variation of volume fraction throughout the thickness (P-FGM)

II.6.2. Exponential Law (E-FGM)

Material properties vary continuously throughout the thickness direction according to the volume fraction of constituents defined exponentially through the thickness. Accordingly, the exponential law is defined as. (Manish B and al., 2015)

$$E(z) = E_m e^{B(Z+h/2)} \tag{II.5}$$

$$B = \frac{h}{2}\ln\left(\frac{E_C}{E_m}\right) \tag{II.6}$$

The variation of the Young's modulus throughout the thickness of the E-FGM structure is depicted in Figure II.13.

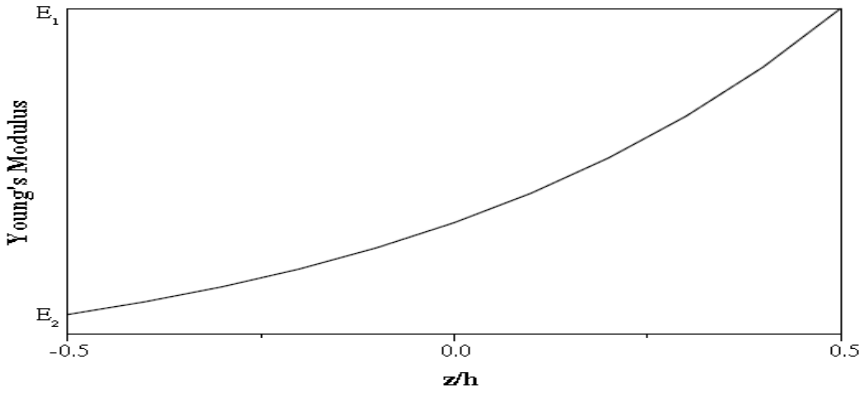

Figure II.13. Variation of Young's modulus across the thickness (E-FGM).

II.6.3. sigmoïd Function (S-FGM)

Chi and Chung (Chi and al., 2003) established the volume fraction of the FGM structure using two power law functions, aiming to ensure a balanced distribution of stresses across all interfaces. These two power law functions are defined as follows:

$$V_c(z)=\left(\frac{h/2+z}{h/2}\right)^P \quad for -h/2 \le z \le 0 \tag{II.7}$$

$$V_m(z)=1-(1/2)\left(\frac{h/2-z}{h/2}\right)^P \quad for 0 \le z \le h/2 \tag{II.8}$$

Using the rule of mixtures, the Young's modulus of the S-FGM plate can be calculated as follows:

$$E(z)=V_c(z)E_c+[1-V_c(z)]E_m \quad for -h/2 \le z \le 0 \tag{II.9}$$

$$E(z)=V_m(z)E_c+[1-V_m(z)]E_m \quad for 0 \le z \le h/2 \tag{II.10}$$

The variation of the Young's modulus according to equations (II.7) and (II.8) is depicted in Figure II.14 with sigmoid distributions.

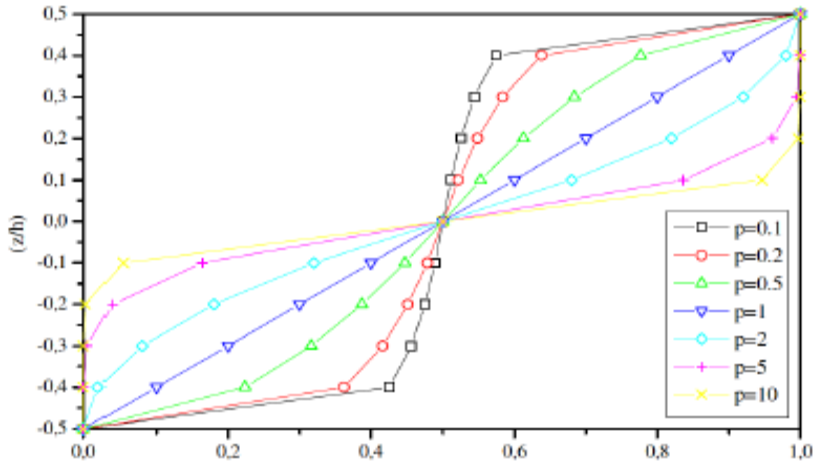

Figure II.14. Variation of volume fraction across thickness (S-FGM).

II.7. Applications of FGMs

The Functionally Graded Materials (FGMs), designed to withstand high thermal gradients, have been specifically developed for use in spacecraft structures, rocket engine components, and similar applications. Over the years, advancements in FGMs have expanded their utility to broader aerospace domains. The Functionally Graded Materials (FGMs), designed to withstand high thermal gradients, have been specifically developed for use in spacecraft structures, rocket engine components, and similar applications. Over the years, advancements in FGMs have expanded their utility to broader aerospace domains.

II.7.1. The Aerospace Industry

The initial application where functionally graded materials were developed was for space plane bodies. The application of this novel material is increased over the years in the

aerospace industry. Most aerospace equipment and structures are now made of functionally graded materials. These include the rocket engine components, the spacecraft truss structure, the heat exchange panels, and some structures, such as the reflectors, the solar panels, the camera housing, the turbine wheels, the turbine blade coatings, the nose caps, the leading edge of missiles, and space shuttles. Functionally graded materials are also used for the structural walls that combine thermal and sound insulation properties. Automobiles are another industry, in which functionally graded materials have been used. These will be presented in the next subsection. (Rasheedat M, 2013).

II.7.2. Biomedical applications

Gradient materials are commonly found in nature, such as the layered shell structures of certain organisms, sturdy animal skeletons, and human skin. Advances in FGM development have enhanced the efficiency and scope of medical care available to patients. Functionally graded materials exhibit characteristics such as high specific strength, high specific modulus, abrasion resistance, and biocompatibility. Leveraging these properties, developed joint prostheses offer strong bonding strength and reliable durability for the patient's skeleton, while demonstrating good biocompatibility as well as self-healing and repair regenerative properties. With their superior properties, FGMs present promising application prospects in biomedical fields, including artificial bones, teeth, and hearts.

II.7.3. Defence applications

It is used in defence application due to its ability to inhibit crack propagation and reduce the weight of vehicles. They are used as Penetration-Resistant materials in the defence industry in applications, such as armour plates and bulletproof vests, in addition to the manufacture of defensive parts such as guide rods, precision rollers, shafts, tubes, latches,axle‟s housings and firing pins .

II.7.4. Marine applications

FGMs also have applications in the marine and submarine industry, including propeller shafts, diving cylinders, sonar domes, composite piping systems, and cylindrical pressure hulls.(Amira S, 2022)

II.7.5. Nuclear Energy Field

FGM materials are renowned for their high mechanical strength, heat resistance, and corrosion resistance, rendering them indispensable for the development of the new generation of the nuclear industry. Given the highly elevated risks associated with nuclear energy production, nuclear power, and nuclear weapons storage, their safety is paramount. In the

event of an accident, the consequences can be severe. Therefore, ensuring their safety is imperative.

In the application of nuclear fusion reactor, FGM materials exhibit a good effect in relieving thermal stresses, thereby making nuclear fusion reaction safer. FGM materials, as high-strength, heat-resistant, and shielding materials, possess significant superiority in the construction materials of nuclear furnaces and the materials of internal furnace walls, considerably enhancing the safety of the nuclear industry.

II.7.6. Electromagnetic field

Functionally Graded Materials (FGMs) find application in various components such as antennas, waveguides, microwave absorbers, and electromagnetic shielding materials. Their tailored electromagnetic properties make them valuable for improving signal transmission, reducing interference, and enhancing the overall performance of electronic devices and communication systems. FGMs play a crucial role in advancing technologies like wireless communication, radar systems, and electromagnetic compatibility (EMC), contributing to the development of more efficient and reliable electromagnetics applications.

II.7.7. Optical field

Ordinary glass has a high hardness but a high brittleness. The glass's service life is significantly shortened by the unpredictability of the outside world. However, common glass's transmittance is unaffected by environmental changes, which has an effect on living, working, and producing particular goods. Thus, enhancing glass's mechanical and optical qualities has emerged as a key area of research and development. The functionally graded material can have its optical characteristics adjusted for the environment by including rare earth elements and materials with varying refractive indices. Materials like glass lasers, optical fiber lenses, anti-reflection films, and discolored glass have been effectively manufactured by the relevant scholars.

II.7.8. Energy

Functionally graded materials find wide applications in the field of energy industries to improve the efficiency of some of their equipment. Some of the applications of the functionally graded materials in the energy industry include the solar panel, the solar cells, the inner of nuclear reactors, the thermo-electric converter for energy conversion, the tubes and pressure vessels, the graded electrode for the production of solid oxide fuel, the piezoelectric

functionally graded materials for the ultrasonic transducer, the dielectric, the fuel cell, the turbine blade coatings, and for thermal barrier coatings . (Asmaa R, 2022)

II.7.9. Automotive industry applications

The use of functional materials in the automotive industry is still limited due to the high cost of producing such materials. However, they are employed in critical parts of vehicles where the current high cost justifies their use. Current applications include engine cylinder liners for diesel engine pistons, leaf springs, spark plugs, combustion chambers, drive shafts, shock absorbers, flywheels, certain body parts, windows, and racing car brakes. Additionally, materials with functional gradients are used in enhanced body coatings for automobiles.

II.7.10. Sports industry applications

FGM, or fiber-reinforced composites, find application in various sports equipment such as golf clubs, tennis rackets, artificial turf layers, and skis.

II.7.11. Other applications of FGMs

Some examples of various applications of FGMs in different sectors are given below:
aerospace (rocket nozzle, heat exchange panels, solar panels, turbine wheels, space plane nose, combustion chamber protective layer, body components, rocket engine components, reflectors, camera housing, caps and leading edge of missiles and space shuttle. etc);

- automobile (combustion chambers, diesel engine pistons, racing car brakes, crown of piston, cylinder liners, exhaust valves and valve seating);
- medicine (medical implants, teeth and bone replacement, artificial skin, drug delivery system);
- construction (roads – e.g. pavement life can be increased by 59% as a result of the grading of the asphalt concrete and base layers together);
- commodities (car body, sport goods, window glass, etc.);
- energy (energy conversion devices, nuclear energy, thermionic and thermoelectric converters, fuel cells, solar batteries, fuel pellet, etc.);
- electronics (graded band semiconductor, substrate, sensors);
- optoelectronic (antireflective layers, fibres, GRIN lenses);
- nanotechnology (nanostructured devices and systems etc);
- chemical plants (heat exchanger, heat pipe, slurry pump, reaction vessel);
- optics (optical fibre, lens);
- nuclear (first wall of fusion reaction, fuel pellets);
- energy conversion (solar cell, fuel cell, thermoelectric generator, thermionic convertor);

- engineering (cutting tools, machine parts, engine components, turbine blade, roller, shaft, etc.) etc. (Adelina M, 2022)

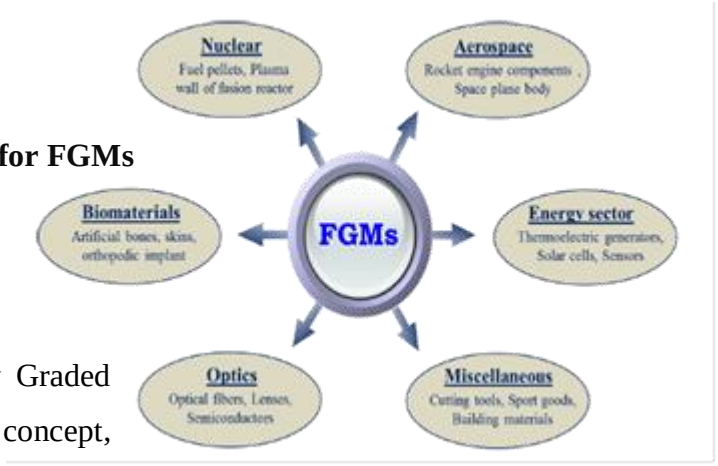

Figure II.15. Various applicable fields for FGMs (Amira S, 2022)

II.8. Conclusion

This chapter deals with Functionally Graded Materials (FGMs), presenting their concept, development, fabrication, and application. The history of FGM fabrication is addressed by describing various modern manufacturing methods and their impact on materials. The effective material properties of FGMs, such as Young's modulus, density, and Poisson's ratio, are also presented along with the different possible laws describing their variation with plate thickness.

The following chapter will focus on the design of plate theories in FGMs by defining various models of composite structures in two-dimensional elasticity.

Chapter III

Reminder on plate theories

III.1. Introduction

An FGM structure can be considered as a heterogeneous material. The primary geometric characteristic of a plate is its small thickness compared to its other dimensions. Modeling modern FGM structures, characterized by strong anisotropy (for example: a low ratio between the transverse shear modulus of the core and the longitudinal elasticity modulus of the skins in the case of sandwich structures), requires advanced theories that account for an accurate description of transverse shear. A three-dimensional approach allows for exact results, but it is limited to cases of simple geometry, stacking, and loading. Comprehensive reviews of various existing models of three-dimensional elasticity or plate type can be found in (Noor and al., 1989).

The three-dimensional (3D) approach in structural analysis offers a major advantage: it provides precise results that accurately reflect the real behavior of the structure in space. This precision makes the 3D approach a valuable reference for validating other, more simplified analysis methods.

During recent years, several two-dimensional models have been developed for modeling multilayer structures, taking into account transverse shear effects. They can be grouped based on the type of approach adopted:

- Equivalent single-layer approach.
- Layer-wise approach.
- Asymptotic expansion approach.

III.2. History

In 1888, Love utilized Gustav Kirchhoff's assumptions, themselves inspired by Euler-Bernoulli's hypotheses, to formulate a theory of thin plates (also known as classical theory or Kirchhoff-Love theory). The theory of semi-thick plates (first-order deformation theory) was further developed by Mindlin based on the works of Rayleigh (1877), Timoshenko, Reissner, and Uflyand. Subsequently, higher-order theories emerged to refine the assumptions of classical and first-order theories when the plate thickness becomes significant. There is also the theory based on three-dimensional elasticity (3-D theory), which imposes no restrictive assumptions on plate displacements. (Chedad A, 2023)

III.3. The various models of composite structures in two-dimensional elasticity

III.3.1. Equivalent single-layer approach

In the equivalent single-layer approach, the number of equations does not depend on the number of layers; the multilayered plate is homogenized and thus considered as a single layer. From Sophie Germain's pioneering work in 1815 on thin plates to the first-order models of Love-Kirchhoff and Reissner-Mindlin, many authors have developed plate theories based on more refined kinematics or stress fields. We review the main models in the following sections. (Nguyen V, 2004).

III.3.1.1. The classical theory of thin plates by Love-Kirchhoff (CPT).

A thin plate is considered when the deflection generated by shear deformations remains negligible compared to the deflection generated by the curvature of the plate. In the case of a homogeneous isotropic plate, the shear contribution to the deflection is directly related to the slenderness ratio (l/h).The classical theory of thin plates (CPT) is based on the Love-Kirchhoff assumptions, which state that a line normal to the mid-plane of the plate remains perpendicular after deformation (Figure III .1), thus neglecting the effects of transverse shear deformation. This plate model can be referred to as Timoshenko and Woinowsky-Krieger [Timoshenko, 1959], [Reddy, 1997], [Reddy, 1999].

Based on these assumptions, the displacement field is determined as follows:

$$u(x,y,z) = u_0(x,y) - z\frac{\partial w_0}{\partial x} \qquad \text{(III.1)}$$

$$V(x,y,z) = v_0(x,y) - z\frac{\partial w_0}{\partial y} \qquad \text{(III.2)}$$

$$W(x,y,z,t) = w_0(x,y) \qquad \text{(III.3)}$$

With (u_0, v_0, w_0) being the components of the displacement field on the mid-plane of the plate $(z = 0)$

refer to the schematic representation of deformations in the case of classical plate theory.

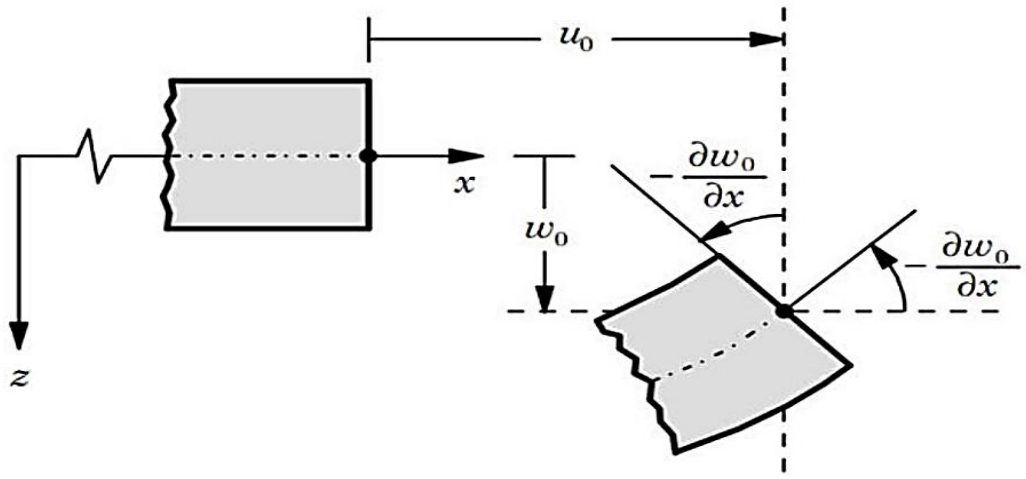

Figure III. 1. An illustration of the Love-Kirchhoff plate. CPT (Reddy and al., 1997).

NOTA: Comme le modèle ne prend pas en compte l'effet de cisaillement transverse, ses résultats ne sont pas précis pour les plaques épaisses.

III.3.1.2. The first-order shear deformation theory by Reissner and Mindlin (FSDT).

The first-order shear deformation theory extended the classical plate theory by taking into account the effect of transverse shear. In this case, stresses and strains are constant through the thickness of the plate (Figure III.2), requiring the introduction of a correction factor. Studies on the first-order shear deformation theory (FSDT) are described in the works of (Reissner and al., 1945) and (Mindlin and al., 1951), which led to the Reissner-Mindlin plate model. This model is also discussed in the works of (Timoshenko and al., 1972); (Reddy and al., 1997 and 1999); (Tlidji and al., 2016).

The first-order theory is based on the following displacement field:

$$u(x,y,z) = u_0(x,y) + z\,\phi_x(x,y) \quad \textbf{(III.4)}$$

$$v(x,y,z) = v_0(x,y) + z\phi_y(x,y) \quad \textbf{(III.5)}$$

$$w(x,y,z) = w_0(x,y) \quad \textbf{(III.6)}$$

with u_0, v_0, w_0 and ϕ_x, ϕ_y representing the membrane displacements and rotations around the x and y, axes, respectively.

By substituting the above expression with the defined displacement field, it is possible to reuse the classical plate theory described in the previous section.

$\phi_x = -\frac{\partial w_0}{\partial x}$ $\phi_y = -\frac{\partial w_0}{\partial y}$ et , Refer to the schematic representation of deformations in the case of the first-order plate theory.

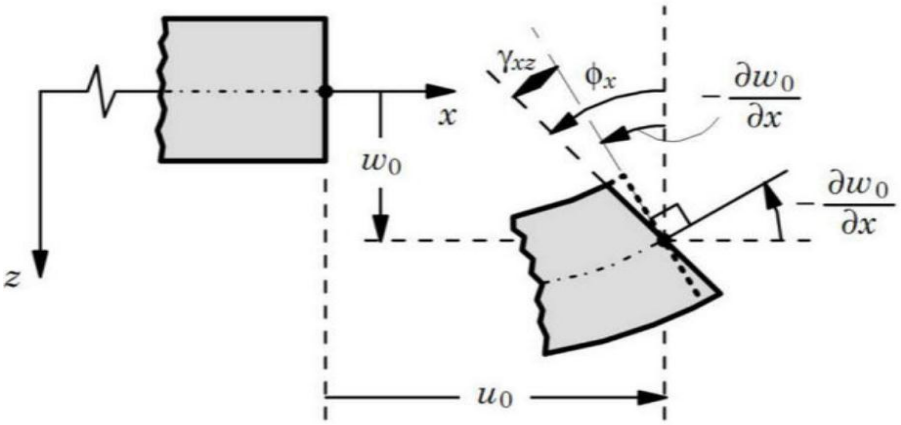

Figure III. 2. An illustration of the Reissner-Mindlin plate. FSDT (Reddy and al., 1997 and 1999).

By choosing a certain form for the displacement fields, the transverse deformations in the material are constant along the z-axis (Figure III.3). However, this results in a uniform distribution of shear stresses between the discontinuous layers, which is not an accurate description of reality.

To correct this in the energy calculation, corrective coefficients must be introduced, which is complex and often empirical in real-world situations. Therefore, using this kinematic approach to study thick composites is random and can lead to unreliable results (Whitney and al., 1973).

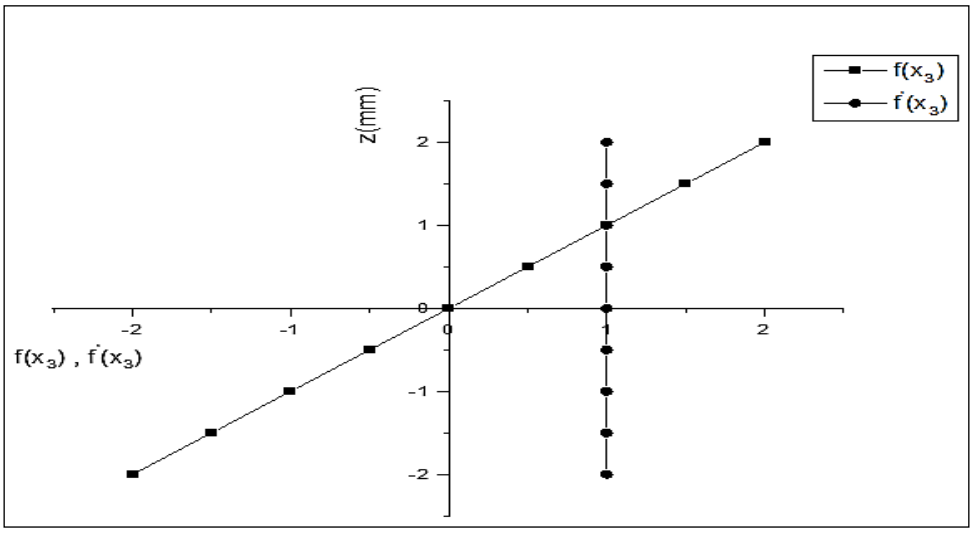

Figure III. 3. The variation of the warping function with respect to thickness.

NOTE: To avoid the need for introducing a correction factor for calculations, higher-order shear deformation theories have been developed.

III.3.1.3. The Higher-Order Shear Deformation Theory by Reddy HSDT (PSDT).

In-order to overcome the limitations of FSDT many HSDTs were developed that involve higher order terms in Taylors expansions of the displacements in the thickness coordinate . Most of these theories do not account for transverse shear stress on the top and bottom surfaces of the plate and transverse extensibility by neglecting the transverse stress in the z-direction (σz). (Redddy B and al. 2014).

Refer to the schematization of deformations in the case of the Higher-Order Plate Theory.

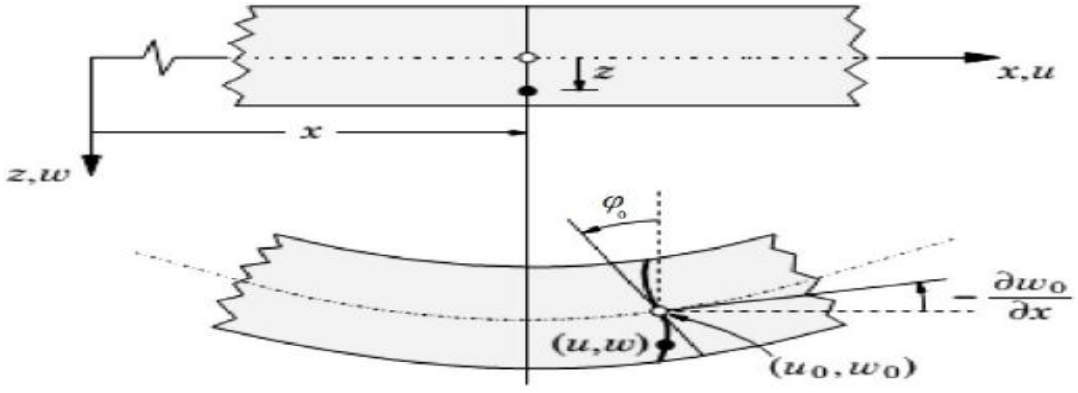

Figure III. 4. Illustration of the Higher-Order Plate. HSDT (Reddy, 1997).

III.3.1.3.1.Displacement field (HSDPT)

In cases where a first-order scheme does not adequately approximate a given problem, it will then be necessary to transition to a higher-order scheme (2nd order, 3rd order, or even higher) in the development of displacement series. Consequently, these theories introduce additional functions whose terms are often difficult to interpret.

Second-order Plate Theories:

The displacement field of the second-order theory is expressed by:

$U(x, y, z,t) = u(x, y,t) + z\varphi x(x, y,t) + z2\psi x(x, y,t)$

$V(x, y, z,t) = v(x, y,t) + z\varphi y(x, y,t) + z2\psi y(x, y,t)$ (3-5)

$W(x, y, z,t) = w(x, y,t) + z\varphi z(x, y,t) + z2\psi z(x, y,t)$

Where : u, v, w, φx, φy, φz, ψx, ψy , ψz Are unknown functions depending on the coordinates x and y and the time t.

This theory brings a substantial improvement compared to the first-order theory while requiring a correction factor similar to the FSDPT.

Third-order Plate Theories:

In the pursuit of more refined theories and the aim to remove limitations of previous theories, new higher-order theories have emerged. The displacement field is written as follows:

$U(x, y, z,t) = u(x, y,t) + z\varphi x(x, y,t) + z2\psi x(x, y,t) + z3\ \chi x(x, y,t)$

$V(x, y, z,t) = v(x, y,t) + z\varphi y(x, y,t) + z2\psi y(x, y,t) + z3\ \chi y(x, y,t)$ (3-6)

$W(x, y, z,t) = w(x, y,t) + z\varphi z(x, y,t) + z2\psi z(x, y,t) + z3\ \chi z(x, y,t)$

Where: u, v, w, φx, φy, φz, ψx, ψy, ψz, χx, χy, χz are unknown functions depending on the coordinates x and y and the time t.(Zemani KADA, 2015)

III.3.2. Layer-wise approach

In the layer-wise approach, the multilayer is subdivided into substructures (corresponding actually to each material layer or to a set of layers). We apply a first-order or higher-order theory to each of the layers. Thus, different models have been developed for elasticity: (Pagano, 1978), (Seide, 1980), (Di Sciuva, 1984), (Chabot, 1997), (Carreira et al., 2002), (Diaz-Diaz et al., 2002). These approaches are generally aimed at better predicting interface effects between layers: sliding, delamination...

These models are more costly (the number of variables depends on the number of layers), but allow for more precise results, especially regarding out-of-plane stress calculation.

We will focus here on the so-called "discrete layer models." These models propose a layer-wise kinematics rather than a global kinematics. The multilayer is represented by a set of

plates interacting with each other through their interfaces. Continuity conditions at the interfaces are ensured.

In the works of Srinivas (1987), Seide (1980), Reddy (1987), Naciri et al. (1998), Tahani and Nosier (2003), a first-order or higher-order kinematics per layer is assumed. The fundamental equations per layer are obtained using the principle of virtual work. Boundary conditions are also provided layer by layer.

Alternatively, some authors use an approximation solely on the stress field per layer (Ying, 1994), or a mixed stress-kinematic approach. Thus, Ren (1986) employs a stress field where the transverse shear component is quadratic per layer, and the displacements are considered cubic per layer and continuous at the interfaces. (Dallot J, 2008)

The layer-wise approach can be classified into two main categories: discrete layer models, where each layer is treated as an individual plate and continuity conditions in terms of displacements or stresses are applied at the interfaces; and zigzag models, where the kinematics are designed to automatically satisfy the contact conditions and are independent of the number of layers. The displacement fields of the modes are illustrated in Figures III.5 and III.6.

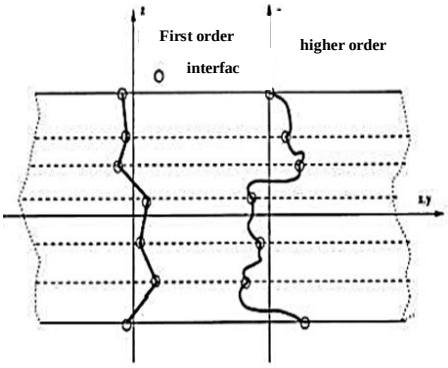

Figure III.5.Displacement field Of discrete layer models, kinematic approach. (Nguyen and al., 2004)

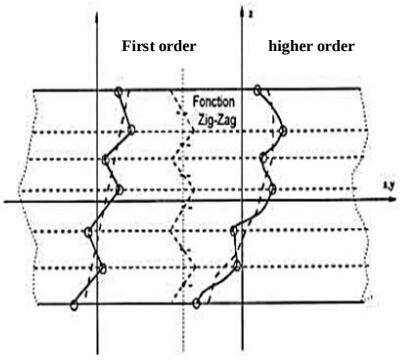

Figure III.6 Displacement field of zigzag models, kinematic approach. (Nguyen and al., 2004)

III.3.2.1.Les modèles zig-zag

To better describe the shear deformation of composite materials, some authors have combined the higher-order theory with the so-called zigzag theory, which is specifically aimed at better describing interface effects. Thus, various models stemming from the layer-wise approach have been proposed. The multilayer is subdivided into substructures (corresponding to each layer or each set of layers). A first-order theory or a higher-order model is applied to each substructure. The kinematics of zigzag models inherently satisfies the contact conditions and is independent of the number of layers.

The main advantage of the displacement field of zigzag models lies in accurately modeling the distortion of the normal to the deformed surface, as well as verifying continuity conditions, without increasing the number and order of fundamental equations of the first-order theory. The need for correction coefficients for transverse shear is avoided. Building on the concept of Di Sciuva, several authors have made significant improvements to the zigzag model.

The main improvement is the introduction of a non-linear distribution of displacements. The zigzag field (piecewise linear) is superimposed with a higher-order displacement field (often cubic) (Figure II.7). Compatibility conditions are satisfied on the upper and lower surfaces of the plates to reduce the number of parameters. (Sedjrari A, 2018)

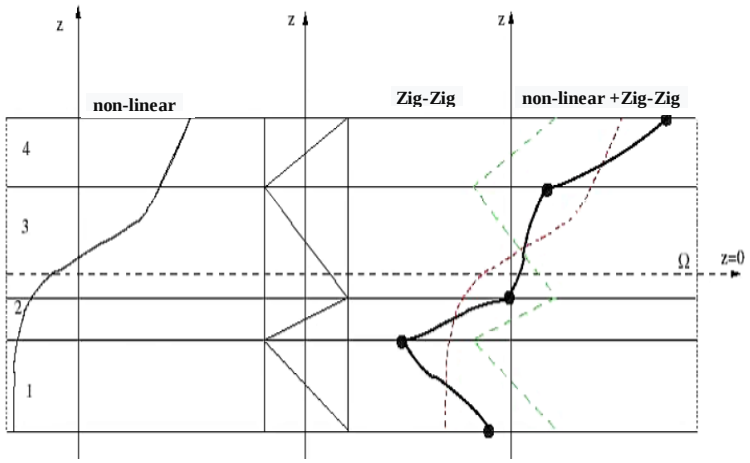

Figure III.7. Higher-order zig-zag model displacement field. (Nguyen, 2004)

III.4. Various shape functions of more recent plate theories.

Other refined theories of isotropic plate approach and FGM have emerged more recently in the unified form as depicted in the following table: (Ait Atmane and al., 2010). Various shape functions of isotropic plate theories in FGM. (Meksi and al., 2016).

Theory	Title	Shape function φ(z)	Distribution of γxz and γyz along z	Shear correction coefficient	Validity
CPT Kirchhoff	Classical plate theory	0	-	-	Thin plates
FSDPT Mindlin	First-order plate deformation theory	z	Constant	Required	Thin and moderately thick plates

Ambartsumian	Higher-order theory	$\frac{z}{2}\left(\frac{h^2}{4}-\frac{z^2}{3}\right)$	Quadratic	Not required	Thin and moderately thick plates
Reissner	Higher-order theory	$\frac{5z}{4}\left(1-\frac{4}{3}\left(\frac{z}{h}\right)^2\right)$	Parabolic	Not required	Thin and thick plates
TSDPT Touratier	Trigonometric plate deformation theory	$\frac{h}{\pi}\sin\left(\frac{\pi z}{h}\right)$	Parabolic	Not equired	Thin and thick plates
ESDPT Karama, Afaq and *al*.	Exponential plate deformation theory	$z\,Exp\left(-2\left(\frac{z}{h}\right)^2\right)$	Parabolic	Not required	Thin and thick plates
PSDPT Levinson Reddy Murthy	Parabolic plate deformation theory	$z\left(1-\frac{4}{3}\left(\frac{z}{h}\right)^2\right)$	Parabolic	Not required	Thin and thick plates
Aydogdu	Exponential Plate Deformation Theory	$z\alpha^{-\frac{2(z/h)^2}{\ln(\alpha)}},\alpha\succ 0$	Parabolic	Not required	Thin and thick plates
El Maiche, Tounsi and *al.*	Refined Plate Theory	$\frac{\frac{h}{\pi}\sin\left(\frac{\pi z}{h}\right)}{\left(\cos h\left(\pi/2\right)-1\right)}$	Parabolic	Not required	Thin and thick plates
Atmane, Tounsi and *al.*	Refined Plate Theory	$\frac{\cos h\left(\pi/2\right)}{\left[\cos\left(\pi/2\right)-1\right]}z-\frac{\frac{h}{\pi}\sin\left(\frac{\pi z}{h}\right)}{\left(\cos h(\pi/2)-1\right)}z$	Parabolic	Not required	Thin and thick plates
Shimpi	Refined Plate Theory	$h\left[\frac{1}{4}\left(\frac{z}{h}\right)-\frac{5}{3}\left(\frac{z}{h}\right)^3\right]$	Parabolic	Not required	Thin and thick plates

III.4.1. New refined theory of plate deformation.

Shimpi (2002) developed a refined model for isotropic plates (RPT: Refined Plate Theory). One of the most interesting features of this method is that it only contains two variables, resulting in only four unknowns instead of the five in the classical case. Additionally, this theory does not require a shear correction factor and provides a parabolic distribution of shear across the plate thickness. Furthermore, it exhibits many similarities with the classical plate theory regarding the equations of motion, boundary conditions, and moment expressions (Shimpi and al., 2002).

• (Ait Atmane and al. 2010) adapted this theory for the bending of FGM plates. Recently (Ait Atmane and al., 2010).

• Ait Yahia, S., Ait Atmane, H., Houari, M.S.A., and Tounsi, A. studied (2015), ("wave propagation in functionally graded plates with porosities using various higher-order shear deformation plate theories"). They published this theory for the shear deformation of FG plates with porosity. (Ait Yahia and al., 2015).

• Thai and Kim (2010, 2011) and Hadji and al. in 2011 successfully adapted RPT to the buckling of orthotropic plates and the free vibration of laminated and sandwich plates, respectively (Thai and al., 2010).

In this thesis, we propose the use of this refined theory to study the mechanical behavior analysis of sandwich plates with multiple porous directions in FGM composite materials, in addition to the exact position of the neutral surface of such a sandwich plate already well determined.

III.5. Conclusion

This chapter provides an introduction to the three most commonly used plate theories. This section discusses various theories related to sandwich plates, including the equivalent single-layer approach, the layer-wise approach, and the asymptotic development approach. We also concluded that the equivalent single-layer approach is better suited for FGM materials, as they do not exhibit abrupt changes in their mechanical properties, unlike conventional composites where delamination can be an issue.

Other plate theories such as layer-wise theory or zig-zag theory are also available but are not discussed here, as well as finite element models of composite structures.

Therefore, we have opted for the use of the equivalent single-layer model for thick and thin plates in different high-order theories, where consideration of transverse shear is necessary for a more precise study.

Chapter IV

Free Vibration Analysis of Multi-directional Porous Functionally Graded Sandwich Plates

IV.1 Introduction

While most research tends to focus on creating and analyzing structures with functionally graded properties along a single direction, the operating conditions of advanced aerospace vehicles involve temperature variations in multiple directions. Consequently, there is a growing interest in studying materials with properties graded in multiple directions to enhance their performance further. Fortunately, modern additive manufacturing techniques now enable the fabrication of such multidirectionally graded structures.

In our current study, we investigate the natural vibration characteristics of sandwich plates composed of multiple layers with functionally graded properties, both with and without porosity. We explore two scenarios: one with functionally graded skins and a homogeneous core, and the other with a functionally graded core and homogeneous skins.

Our findings highlight the critical role of grading parameters in achieving optimal natural frequencies for both scenarios. Additionally, we examine how different types of imperfections and the length-to-thickness ratio influence the natural frequency. Imperfections in the functionally graded core decrease natural frequencies, while in the functionally graded skin, they have the opposite effect.

We employ a methodology that results in a hyperbolic distribution of shear stress across the structure, with zero shear stress at the upper and lower faces of the plate. By applying Hamilton's principle to the governing equations of motion, we conduct a thorough analysis of free vibrations under simply supported boundary conditions.

From a manufacturing perspective, our study sheds light on how frequency variations correlate with porosity distribution, which varies across different fabrication approaches. This insight can guide the selection of manufacturing methods, considering the diverse porosity distributions associated with each technique.

IV.2. Problem formulation

IV.2.1 Preliminary concepts and definitions

Fig. 1 illustrates a multi-directional FGM sandwich plate having a length (a), width (b), and thickness (h) along the x, y, and z axes. The sandwich plate consists of three parts, two face sheets (top and bottom) embedded with a core in between. The x and y axes are considered to be the midplane in Fig. 1, while the z-axis is perpendicular to the midplane.

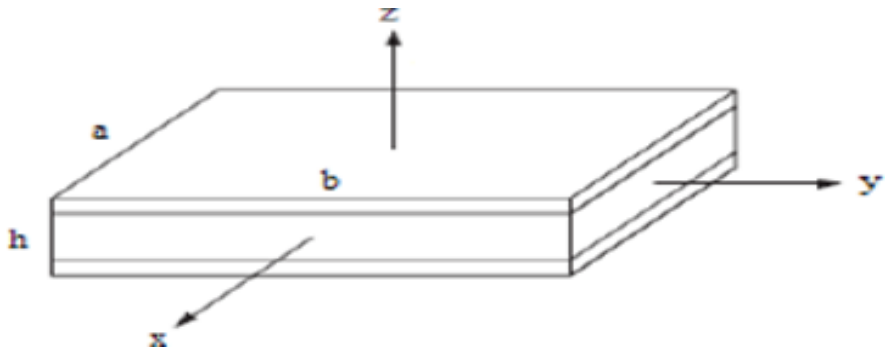

Figure IV.1. Multi-directional graded sandwich plate (Hadji. 2012)

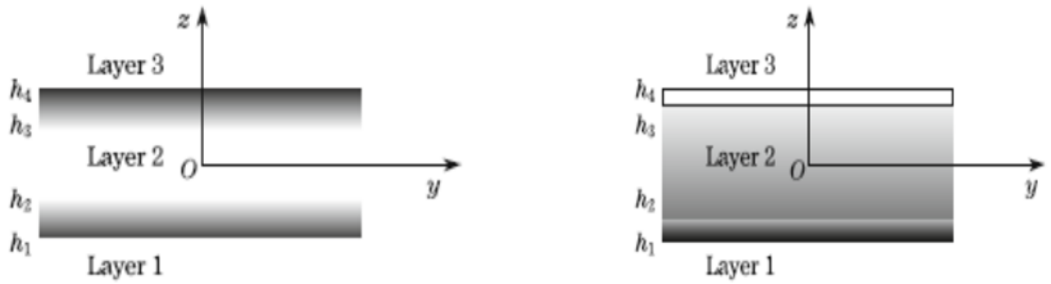

(a) FG face-sheet and homogeneous core **(b)** FG core and homogeneous face sheet

Figure IV. 2 .Multi-directional FGM sandwich plate (Hadji. 2012)

The layer thickness is given by h1, h2, h3, and h4 which defines the sandwich configuration. A power law variation of volume fraction variation of metal and ceramic was considered as given by Eq. (1-2). The study considers metal (Al) and ceramic (Al2O3) whose composition changes longitudinal (nx) and transverse direction (nz). Material properties of FGM sandwich plate depend upon the volume fraction of material constituents in longitudinal and transverse directions based on power law.

The volume fraction of metal for a multi-directional sandwich plate can be expressed as:

Type A: FG face-sheet and homogeneous core

$$V^{(1)}(x,z)=\left(\frac{z-h_2}{h_1-h_2}\right)^{n_z}\left(1-\frac{x}{2a}\right)^{n_x} \quad \text{(IV.1)}$$

$$V^{(2)}(x,z)=0 \quad \text{(IV.2)}$$

$$V^{(3)}(x,z)=\left(\frac{z-h_3}{h_4-h_3}\right)^{n_z}\left(1-\frac{x}{2a}\right)^{n_x} \quad \text{(IV.3)}$$

Where V(n) (n = 1, 2, 3) is the volume fraction. Layer n defines the grading index; nx and nz are the gradations along with longitudinal and transverse directions respectively.

Type B: FG core and homogeneous face sheet

$$V^{(1)}(x,z)=0 \tag{IV.4}$$

$$V^{(1)}(x,z)=\left(\frac{z-h_2}{h_3-h_2}\right)^{n_z}\left(1-\frac{x}{2a}\right)^{n_x} \tag{IV .5}$$

$$V^{(3)}(x,z)=1 \tag{IV.6}$$

IV.3. Modeling of porous FG sandwich plate

Using rule of mixture, the mechanical properties of porous functionally graded sandwich plate, such as Young's modulus and density, were determined. To account for the effect of porosity developed in a material as a result of various fabrication procedures, three different porosity distributions in the material were studied, which are primarily classified as uniform and non-uniform.

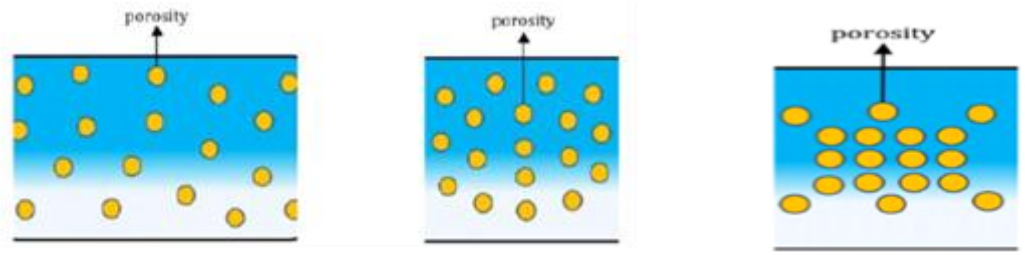

I .Uniform distribution | II. Non uniform distribution | III. non uniform Logarithmic distribution

Figure IV.3.Modeling of porous FG sandwich plate (Hadji. 2012)

IV.3.1. Modeling of porous FG sandwich plate (Type A)

IV .3.1.1. Imperfect I: Porosity distributed evenly

$$P_1(x,z)=(P_m-P_c)V_1(x,z)+P_c-\frac{\alpha}{2}(P_c+P_m) \tag{IV.7}$$

$$P_2(x,z)=(P_m-P_c)V_2(x,z)+P_c \tag{IV.8}$$

$$P_3(x,z)=(P_m-P_c)V_3(x,z)+P_c-\frac{\alpha}{2}(P_c+P_m) \tag{IV.9}$$

Where α, defines the porosity volume fraction, when α is 0, means no porosity (perfect). A higher value of α indicates higher porosity in a material. The material properties of metal and ceramic were given by Pm and P, respectively. The overall effective properties of FGM were given by $P1(x, z)$, $P2(x, z)$, and $P3(x, z)$ of the bottom layer, core, and top layer respectively.

IV .3.1.2. Imperfect II: Porosity distributed unevenly

$$P_1(x,z)=(P_m-P_c)V_1(x,z)+P_c-\frac{\alpha}{2}(P_c+P_m)\left[1-\frac{\left|2z-(h_1+h_2)\right|}{(h_2-h_1)}\right] \quad \text{(VI.10)}$$

$$P_2(x,z)=(P_m-P_c)V_2(x,z)+P_c \quad \text{(IV.11)}$$

$$P_3(x,z)=(P_m-P_c)V_3(x,z)+P_c-\frac{\alpha}{2}(P_c+P_m)\left[1-\frac{\left|2z-(h_4+h_3)\right|}{(h_4-h_3)}\right] \quad \text{(IV.12)}$$

IV.3.1.3 (Imperfect III): logarithmic uneven porosities

$$P_1(x,z)=(P_m-P_c)V_1(x,z)+P_c-\log\left(1+\frac{\alpha}{2}\right)(P_c+P_m)\left[1-\frac{\left|2z-(h_1+h_2)\right|}{(h_2-h_1)}\right] \quad \text{(IV.13)}$$

$$P_2(x,z)=(P_m-P_c)V_2(x,z)+P_c \quad \text{(IV.14)}$$

$$P_3(x,z)=(P_m-P_c)V_3(x,z)+P_c-\log\left(1+\frac{\alpha}{2}\right)(P_c+P_m)\left[1-\frac{\left|2z-(h_4+h_3)\right|}{(h_4-h_3)}\right] \quad \text{(IV.15)}$$

IV.3.2. Modeling of porous FG sandwich plate (Type B)

IV .3.2.1. Imperfect I: Porosity distributed evenly

$$P_1(x,z)=(P_m-P_c)V_1(x,z)+P_c \quad \text{(IV.16)}$$

$$P_2(x,z)=(P_m-P_c)V_2(x,z)+P_c-\frac{\alpha}{2}(P_c+P_m) \quad \text{(IV.17)}$$

$$P_3(x,z)=(P_m-P_c)V_3(x,z)+P_c \quad \text{(IV.18)}$$

IV .3.2.2. Imperfect II: Porosity distributed unevenly

$$P_1(x,z)=(P_m-P_c)V_1(x,z)+P_c \quad \text{(IV.19)}$$

$$P_2(x,z)=(P_m-P_c)V_2(x,z)+P_c-\frac{\alpha}{2}(P_c+P_m)\left[1-\frac{\left|2z-(h_2+h_2)\right|}{(h_3-h_2)}\right] \quad \text{(IV.20)}$$

$$P_3(x,z)=(P_m-P_c)V_3(x,z)+P_c \quad \text{(IV.21)}$$

IV .3.2.3 . (Imperfect III): logarithmic uneven porosities

$$P_1(x,z)=(P_m-P_c)V_1(x,z)+P_c \quad \text{(IV.22)}$$

$$P_2(x,z)=(P_m-P_c)V_2(x,z)+P_c-\log\left(1+\frac{\alpha}{2}\right)(P_c+P_m)\left[1-\frac{\left|2z-(h_2+h_3)\right|}{(h_3-h_2)}\right] \quad \text{(IV.23)}$$

$$P_3(x,z)=(P_m-P_c)V_3(x,z)+P_c \quad \text{(IV.24)}$$

IV .4. Displacement field and strains

In the multi-directional FGM sandwich plate, in-plane displacement $u$and$v$ is considered in $x$and $y$direction and transverse displacement w in z direction. The in-plane and transverse displacements can be represented as follows using refined shear deformation theory (El Meiche and al.2011, Hadji and al. 2011, Kettaf and al. 2013):

$$u(x,y,z,t)=u_0(x,y,t)-z\frac{\partial w_b}{\partial x}-f(z)\frac{\partial w_s}{\partial x} \quad \textbf{(IV.25)}$$

$$V(x,y,z,t)=v_0(x,y)-z\frac{\partial w_b}{\partial y}-f(z)\frac{\partial w_s}{\partial y} \quad \textbf{(IV.26)}$$

$$W(x,y,z,t)=w_b(x,y,t)+w_s(x,y,t) \quad \textbf{(IV.27)}$$

Where

$$f(z)=z\left[1+\frac{3\pi}{2}sech(\frac{1}{2})^2\right]-\frac{3\pi}{2}h*tanh(\frac{z}{h}) \quad \text{(IV.28)}$$

$u0$, $v0$, wb and ws are in-plane and transverse displacements at the middle plane. The strains associated with the displacements in Eq. (9) are given by

$$\varepsilon_x=\varepsilon_x^0+z\,k_x^b+f\,k_x^s \quad \text{(IV.29)}$$

$$\varepsilon_y=\varepsilon_y^0+z\,k_y^b+f\,k_y^s \quad \text{(IV.30)}$$

$$\gamma_{xy} = \gamma_{xy}^{0} + z\ k_{xy}^{b} + f\ k_{xy}^{s} \tag{IV.31}$$

$$\gamma_{yz} = g\ \gamma_{yz}^{s} \tag{IV.32}$$

$$\gamma_{xz} = g\ \gamma_{xz}^{s} \tag{IV.33}$$

$$\varepsilon_{z} = 0 \tag{IV.34}$$

Where

$$\varepsilon_{x}^{0} = \frac{\partial u_0}{\partial x},\ k_{x}^{b} = -\frac{\partial^2 w_b}{\partial x^2},\ k_{x}^{s} = -\frac{\partial^2 w_s}{\partial x^2}$$

$$\varepsilon_{y}^{0} = \frac{\partial v_0}{\partial y},\ k_{y}^{b} = -\frac{\partial^2 w_b}{\partial y^2},\ k_{y}^{s} = -\frac{\partial^2 w_s}{\partial y^2}$$

$$\gamma_{xy}^{0} = \frac{\partial u_0}{\partial y} + \frac{\partial v_0}{\partial x},\quad k_{xy}^{b} = -2\frac{\partial^2 w_b}{\partial x \partial y}$$

$$k_{xy}^{s} = -2\frac{\partial^2 w_s}{\partial x \partial y} \tag{IV.35}$$

$$\gamma_{yz}^{s} = \frac{\partial w_s}{\partial y},\ \gamma_{xz}^{s} = \frac{\partial w_s}{\partial x}$$

$$f(z) = z\left[1 + \frac{3\pi}{2} sech\left(\frac{1}{2}\right)^2\right] - \frac{3\pi}{2} h * tanh\left(\frac{z}{h}\right),\quad g(z) = 1 - \frac{df(z)}{dz}$$

For a multi-directional FGM sandwich plate, the stress-strain relationship is as follows

$$\begin{Bmatrix} \sigma_x \\ \sigma_y \\ \tau_{xy} \end{Bmatrix}^{(n)} = \begin{bmatrix} Q_{11} & Q_{12} & 0 \\ Q_{12} & Q_{22} & 0 \\ 0 & 0 & Q_{66} \end{bmatrix}^{(n)} \begin{Bmatrix} \varepsilon_x \\ \varepsilon_y \\ \gamma_{xy} \end{Bmatrix} \textbf{ and } \begin{Bmatrix} \tau_{yz} \\ \tau_{zx} \end{Bmatrix}^{(n)} = \begin{bmatrix} Q_{44} & 0 \\ 0 & Q_{55} \end{bmatrix}^{(n)} \begin{Bmatrix} \gamma_{yz} \\ \gamma_{zx} \end{Bmatrix} \tag{IV.36}$$

Where

$$Q_{11}^{(n)}(x,z) = Q_{22}^{(n)}(x,z) = \frac{E^{(n)}(x,z)}{1-\nu^2} \tag{IV.37}$$

$$Q_{12} = \nu Q_{11}^{(n)}(x,z) \tag{IV.38}$$

$$Q_{44}^{(n)}(x,z) = Q_{55}^{(n)} = Q_{66}^{(n)} = \frac{E^{(n)}(x,z)}{2(1+\nu)} \tag{IV.39}$$

IV .5. Equations of motion

The equation of motion for the FG plate is derived using Hamilton's energy principle (Delale F et al, 1983).

$$\int_{t_1}^{t_2}\left(\delta U-\delta T\right)dt=0 \tag{IV.40}$$

where T and U are the kinetic energy and strain energy of the plate, respectively. The total potential energy of the multi-directional FGM sandwich plate is given by the following equation

$$U=\frac{1}{2}\int_{V}\left[\sigma_x^{(n)}\ \varepsilon_x+\sigma_y^{(n)}\ \varepsilon_y+\tau_{xy}^{(n)}\ \gamma_{xy}+\tau_{yz}^{(n)}\ \gamma_{yz}+\tau_{xz}^{(n)}\ \gamma_{zx}\right]dV \tag{IV.41}$$

The strain energy change for the FGM sandwich plate is represented as follows:

$$\begin{aligned}\delta\ U=\int_{A}\Big[&N_x\delta\ \varepsilon_x^0+N_y\delta\ \varepsilon_y^0+N_{xy}\delta\ \gamma_{xy}^0+M_x^b\delta\ k_x^b+M_y^b\delta\ k_y^b+M_{xy}^b\delta\ k_{xy}^b\\&+M_x^s\delta\ k_x^s+M_y^s\delta\ k_y^s+M_{xy}^s\delta\ k_{xy}^s+S_{yz}^s\delta\ \gamma_{yz}^s+S_{xz}^s\delta\ \gamma_{xz}^s\Big]\ dA=0\end{aligned} \tag{IV.42}$$

Where A is the top surface and the stress resultants N, M, and S are defined by

$$\left(N_x,N_y,N_{xy}\right)=\sum_{n=1}^{3}\int_{h_n}^{h_{n+1}}\left(\sigma_x,\sigma_y,\tau_{xy}\right)dz \tag{IV.43}$$

$$\left(M_x^b,M_y^b,M_{xy}^b\right)=\sum_{n=1}^{3}\int_{h_n}^{h_{n+1}}\left(\sigma_x,\sigma_y,\tau_{xy}\right)zdz \tag{IV.44}$$

$$\left(M_x^s,M_y^s,M_{xy}^s\right)=\sum_{n=1}^{3}\int_{h_n}^{h_{n+1}}\left(\sigma_x,\sigma_y,\tau_{xy}\right)fdz \tag{IV.45}$$

$$\left(S_{xz}^s,S_{yz}^s\right)=\sum_{n=1}^{3}\int_{h_n}^{h_{n+1}}\left(\tau_{xz},\tau_{yz}\right)gdz \tag{IV.46}$$

Substituting Eq (IV.36). into Eq. (IV.43) to (IV.46) and integrating through the thickness of the plate, the stress resultants are given as

$$\begin{Bmatrix}N\\M^b\\M^s\end{Bmatrix}=\begin{bmatrix}A&B&B^s\\B&D&D^s\\B^s&D^s&H^s\end{bmatrix}\begin{Bmatrix}\varepsilon\\k^b\\k^s\end{Bmatrix},\ \textbf{and}\begin{Bmatrix}S_{yz}^s\\S_{xz}^s\end{Bmatrix}=\begin{bmatrix}A_{44}^s&0\\0&A_{55}^s\end{bmatrix}\begin{Bmatrix}\gamma_{yz}^s\\\gamma_{xz}^s\end{Bmatrix} \tag{IV.47}$$

In which

$$N=\left\{N_x,N_y,N_{xy}\right\}^t,\ M^b=\left\{M_x^b,M_y^b,M_{xy}^b\right\}^t,\ M^b=\left\{M_x^b,M_y^b,M_{xy}^b\right\}^t \tag{IV.48}$$

$$\varepsilon=\left\{\varepsilon_x^0,\varepsilon_y^0,\gamma_{xy}^0\right\}^t,\ k^b=\left\{k_x^b,k_y^b,k_{xy}^b\right\}^t,\ k^s=\left\{k_x^s,k_y^s,k_{xy}^s\right\}^t \tag{IV.49}$$

$$A=\begin{bmatrix}A_{11}&A_{12}&0\\A_{12}&A_{22}&0\\0&0&A_{66}\end{bmatrix},B=\begin{bmatrix}B_{11}&B_{12}&0\\B_{12}&B_{22}&0\\0&0&B_{66}\end{bmatrix} \tag{IV.50}$$

$$D=\begin{bmatrix}D_{11}&D_{12}&0\\D_{12}&D_{22}&0\\0&0&D_{66}\end{bmatrix} \tag{IV.51}$$

$$B^s=\begin{bmatrix}B_{11}^s&B_{12}^s&0\\B_{12}^s&B_{22}^s&0\\0&0&B_{66}^s\end{bmatrix},\ D^s=\begin{bmatrix}D_{11}^s&D_{12}^s&0\\D_{12}^s&D_{22}^s&0\\0&0&D_{66}^s\end{bmatrix} \tag{IV.52}$$

$$H^s=\begin{bmatrix}H_{11}^s&H_{12}^s&0\\H_{12}^s&H_{22}^s&0\\0&0&H_{66}^s\end{bmatrix}$$

$$S=\left\{S_{xz}^s,S_{yz}^s\right\}^t,\gamma=\left\{\gamma_{xz}^0,\gamma_{yz}^0\right\}^t,A^s=\begin{bmatrix}A_{44}^s&0\\0&A_{55}^s\end{bmatrix} \tag{IV.53}$$

and stiffness components are given as:

$$\begin{Bmatrix}A_{11}&B_{11}&D_{11}&B_{11}^s&D_{11}^s&H_{11}^s\\A_{12}&B_{12}&D_{12}&B_{12}^s&D_{12}^s&H_{12}^s\\A_{66}&B_{66}&D_{66}&B_{66}^s&D_{66}^s&H_{66}^s\end{Bmatrix}$$

$$=\sum_{n=1}^{3}\int_{h_n}^{h_{n+1}}Q_{ij}^{(n)}\left(1,z,z^2,f(z),z\,f(z),f^2(z)\right)\begin{Bmatrix}1\\\nu\\\dfrac{1-\nu}{2}\end{Bmatrix}dz \tag{IV.54}$$

$$\left(A_{22},B_{22},D_{22},B_{22}^s,D_{22}^s,H_{22}^s\right)=\left(A_{11},B_{11},D_{11},B_{11}^s,D_{11}^s,H_{11}^s\right) \tag{IV.55}$$

$$A_{44}^{s} = A_{55}^{s} = \sum_{n=1}^{3} \int_{-h/2}^{h/2} Q_{ij}^{(n)} \left[g(z) \right]^2 dz \tag{IV.56}$$

The variation of kinetic energy can be expressed as:

$$\begin{aligned}
\delta T &= \int_{-\frac{h}{2}}^{\frac{h}{2}} \int_{\Omega} \left[\dot{u}\delta \dot{u} + \dot{v}\delta \dot{v} + \dot{w}\delta \dot{w} \right] \rho(z)\, d\Omega\, dz \\
&= \int_{A} \Big\{ I_0 \left[\dot{u}_0 \delta \dot{u}_0 + \dot{v}_0 \delta \dot{v}_0 + \left(\dot{w}_b + \dot{w}_s \right) \left(\delta \dot{w}_b + \delta \dot{w}_s \right) \right] \\
&- I_1 \left(\dot{u}_0 \frac{\partial \delta \dot{w}_b}{\partial x} + \frac{\partial \dot{w}_b}{\partial x} \delta \dot{u}_0 + \dot{v}_0 \frac{\partial \delta \dot{w}_b}{\partial y} + \frac{\partial \dot{w}_b}{\partial y} \delta \dot{v}_0 \right) \\
&- I_2 \left(\dot{u}_0 \frac{\partial \delta \dot{w}_s}{\partial x} + \frac{\partial \dot{w}_s}{\partial x} \delta \dot{u}_0 + \dot{v}_0 \frac{\partial \delta \dot{w}_s}{\partial y} + \frac{\partial \dot{w}_s}{\partial y} \delta \dot{v}_0 \right) \\
&+ J_1 \left(\frac{\partial \dot{w}_b}{\partial x} \frac{\partial \delta \dot{w}_b}{\partial x} + \frac{\partial \dot{w}_b}{\partial y} \frac{\partial \delta \dot{w}_b}{\partial y} \right) + K_2 \left(\frac{\partial \dot{w}_s}{\partial x} \frac{\partial \delta \dot{w}_s}{\partial x} + \frac{\partial \dot{w}_s}{\partial y} \frac{\partial \delta \dot{w}_s}{\partial y} \right) \\
&+ J_2 \left(\frac{\partial \dot{w}_b}{\partial x} \frac{\partial \delta \dot{w}_s}{\partial x} + \frac{\partial \dot{w}_s}{\partial x} \frac{\partial \delta \dot{w}_b}{\partial x} + \frac{\partial \dot{w}_b}{\partial y} \frac{\partial \delta \dot{w}_s}{\partial y} + \frac{\partial \dot{w}_s}{\partial y} \frac{\partial \delta \dot{w}_b}{\partial y} \right) \Big\} dA
\end{aligned} \tag{IV.57}$$

Where dot-superscript convention indicates the differentiation concerning the time variable t; $\rho(z)$ is themass density; and (Ii , Ji ,Ki) are mass inertias expressed by

$$\left(I_0, I_1, I_2 \right) = \int_{A} \left(1, z, z^2 \right) \rho(z) dA \tag{IV.58}$$

$$\left(J_1, J_2, K_2 \right) = \int_{A} \left(f(z), z f(z), f^2(z) \right) \rho(z) dA \tag{IV.59}$$

By substituting Eqs(IV.42). and (IV.57) into Eq. (IV.40), the following can be derived

$$
\begin{aligned}
&\delta u_0: \quad \frac{\partial N_x}{\partial x}+\frac{\partial N_{xy}}{\partial y}=I_0\ddot{u}_0-I_1\frac{\partial \ddot{w}_b}{\partial x}-J_1\frac{\partial \ddot{w}_s}{\partial x}\\
&\delta v_0: \quad \frac{\partial N_{xy}}{\partial x}+\frac{\partial N_y}{\partial y}=I_{01}\ddot{v}_0-I_1\frac{\partial \ddot{w}_b}{\partial y}-J_1\frac{\partial \ddot{w}_s}{\partial y}\\
&\delta w_b: \quad \frac{\partial^2 M_x^b}{\partial x^2}+2\frac{\partial^2 M_{xy}^b}{\partial x\partial y}+\frac{\partial^2 M_y^b}{\partial y^2}\\
&=I_0\left(\ddot{w}_b+\ddot{w}_s\right)+I_1\left(\frac{\partial \ddot{u}_0}{\partial x}+\frac{\partial \ddot{v}_0}{\partial y}\right)-I_2\nabla^2\ddot{w}_b-J_2\nabla^2\ddot{w}_s\\
&\delta w_s: \quad \frac{\partial^2 M_x^s}{\partial x^2}+2\frac{\partial^2 M_{xy}^s}{\partial x\partial y}+\frac{\partial^2 M_y^s}{\partial y^2}+\frac{\partial S_{xz}^s}{\partial x}+\frac{\partial S_{yz}^s}{\partial y}\\
&=I_0\left(\ddot{w}_b+\ddot{w}_s\right)+J_1\left(\frac{\partial \ddot{u}_0}{\partial x}+\frac{\partial \ddot{v}_0}{\partial y}\right)-J_2\nabla^2\ddot{w}_b-K_2\nabla^2\ddot{w}_s
\end{aligned}
\tag{IV.60}
$$

By substituting Eq(IV.47). in Eq. (IV.60), the equations of motion can be written in terms of displacements ($u0$, $v0$,wb , ws) and the corresponding equations take thefollowing form:

$$
\begin{aligned}
&A_{11}\frac{\partial^2 u_0}{\partial x^2}+A_{66}\frac{\partial^2 u_0}{\partial y^2}+\left(A_{12}+A_{66}\right)\frac{\partial^2 v_0}{\partial x\partial y}-B_{11}\frac{\partial^3 w_b}{\partial x^3}-\left(B_{12}+2B_{66}\right)\frac{\partial^3 w_b}{\partial x\partial y^2}\\
&-B_{11}^s\frac{\partial^3 w_s}{\partial x^3}-\left(B_{12}^s+2B_{66}^s\right)\frac{\partial^3 w_s}{\partial x\partial y^2}=I_0\ddot{u}_0-I_1\frac{\partial \ddot{w}_b}{\partial x}-J_1\frac{\partial \ddot{w}_s}{\partial x},
\end{aligned}
\tag{IV.61}
$$

$$
\begin{aligned}
&\left(A_{12}+A_{66}\right)\frac{\partial^2 u_0}{\partial x\partial y}+A_{66}\frac{\partial^2 v_0}{\partial x^2}+A_{22}\frac{\partial^2 v_0}{\partial y^2}-\left(B_{12}+2B_{66}\right)\frac{\partial^3 w_b}{\partial x^2\partial y}-B_{22}\frac{\partial^3 w_b}{\partial y^3}\\
&-B_{22}^s\frac{\partial^3 w_s}{\partial y^3}-\left(B_{12}^s+2B_{66}^s\right)\frac{\partial^3 w_s}{\partial x^2\partial y}=I_0\ddot{v}_0-I_1\frac{\partial \ddot{w}_b}{\partial y}-J_1\frac{\partial \ddot{w}_s}{\partial y}
\end{aligned}
\tag{IV.62}
$$

$$
\begin{aligned}
&B_{11}\frac{\partial^3 u_0}{\partial x^3}+\left(B_{12}+2B_{66}\right)\frac{\partial^3 u_0}{\partial x\partial y^2}+\left(B_{12}+2B_{66}\right)\frac{\partial^3 v_0}{\partial x^2\partial y}+B_{22}\frac{\partial^3 v_0}{\partial y^3}-D_{11}\frac{\partial^4 w_b}{\partial x^4}\\
&-2\left(D_{12}+2D_{66}\right)\frac{\partial^4 w_b}{\partial x^2\partial y^2}-D_{22}\frac{\partial^4 w_b}{\partial y^4}-D_{11}^s\frac{\partial^4 w_s}{\partial x^4}-2\left(D_{12}^s+2D_{66}^s\right)\frac{\partial^4 w_s}{\partial x^2\partial y^2}\\
&-D_{22}^s\frac{\partial^4 w_s}{\partial y^4}=I_0\left(\ddot{w}_b+\ddot{w}_s\right)+I_1\left(\frac{\partial \ddot{u}_0}{\partial x}+\frac{\partial \ddot{v}_0}{\partial y}\right)-I_2\nabla^2\ddot{w}_b-J_2\nabla^2\ddot{w}_s,
\end{aligned}
\tag{IV.63}
$$

$$
\begin{aligned}
&B_{11}^{s}\frac{\partial^3 u}{\partial x^3}+\left(B_{12}^{s}+2B_{66}^{s}\right)\frac{\partial^3 u}{\partial x\partial y^2}+\left(B_{12}^{s}+2B_{66}^{s}\right)\frac{\partial^3 v}{\partial x^2\partial y}+B_{22}^{s}\frac{\partial^3 v}{\partial y^3}-D_{11}^{s}\frac{\partial^4 w_b}{\partial x^4}\\
&-2\left(D_{12}^{s}+2D_{66}^{s}\right)\frac{\partial^4 w_b}{\partial x^2\partial y^2}-D_{22}^{s}\frac{\partial^4 w_b}{\partial y^4}-H_{11}^{s}\frac{\partial^4 w_s}{\partial x^4}-2\left(H_{12}^{s}+2H_{66}^{s}\right)\frac{\partial^4 w_s}{\partial x^2\partial y^2}-H_{22}^{s}\frac{\partial^4 w_s}{\partial y^4}\\
&+A_{55}^{s}\frac{\partial^2 w_s}{\partial x^2}+A_{44}^{s}\frac{\partial^2 w_s}{\partial y^2}=I_0\left(\ddot{w}_b+\ddot{w}_s\right)+J_1\left(\frac{\partial\ddot{u}_0}{\partial x}+\frac{\partial\ddot{v}_0}{\partial y}\right)-J_2\nabla^2\ddot{w}_b-K_2\nabla^2\ddot{w}_s
\end{aligned}
\qquad \textbf{(IV.64)}
$$

IV.6 .Navier solution for simply supported rectangular multi-directional FGM sandwich plate

Sandwich plates are categorized based on boundary conditions. For a simply supported plate, the analytical solutions were given by Eqs. (IV.61) to (IV.64) .At the side edges, the following boundary conditions were imposed.

$$
\begin{aligned}
&v_0(-a/2,y)=w_b(-a/2,y)=w_s(-a/2,y)\\
&=\frac{\partial w_b}{\partial y}(-a/2,y)=\frac{\partial w_s}{\partial y}(-a/2,y)=0
\end{aligned}
\qquad \text{(IV.65)}
$$

$$
\begin{aligned}
&v_0(a/2,y)=w_b(a/2,y)=w_s(a/2,y)\\
&=\frac{\partial w_b}{\partial y}(a/2,y)=\frac{\partial w_s}{\partial y}(a/2,y)=0
\end{aligned}
\qquad \text{(IV.66)}
$$

$$
\begin{aligned}
&N_x(-a/2,y)=M_x^b(-a/2,y)=M_x^s(-a/2,y)\\
&=N_x(a/2,y)=M_x^b(a/2,y)=M_x^s(a/2,y)=0
\end{aligned}
\qquad \text{(IV.67)}
$$

$$
\begin{aligned}
&u_0(x,-b/2)=w_b(x,-b/2)=w_s(x,-b/2)\\
&=\frac{\partial w_b}{\partial x}(x,-b/2)=\frac{\partial w_s}{\partial x}(x,-b/2)=0
\end{aligned}
\qquad \text{(IV.68)}
$$

$$
\begin{aligned}
&u_0(x,b/2)=w_b(x,b/2)=w_s(x,b/2)\\
&=\frac{\partial w_b}{\partial x}(x,b/2)=\frac{\partial w_s}{\partial x}(x,b/2)=0
\end{aligned}
\qquad \text{(IV.69)}
$$

$$
\begin{aligned}
&N_y(x,-b/2)=M_y^b(x,-b/2)=M_y^s(x,-b/2)\\
&=N_y(x,b/2)=M_y^b(x,b/2)=M_y^s(x,b/2)=0
\end{aligned}
\qquad \text{(IV.70)}
$$

The following Fourier series was used to select the displacement functions that satisfy the equations of boundary conditions, Eqs (IV.65) to (IV.70)

$$\begin{Bmatrix} u_0 \\ v_0 \\ w_b \\ w_s \end{Bmatrix} = \sum_{m=1}^{\infty}\sum_{n=1}^{\infty} \begin{Bmatrix} U_{mn}\cos(\lambda x)\sin(\mu y)\, e^{i\omega t} \\ V_{mn}\sin(\lambda x)\cos(\mu y)\, e^{i\omega t} \\ W_{bmn}\sin(\lambda x)\sin(\mu y)\, e^{i\omega t} \\ W_{smn}\sin(\lambda x)\sin(\mu y)\, e^{i\omega t} \end{Bmatrix} \tag{IV.71}$$

where Umn , Vmn , $Wbmn$, and $Wsmn$ are arbitrary parameters and $\omega = \omega mn$ denote the eigenfrequency associated with $(m, n)th$ eigenmode and $\lambda = m\pi/a$, $\mu = n\pi/b$.

By substituting Eqs. (IV.71) in Eqs (IV.61) to (IV.64) , the following general governing equation for free vibration studies of amultidirectional FGM sandwich plate was obtained:

$$\left(\begin{bmatrix} a_{11} & a_{12} & a_{13} & a_{14} \\ a_{12} & a_{22} & a_{23} & a_{24} \\ a_{13} & a_{23} & a_{33} & a_{34} \\ a_{14} & a_{24} & a_{34} & a_{44} \end{bmatrix} - \omega^2 \begin{bmatrix} m_{11} & 0 & 0 & 0 \\ 0 & m_{22} & 0 & 0 \\ 0 & 0 & m_{33} & m_{34} \\ 0 & 0 & m_{43} & m_{44} \end{bmatrix} \right) \begin{Bmatrix} U_{mn} \\ V_{mn} \\ W_{bmn} \\ W_{smn} \end{Bmatrix} = \begin{Bmatrix} 0 \\ 0 \\ 0 \\ 0 \end{Bmatrix} \tag{IV.72}$$

In which

$$a_{11} = \int_0^a \left(A_{11}\lambda^2 + A_{66}\mu^2\right)dx$$

$$a_{12} = \int_0^a \lambda\mu\ \left(A_{12} + A_{66}\right)dx$$

$$a_{13} = \int_0^a -\lambda\left(B_{11}\lambda^2 + \left(B_{12} + 2B_{66}\right)\mu^2\right)dx$$

$$a_{14} = \int_0^a -\lambda\left(B_{11}^s\lambda^2 + \left(B_{12}^s + 2B_{66}^s\right)\mu^2\right)dx$$

$$a_{22} = \int_0^a \left(A_{66}\lambda^2 + A_{22}\mu^2\right)dx$$

$$a_{23} = \int_0^a -\mu\left(\left(B_{12} + 2B_{66}\right)\lambda^2 + B_{22}\mu^2\right)dx \tag{IV.73a}$$

$$a_{24} = \int_0^a -\mu\left(\left(B_{12}^s + 2B_{66}^s\right)\lambda^2 + B_{22}^s\mu^2\right)dx$$

$$a_{33} = \int_0^a \left(D_{11}\lambda^4 + 2(D_{12} + 2D_{66})\lambda^2\mu^2 + D_{22}\mu^4\right)dx$$

$$a_{34} = \int_0^a \left(D_{11}^s\lambda^4 + 2\left(D_{12}^s + 2D_{66}^s\right)\lambda^2\mu^2 + D_{22}^s\mu^4\right)dx$$

$$a_{44}=\int_0^a\left(H_{11}^s\lambda^4+2\left(H_{12}^s+2H_{66}^s\right)\lambda^2\mu^2+H_{22}^s\mu^4+A_{55}^s\lambda^2+A_{44}^s\mu^2\right)dx$$

and

$$\begin{aligned}
m_{11}&=m_{22}=\int_0^a I_0\,dx\\
m_{33}&=\int_0^a I_0+I_2\left(\lambda^2+\mu^2\right)dx\\
m_{34}&=\int_0^a I_0+J_2\left(\lambda^2+\mu^2\right)dx\\
m_{44}&=\int_0^a I_0+K_2\left(\lambda^2+\mu^2\right)dx
\end{aligned}\qquad\text{(IV.73b)}$$

Eq. (IV.72) is a general governing equation used to performfree vibration analysis on FGM sandwich plates.

The non-dimensional frequency parameter can be expressed as

$$\overline{\omega}=\frac{\omega a}{h}\sqrt{\frac{\rho_0}{E_0}}\qquad\text{(IV.74)}$$

The following is the general governing equation for free vibration analysis of a multi-directional FGM sandwich beam:

$$\left(\begin{bmatrix}a_{11}&a_{12}&a_{13}\\a_{12}&a_{22}&a_{23}\\a_{13}&a_{23}&a_{33}\end{bmatrix}-\omega^2\begin{bmatrix}m_{11}&m_{12}&m_{13}\\m_{12}&m_{22}&m_{23}\\m_{13}&m_{23}&m_{33}\end{bmatrix}\right)\begin{Bmatrix}U_m\\W_{bm}\\W_{sm}\end{Bmatrix}=\begin{Bmatrix}0\\Q_m\\Q_m\end{Bmatrix}\qquad\text{(IV.75)}$$

Where

$$\begin{aligned}
&a_{11}=A_{11}\lambda^2\ ,\ a_{12}=-B_{11}\lambda^3\,,a_{13}=-B_{11}^s\lambda^3\,,a_{22}=D_{11}\lambda^4\\
&a_{23}=D_{11}^s\lambda^4\,,a_{33}=H_{11}^s\lambda^4+A_{55}^s\lambda^2\qquad\text{(IV.75)}\\
&m_{11}=I_1\,,\ \ m_{12}=-I_2\lambda\ ,\ \ m_{13}=-I_3\lambda\ ,\ m_{22}=I_1+I_4\lambda^2\ ,\\
&m_{22}=I_1+I_4\lambda^2\,,\ m_{23}=I_1+I_5\lambda^2\,,\ m_{33}=I_1+I_6\lambda^2\qquad\text{(IV.76)}
\end{aligned}$$

IV.7. Conclusion

This chapter introduces a novel theory of transverse shear for sandwich plates, aimed at analyzing the free vibration of multidirectionally functionally graded plates. This theory considers the effects of transverse shear and the distribution of shear stresses throughout the plate's thickness, meeting the condition of shear stress nullity on both the upper and lower faces of the FGM plate without requiring shear correction factors. It is assumed that the material properties of the plate follow a power law P-FGM. The equations of motion for the FGM sandwich plate are derived using Hamilton's energy principle. Solutions are obtained through Navier's equations, and the fundamental frequencies are determined by solving the eigenvalue problem.

Chapter V

Results and discussions

V.1. Introduction

In this chapter, we present and analyze various models to validate the accuracy of the refined theory in predicting vibration when porosity is present in simply supported multidirectional FGM sandwich plates. We consider two types of porous FGM sandwich plates:

Type A: Sandwich with FGM skins and a homogeneous core (core)

Type B: Sandwich with an FGM core and homogeneous skins.

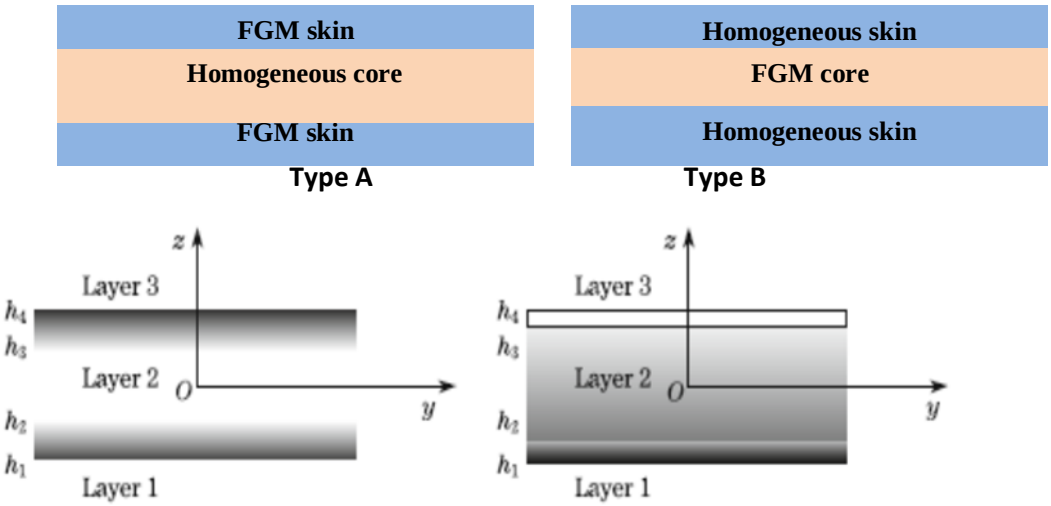

Figure V. 1. Configuration of the FGM sandwich plate, (Type A and B).

For the FGM sandwich plate, the material properties used in this study are summarized in the following table:

Table V. 1. Material properties of metal and ceramic

	Material	**Properties**	**Symbol**
1	Ceramic (Alumina, Al_2O_3)	Elasticity modulus	E_c = 380 GPa
		Poisson coefficient	$\nu = 0.3$
		Mass density	ρ_c=3800kg/m^3
2	Metal (Aluminum, Al)	Elasticity modulus	E_m = 70 GPa
		Poisson coefficient	$\nu = 0.3$
		Mass density	ρ_m=2707kg/m^3

For verification purposes, the results obtained are compared to those reported in the literature. In all examples, no shear correction factor is used for this theory. The Poisson's ratio of the plate is assumed to be constant across the thickness and equal to 0.3.

The numerical results are presented in terms of non-dimensional frequencies. The non-dimensional parameter used is defined as:

$$\overline{\omega} = \frac{\omega a}{h}\sqrt{\frac{\rho_0}{E_0}}$$

Where ρ_0= 1 kg/m^3 and E_0 =1GPa.

Several kinds of symetric and non-symetric FGM sandwich plate are used as shown in table V.2:

Table V. 2. Differents models of symetric and non-symetric FGM sandwich plates

Models	Symbol	FGM sandwich plate definitions	Geometric characteristics
Model 1	1-0-1	The plate is made of two layers of equal thickness without a core.	$h_1=h_2=0$
Model 2	1-1-1	The plate is made of three equal-thickness layers.	$h_1 = -h_2 = h/6.$
Model 3	1-2-1	The core thickness equals the sum of faces thickness.	$h_1 = -h_2 = h/4.$
Model 4	2-1-2	The upper layer thickness is twice the core layer while its the same as the lower one.	$h_1 = -h_2 = h/10.$
Model 5	2-2-1	The core thickness is twice the upper face while it is the same as the lower one.	$h_1 = -h/10\ h_2 = 3h/10$
Model 6	1-1-2	The thickness of the core is the same as the bottom while it is half that of the upper face.	h_1= - $h/4$ $h_2=0$

V.2. Validation

The results are validated with published works on free vibration analysis of sandwich plates with functionally graded skin and homogenous core. It can be seen from Table 1 that the results of the present method, i.e., the frequency parameter of multidirectional sandwich plate sandwich models at mode 2, are in agreement with the existing solutions (Kumar Sah and Ghosh 2022). Therefore, demonstrating the validity of the solution methodology

V.2.1. Free vibration analysis of perfect (non-porous) sandwich plate:

V.2.1.1. Sandwich plate with FGM skin and homogeneous core (type A)

The face sheet is made of functionally graded material and a power-law variation of metal and ceramic was considered. In the present study, the core material was made of ceramic (alumina) and is known as hardcore whereas when the core material is metal then it is known as softcore. The two skins are made of FGM in which the material properties are varied as per power law. On solving, the maximum frequency parameter was obtained for type: (1-2-1), because in this case, the core thickness is more and so its stiffness will be higher. Also, when the core material is ceramic then increasing the thickness of ceramic layers generates additional stiffer plates which give higher frequency whereas when the core is metal-based, incrementing the metal core thickness adds flexibility to the system which reduces the natural frequency (Tahir et al., 2021). A further decrease in natural frequency is seen for (2-2-1), followed by (1-1-1), (1-1-2), and (2-1-2). The frequency increases as the grading parameter, nx and nz increases. Considering mode-1 and mode-2, for type 1-2-1, when nx=0 and nz are incremented from 0 to 0.5, the percentage increases in frequency are 7.53% and 3.10%. On the other hand, when nz =0.5, and nx is incremented from 0 to 0.5, the percentage increase in frequency is 5.88% and 1.77%, for mode-1 and mode -2 respectively. See table V.3

Table V. 3. Free vibration of multi-directional FGM sandwich plate with n_x and n_z. (Type A)

a/h	n_x	n_z	Theory	Multi-directional FGM models				
				1-1-1	1-2-1	1-1-2	2-1-2	2-2-1
5	0	0.5	Present (Mode 1)	1.1566	1.2453	1.1405	1.1069	1.2008
			Present (Mode 2)	3.7245	3.9095	3.6229	3.5588	3.8012
			Kumar and Ghosh (2021) (Mode 2)	3.7245	3.9095	3.6166	3.5588	3.7955
		1	Present (Mode 1)	1.2714	1.3468	1.2516	1.2235	1.3076

			Present (Mode 2)	3.9095	4.0348	3.8427	3.8012	3.9609
			Kumar and Ghosh (2021) (Mode 2)	3.9095	4.0348	3.8381	3.8012	3.9571
		5	Present (Mode 1)	1.5180	1.5523	1.5041	1.4924	1.5330
			Present (Mode 2)	4.2225	4.2572	4.2048	4.1941	4.2365
			Kumar and Ghosh (2021) (Mode 2)	4.2225	4.2572	4.2038	4.1941	4.2358
	0.5	0.5	Present (Mode 1)	1.2569	1.3231	1.2484	1.2212	1.2921
			Present (Mode 2)	3.8294	3.9800	3.7481	3.6973	3.8915
			Kumar and Ghosh (2021) (Mode 2)	3.8294	3.9800	3.7439	3.6973	3.8875
		1	Present (Mode 1)	1.3433	1.4021	1.3300	1.3069	1.3728
			Present (Mode 2)	3.9800	4.0838	3.9253	3.8915	4.0224
			Kumar and Ghosh (2021) (Mode 2)	3.9800	4.0838	3.9221	3.8915	4.0197
		5	Present (Mode 1)	1.5412	1.5698	1.5299	1.5199	1.5539
			Present (Mode 2)	4.2418	4.2714	4.2268	4.2177	4.2537
			Kumar and Ghosh (2021) (Mode 2)	4.2418	4.2714	4.2260	4.2177	4.2532
	2	0.5	Present (Mode 1)	1.4219	1.4569	1.4201	1.4039	1.4427
			Present (Mode 2)	4.0214	4.1128	3.9735	3.9440	4.0587
			Kumar and Ghosh (2021) (Mode 2))	4.0214	4.1128	3.9719	3.9440	4.0570
		1	Present (Mode 1)	1.4683	1.5015	1.4627	1.4484	1.4862
			Present (Mode 2)	4.1128	4.1778	4.0792	4.0587	4.1392
			Kumar and Ghosh (2021) (Mode 2)	4.1128	4.1778	4.0779	4.0587	4.1380
		5	Present (Mode 1)	1.5857	1.6039	1.5789	1.5724	1.5939
			Present (Mode 2)	4.2799	4.2995	4.2700	4.2641	4.2878
			Kumar and Ghosh (2021) (Mode 2)	4.2799	4.2995	4.2697	4.2641	4.2876
10	0	0.5	Present (Mode 1)	1.2239	1.3229	1.2102	1.1709	1.2748
			Present (Mode 2)	7.4489	7.8189	7.2459	7.1175	7.6023
			Kumar and Ghosh (2021) (Mode 2)	7.4489	7.8190	7.2427	7.1175	7.5995
		1	Present (Mode 1)	1.3533	1.4393	1.3333	1.3001	1.3956

			Present (Mode 2)	7.8189	8.0696	7.6854	7.6023	7.9218
			Kumar and Ghosh (2021) (Mode 2)	7.8190	8.0696	7.6831	7.6023	7.9199
		5	Present (Mode 1)	1.6408	1.6819	1.6243	1.6102	1.6588
			Present (Mode 2)	8.4449	8.5145	8.4096	8.3881	8.4729
			Kumar and Ghosh (2021) (Mode 2)	8.4450	8.5145	8.4091	8.3881	8.4726
	0.5	0.5	Present (Mode 1)	1.3373	1.4116	1.3319	1.2996	1.3785
			Present (Mode 2)	7.6588	7.9600	7.4963	7.3945	7.7829
			Kumar and Ghosh (2021) (Mode 2)	7.6588	7.9600	7.4941	7.3945	7.7809
		1	Present (Mode 1)	1.4357	1.5033	1.4229	1.3951	1.4705
			Present (Mode 2)	7.9600	8.1675	7.8505	7.7829	8.0448
			Kumar and Ghosh (2021) (Mode 2)	7.9600	8.1675	7.8489	7.7829	8.0434
		5	Present (Mode 1)	1.6684	1.7029	1.6549	1.6429	1.6837
			Present (Mode 2)	8.4836	8.5428	8.4535	8.4353	8.5074
			Kumar and Ghosh (2021) (Mode 2)	8.4836	8.5428	8.4531	8.4353	8.5071
	2	0.5	Present (Mode 1)	1.5277	1.5673	1.5294	1.5094	1.5527
			Present (Mode 2)	8.0428	8.2257	7.9469	7.8879	8.1173
			Kumar and Ghosh (2021) (Mode 2)	8.0428	8.2257	7.9461	7.8879	8.1165
		1	Present (Mode 1)	1.5813	1.6201	1.5769	1.5592	1.6030
			Present (Mode 2)	8.2257	8.3556	8.1584	8.1173	8.2783
			Kumar and Ghosh (2021) (Mode 2)	8.2257	8.3556	8.1577	8.1173	8.2778
		5	Present (Mode 1)	1.7217	1.7439	1.7135	1.7055	1.7317
			Present (Mode 2)	8.5599	8.5990	8.5401	8.5282	8.5756
			Kumar and Ghosh (2021) (Mode 2)	8.5599	8.5990	8.5400	8.5282	8.5755

From the results, it is interesting to note that increasing the parameter nz, has a greater influence on the frequency parameter than with nx. Therefore, an increase in the ceramic composition along the transverse direction is more beneficial than varying the ceramic

composition in the longitudinal direction. The effect of nx and nz, becomes more important for lower modes than higher modes.

V.2.1.2. sandwich plate with FGM core and homogeneous skin (type B)

In this case, the core is made of FGM and the skin is made of homogeneous material. The frequency parameter is maximum for (2-2-1), followed by (1-2-1), (1-1-1), (2-1-2), and (1-1-2).

The homogeneous skin material is made of metal which has lesser stiffness than the FG core. Therefore, in cases where the skin thickness is twice that of the core for ex. in (2-1-2) and (1-1-2), the overall stiffness of the structure reduces resulting in lower natural frequency

On the other hand, type-(1-2-1), has a higher core-to-face sheet ratio and so has a higher natural frequency. Considering mode-1 and mode-2 values for type (2-2-1), when nx =0 and nz are incremented from 0.5 to 1, the percentage increases in frequency are 3.08% and 3.06%. Alternatively, when nz =0.5, and nx is incremented from 0 to 0.5, the percentage increase in frequency is 3.16% and 1.74%, for mode-1 and mode-2 respectively. Unlike, case-1, in the present case, the effect of parameter nx is more significant than nz for mode-1, but for mode-2, the parameter nz is more significant than nx.

Out of the two cases, the natural frequency is higher for case-1 (FGM skin) compared to case-2 (FGM core). Comparing the results of both cases, the study shows the importance of grading indices on the frequency parameter. In situations where the results of both cases are comparable, it provides an option to fabricate either the FGM skin or FGM core whichever is easier and economical. As the a/h ratio increases, the natural frequency increases.

Table V. 4. Free vibration of multi-directional FGM sandwich plate with FGM core with n_x and n_z (Type B)

a/h	n_x	n_z	Theory	Multi-directional FGM models				
				1-1-1	1-2-1	1-1-2	2-1-2	2-2-1
5	0	0.5	Present (Mode 1)	1.1445	1.1583	1.1120	1.1387	1.1943
			Present (Mode 2)	3.5145	3.4574	3.2728	3.5588	3.6847
		1	Present (Mode 1)	1.1626	1.1861	1.1181	1.1499	1.2323
			Present (Mode 2)	3.6229	3.6229	3.3677	3.6229	3.8012
		5	Present (Mode 1)	1.2092	1.2619	1.1309	1.1764	1.3232

			Present (Mode 2)	3.8198	3.9095	3.5423	3.7440	4.0106
	0.5	0.5	Present (Mode 1)	1.1643	1.1945	1.1188	1.1485	1.2333
			Present (Mode 2)	3.5753	3.5509	3.3259	3.5945	3.7501
		1	Present (Mode 1)	1.1777	1.2139	1.1228	1.1573	1.2613
			Present (Mode 2)	3.6658	3.6868	3.4055	3.6488	3.8469
		5	Present (Mode 1)	1.2149	1.2728	1.1327	1.1792	1.3335
			Present (Mode 2)	3.8325	3.9274	3.5537	3.7520	4.0240
	2	0.5	Present (Mode 1)	1.1979	1.2529	1.1293	1.1661	1.2975
			Present (Mode 2)	3.6914	3.7245	3.4280	3.6644	3.8742
		1	Present (Mode 1)	1.2044	1.2609	1.1308	1.1711	1.3114
			Present (Mode 2)	3.7488	3.8082	3.4790	3.6997	3.9354
		5	Present (Mode 1)	1.2262	1.2935	1.1361	1.1846	1.3532
			Present (Mode 2)	3.8578	3.9629	3.5764	3.7681	4.0508
10	0	0.5	Present (Mode 1)	1.2373	1.2573	1.2202	1.2270	1.2839
			Present (Mode 2)	7.0289	6.9148	6.5457	7.1175	7.3693
		1	Present (Mode 1)	1.2502	1.2778	1.2186	1.2353	1.3207
			Present (Mode 2)	7.2459	7.2459	6.7355	7.2459	7.6023
		5	Present (Mode 1)	1.2915	1.3484	1.2193	1.2579	1.4155
			Present (Mode 2)	7.6395	7.8189	7.0846	7.4880	8.0212
	0.5	0.5	Present (Mode 1)	1.2559	1.2933	1.2224	1.2358	1.3261
			Present (Mode 2)	7.1506	7.1019	6.6519	7.1891	7.5002
		1	Present (Mode 1)	1.2649	1.3065	1.2205	1.2421	1.3524
			Present (Mode 2)	7.3316	7.3736	6.8109	7.2976	7.6939

		5	Present (Mode 1)	1.2975	1.3603	1.2205	1.2606	1.4270
			Present (Mode 2)	7.6649	7.8549	7.1074	7.5040	8.0480
	2	0.5	Present (Mode 1)	1.2869	1.3495	1.2253	1.2513	1.3945
			Present (Mode 2)	7.3827	7.4489	6.8561	7.3287	7.7485
		1	Present (Mode 1)	1.2907	1.3542	1.2235	1.2547	1.4067
			Present (Mode 2)	7.4977	7.6163	6.9581	7.3994	7.8708
		5	Present (Mode 1)	1.3092	1.3828	1.2226	1.2659	1.4492
			Present (Mode 2)	7.7156	7.9259	7.1528	7.5362	8.1015

V.3. Free vibration analysis of porous functionally graded sandwich plate:

The porosity has a detrimental effect on structural elements due to the reduction in the material properties. In powder metallurgy, the porosity grows because of improper sintering, and in centrifugal casting, it develops because of poor solidification. The percentage of porosity fraction depends on the amount of reinforcement and their shape as well, because powder comes in a variety of shapes such as angular, rounded, rod, etc. Spherical powders show good mobility and pack quite densely when compared to irregular particles (Kamrani and al. 2010).

The addition of an irregular shaped particles increases the porosity because of the presence of voids, and it gets worse for greater reinforcement volume fractions. Increasing the volume fraction of reinforcement or decreasing its size enhances the contribution of particle rearrangement to densification while restricting plastic deformation. The grain size decreases with the addition of reinforcements leading to an increase in material properties such as Young's modulus and yield strength (Madan and Bhowmick 2022).

Additionally, the solid reinforcement particles inhibit the metal-matrix sintering response. The maximum density can be achieved when the fraction of hard particles is relatively low (Hafizpour and Simchi 2008). Therefore, the formation of imperfections during the fabrication is inevitable but its variation over the volume can be controlled by selecting a suitable fabrication technique.

V.3.1. Free vibration analysis of imperfect sandwich plate (type A)

- FGM skin and homogeneous core

Considering all schemes, the natural frequency of imperfect FGM skin and homogeneous core is maximum for (1-2-1), followed by (2-2-1), (1-1-1), (2-2-1).

Table V.5 to V.8 shows the effect of different porosity types on the natural frequency of such schemes. It is a fact that porosity in structures dampens the vibrations and results in higher natural frequency. The trend of natural frequency change is dependent on the type of porosity distribution (Van Vinh and Huy 2022).

Hence, the frequency is higher for imperfect cases compared to the perfect sandwich plate. Also, it is worth noting that the frequency of imperfect- III is maximum followed by imperfect- II and imperfect- I for scheme (2-1-2). The rest of the schemes follow the same trend i.e., imperfect- I has a maximum frequency then imperfect- II and imperfect- III .

Table V. 5. Variation of frequency of Model 2 of FGM sandwich ($\alpha = 0.2$ and a=5h)

n_x	n_z	FGM Multidirectionnel M2 (1-1-1)			
		Parfect	Imperfect I	Imperfect II	Imperfect III
		($\alpha = 0$)	($\alpha = 0.2$)		
0	0.5	3.7245	3.7395	3.7315	3.7311
	1	3.9095	3.9492	3.9281	3.9271
	2	4.0743	4.1331	4.1019	4.1006
0.5	0.5	3.8294	3.8589	3.8431	3.8425
	1	3.9800	4.0282	4.0026	4.0014
	2	4.1168	4.1801	4.1465	4.1451
2	0.5	4.0214	4.0743	4.0462	4.0449
	1	4.1128	4.1757	4.1424	4.1409
	2	4.1988	4.2704>>	4.2325	4.2308

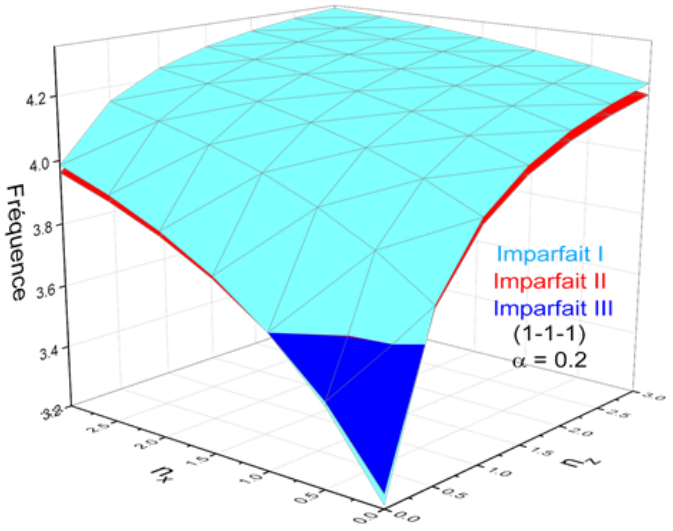

Figure V.2. Variation of frequency as a function of n_x and n_z, and ($\alpha = 0.2$) of model 2 (1.1.1), for various cumulative imperfections of the FGM plate, (Type A).

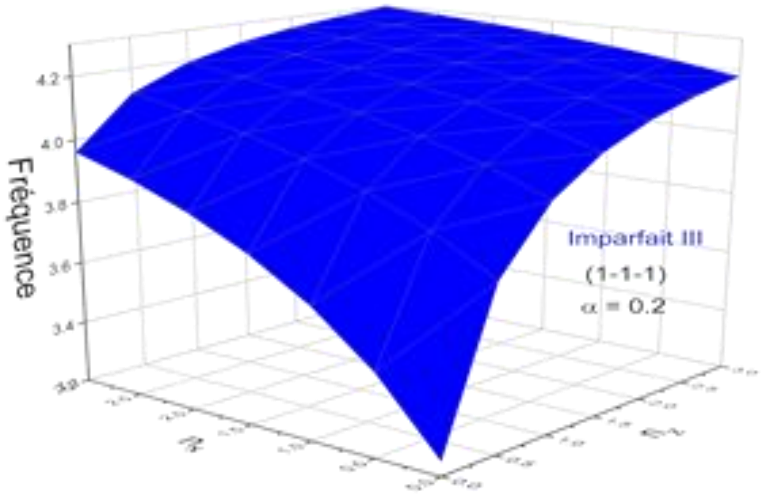

Figure V. 2. Variation of frequency as a function of n_x and n_z, and ($\alpha = 0.2$) of model 2 (1.1.1), for various cumulative imperfections of the FGM plate, (Type A).

Table V. 6. Variation of frequency parameter of imperfect multi-directional FGM sandwich of model 3 with *nx* and *nz* ($\alpha = 0.2$ and a=5h)

n_x	n_z	FGM Multidirectionnel M3 (**1-2-1**)			
		Perfect	Imperfect I	Imperfect II	Imperfet III
		($\alpha = 0$)	($\alpha = 0.2$)		
0	0.5	3.9095	3.9383	3.9232	3.9225
	1	4.0348	4.0743	4.0537	4.0527
	2	4.1503	4.1988	4.1735	4.1724
0.5	0.5	3.9800	4.0149	3.9967	3.9958
	1	4.0838	4.1272	4.1045	4.1035
	2	4.1807	4.2314	4.2049	4.2037
2	0.5	4.1128	4.1585	4.1347	4.1336
	1	4.1778	4.2283	4.2019	4.2008
	2	4.2399	4.2949	4.2662	4.2649

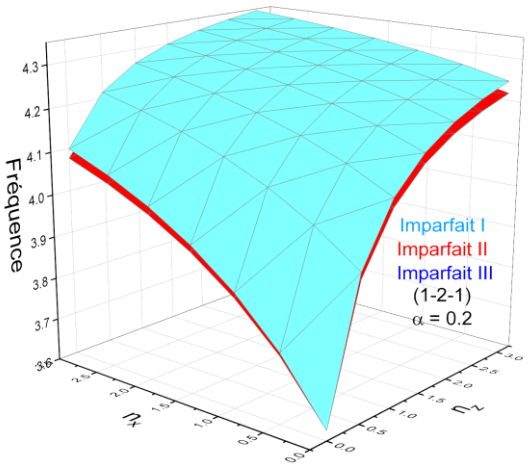

Figure V.4. Variation of frequency as a function of nx and nz and ($\alpha = 0.2$) of model 3 (1.2.1), for the various cumulative imperfections of the FGM plate, (Type A).

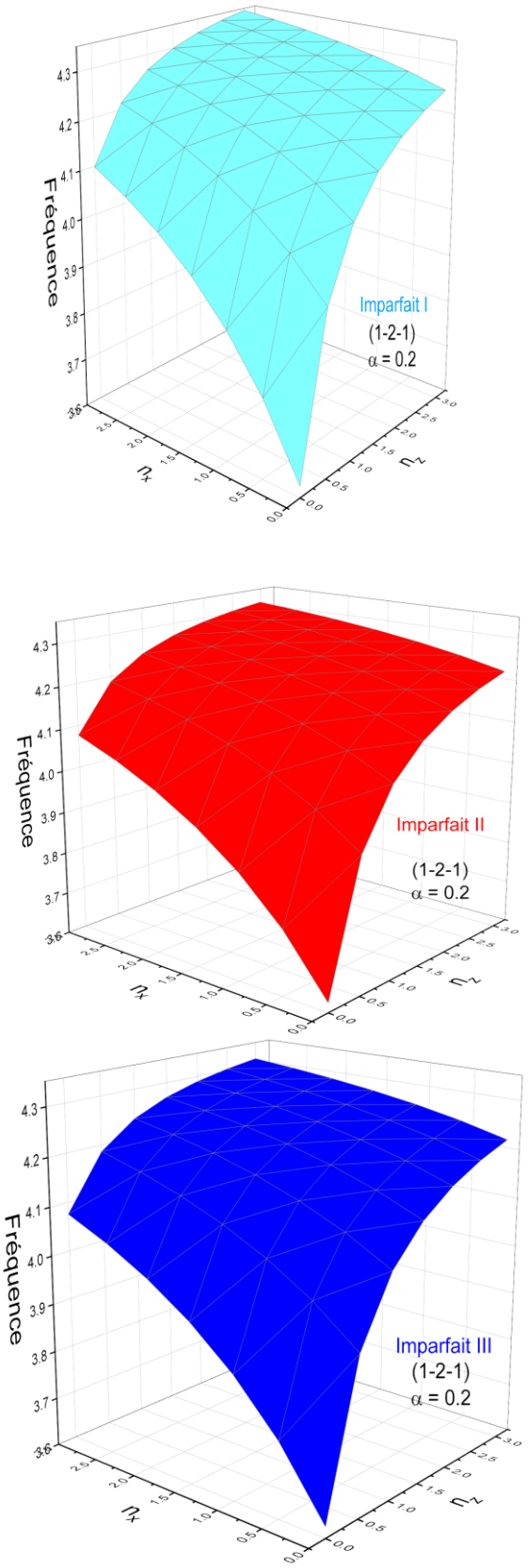

Figure V.5. Variation of frequency as a function of nx and nz and ($\alpha = 0.2$) of model 3 (1.2.1), for the different imperfections of the FGM plate, (Type A)

Tableau V. 7 Variation of frequency parameter of imperfect multi-directional FGM sandwich of model 4 with *nx* and *nz* ($\alpha = 0.2$ and a=5h)

n_x	n_z	FGM Multidirectionnel M4(2-1-2)			
		Parfaite	**Imperfection I**	**Imperfection II**	**Imperfection III**
		($\alpha = 0$)	($\alpha = 0.2$)		
0	0.5	3.5588	3.5462	3.5531	3.5534
	1	3.8012	3.8329	3.8157	3.8150
	2	4.0106	4.0743	4.0400	4.0385
0.5	0.5	3.6973	3.7110	3.7035	3.7032
	1	3.8915	3.9377	3.9127	3.9117
	2	4.0636	4.1346	4.0964	4.0948
2	0.5	3.9439	3.9981	3.9689	3.9677
	1	4.0587	4.1290	4.0912	4.0896
	2	4.1650	4.2490>	4.2040	4.2021

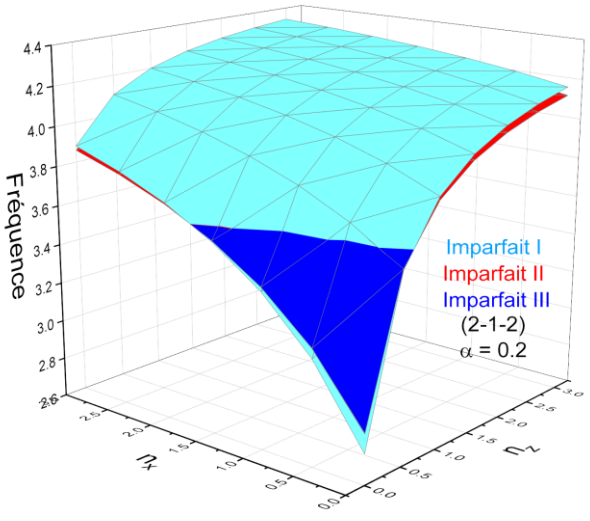

Figure V.6. Variation of frequency as a function of nx and nz and ($\alpha = 0.2$) of model 4 (2.1.2), for the various cumulative imperfections of the FGM plate, (Type A).

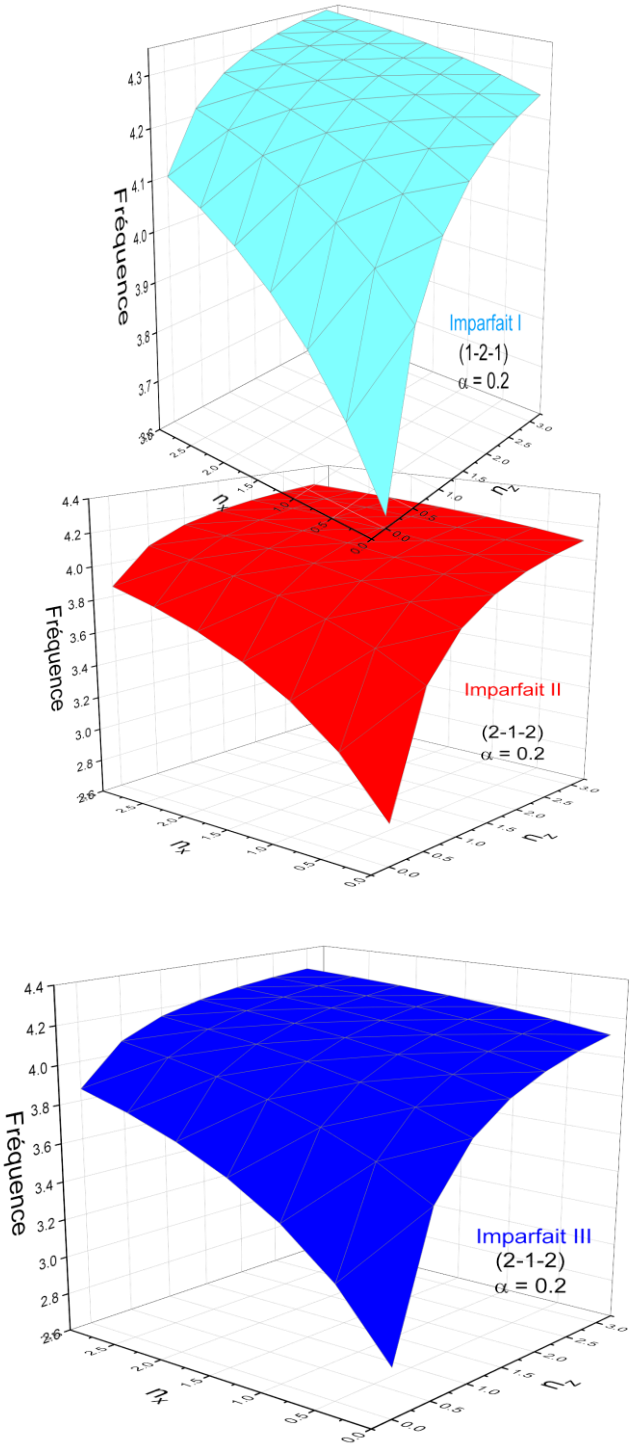

Figure V.7. Variation of frequency as a function of nx and nz and ($\alpha = 0.2$) of model 4 (2.1.2), for the different imperfections of the FGM plate, (Type A).

Table V. 8. Variation of frequency parameter of imperfect multi-directional FGM sandwich of model 5 with *nx* and *nz* ($\alpha = 0.2$ and a=5h)

n_x	n_z	FGM Multidirectionnel M5 (**2-2-1**)			
		Parfaite	Imperfection I	Imperfection II	Imperfection III
		($\alpha = 0$)	($\alpha = 0.2$)		
0	0.5	3.8012	3.8239	3.8119	3.8114
	1	3.9609	4.0017	3.9801	3.9792
	2	4.1052	4.1604	4.1313	4.1300
0.5	0.5	3.8915	3.9247	3.9071	3.9063
	1	4.0224	4.0695	4.0446	4.0435
	2	4.1427	4.2013	4.1704	4.1691
2	0.5	4.0587	4.1094	4.0826	4.0814
	1	4.1392	4.1975	4.1668	4.1654
	2	4.2154	4.2805>>>	4.2462	4.2447

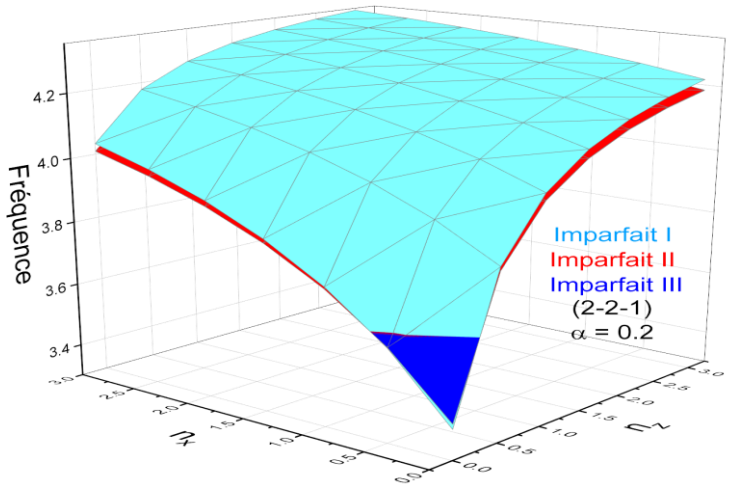

Figure V.8. Variation of frequency as a function of nx and nz and ($\alpha = 0.2$) of model 5 (2.2.1), for the various cumulative imperfections of the FGM plate, (Type A).

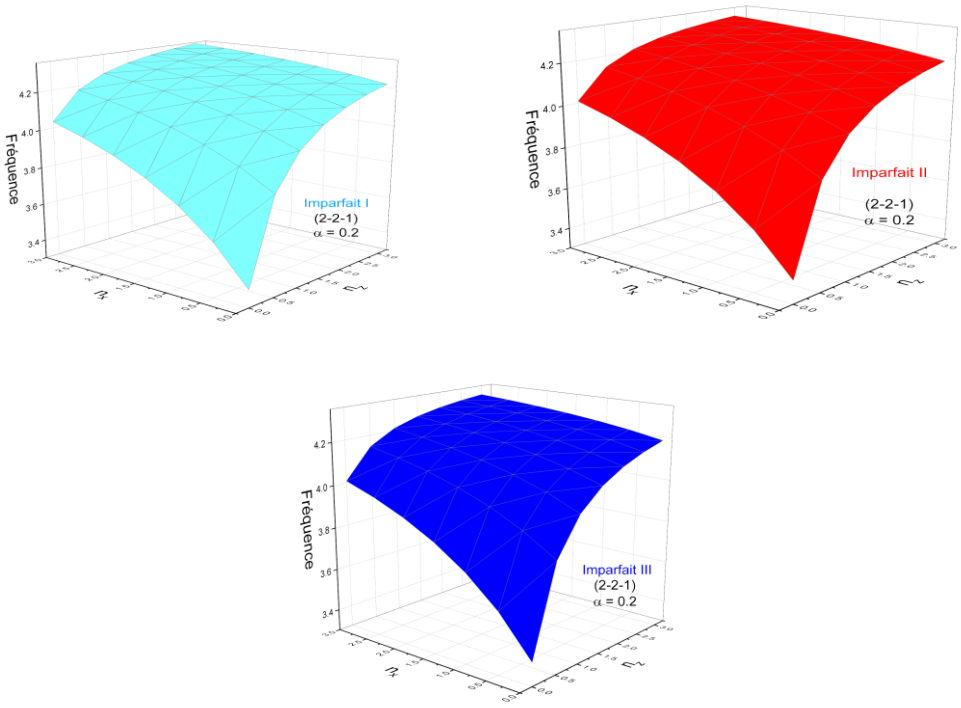

Figure V.9. Frequency variation as a function of nx and nz and ($\alpha = 0.2$) of model 5 (2.2.1), for the various imperfections of the FGM plate, (Type A).

Figures V.2 to V.9 represent the comparison of frequency parameters for the three imperfect I.II.III (cumulated and dispersed) of multidirectional imperfect sandwich plate in FGM (type A FGM skins and homogeneous core).

On these figures, it can be observed that the frequency decreases with increasing porosity coefficients for nx and nz less than 0.5.

Similarly, the frequency increases with increasing porosity coefficient for nx and nz greater than 0.5. It is also noteworthy that for nx and nz less than 0.5, the frequency in the case of type A FGM sandwich plates is the highest for Imperfection I, while it is the lowest for Imperfections II and III. Similarly, for nx and nz greater than 0.5, the frequency of type A multidirectional FGM sandwich plate is highest for Imperfection I and lowest for Imperfections II and III.

V.3.2. Free vibration analysis of imperfect sandwich plate (type B)

- FGM core and homogeneous skin

The natural frequency of imperfect FGM core and homogeneous skin is maximum for (2-2-1), followed by (2-1-2), (1-1-1), (1-2-1).

Table V.9-V.12 shows the effect of different porosity types on the natural frequency of such schemes.

Unlike case-1, here the frequency decreases for imperfect cases compared to perfect cases. Also, it is worth noting that the frequency of imperfect- III is maximum followed by imperfect- II and imperfect- I for scheme 2-2-1.

The rest of the schemes, follow the same trend i.e., imperfect- I has a maximum frequency then imperfect- II and imperfect- III.

Table V. 9. Variation of frequency parameter of imperfect multi-directional FGM sandwich of model 2 ($\alpha = 0.2$ and a=5h).

n_x	n_z	FGM Multidirectionnel M2 (**1-1-1**)			
		Perfect	Imperfect I	Imperfect II	Imperfect III
		($\alpha = 0$)	($\alpha = 0.2$)		
0	0.5	3.5145	3.5065	3.5106	3.5108
	1	3.6229	3.6229	3.6229	3.6229
	2	3.7245	3.7315	3.7279	3.7277
0.5	0.5	3.5753	3.5719	3.5736	3.5737
	1	3.6658	3.6688	3.6673	3.6672
	2	3.7514	3.7602	3.7556	3.7554
2	0.5	3.6914	3.6961	3.6937	3.6936
	1	3.7488	3.7575	3.7530	3.7528
	2	3.8043	3.8165>>	3.8102	3.8099

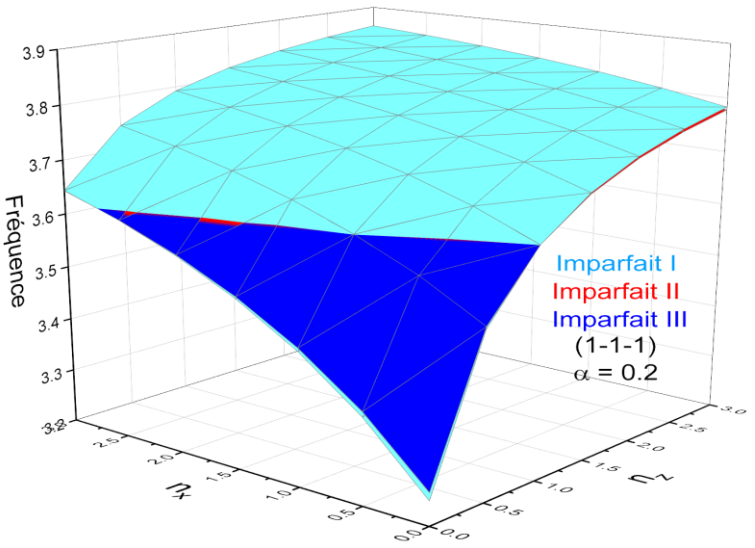

Figure V.10. Variation of frequency as a function of nx and nz and ($\alpha = 0.2$) of model 2 (1.1.1), for the various cumulative imperfections of the FGM plate, (Type B).

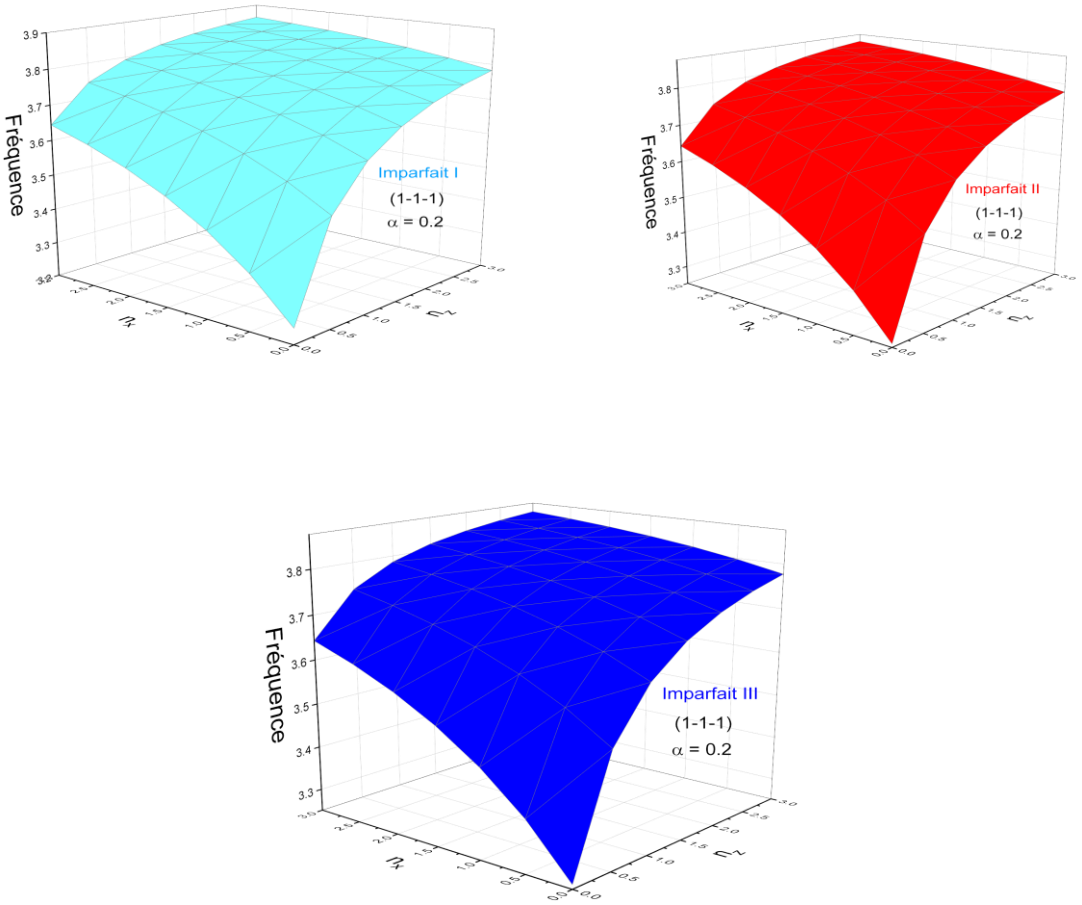

Figure V.11. Variation of frequency as a function of nx and nz and ($\alpha = 0.2$) of model 2 (1.1.1), for the different imperfections of the FGM plate, (Type B).

Table V. 10. Variation of frequency parameter of imperfect multi-directional FGM sandwich of model 3($\alpha = 0.2$ and a=5h).

n_x	n_z	FGM Multidirectionnel M3 (**1-2-1**)			
		Perfect	Imperfect I	Imperfect II	Imperfect III
		($\alpha = 0$)	($\alpha = 0.2$)		
0	0.5	3.4574	3.4379	3.4482	3.4486
	1	3.6229	3.6229	3.6229	3.6229
	2	3.7729	3.7887	3.7804	3.7799
0.5	0.5	3.5509	3.5427	3.5471	3.5473
	1	3.6868	3.6937	3.6901	3.6899
	2	3.8118	3.8315	3.8212	3.8207
2	0.5	3.7245	3.7354	3.7296	3.7294
	1	3.8082	3.8275	3.8173	3.8169
	2	3.8876	3.9143>>>	3.9003	3.8997

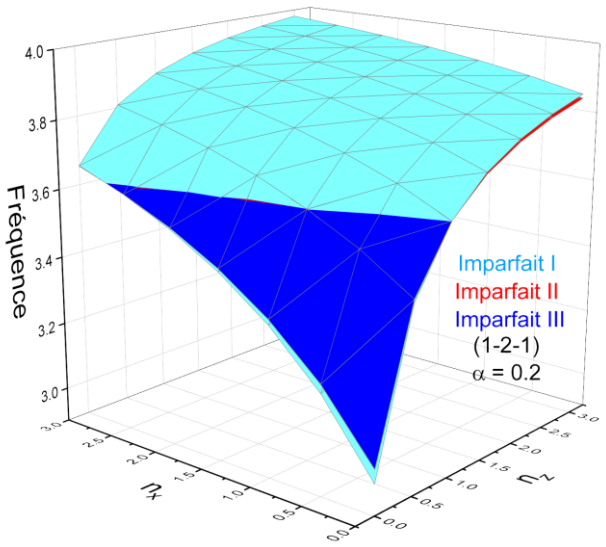

Figure V.12. Variation of frequency as a function of nx and nz and ($\alpha = 0.2$) of model 3 (1.2.1), for the various cumulative imperfections of the FGM plate, (Type B).

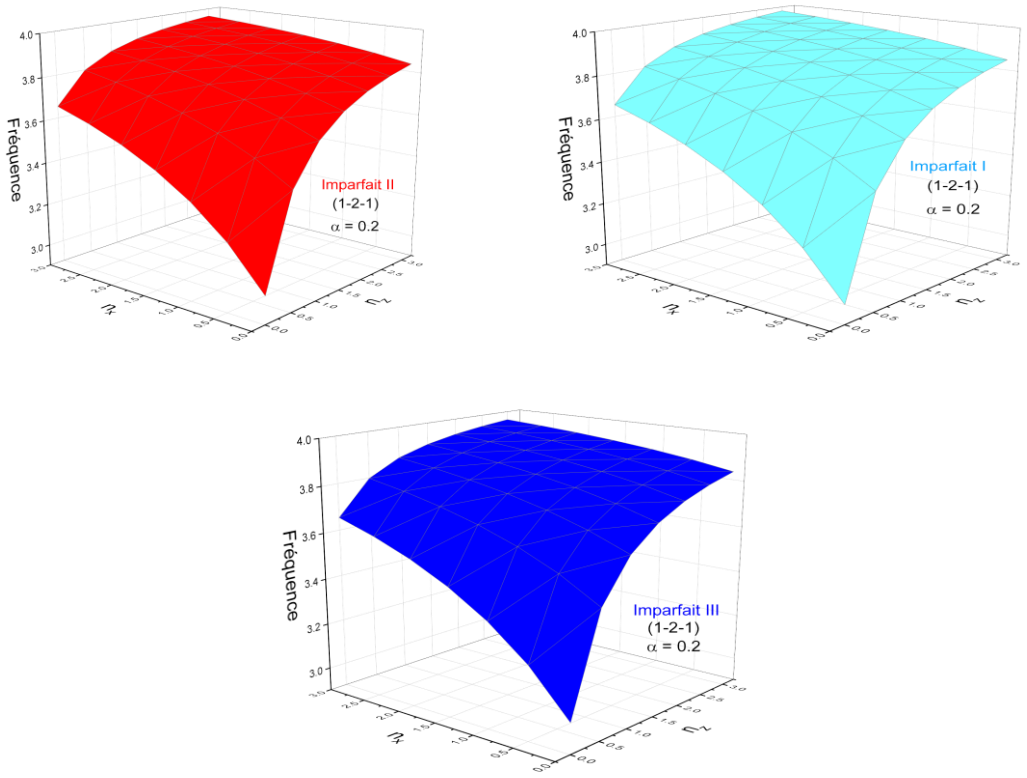

Figure V.13. Variation of frequency as a function of nx and nz and ($\alpha = 0.2$) for model 3 (1.2.1), for the different imperfections of the FGM plate, (Type B).

Table V. 11. Variation of frequency parameter of imperfect multi-directional FGM sandwich of model 4 ($\alpha = 0.2$ and a=5h).

n_x	n_z	FGM Multidirectionnel M4 (**2-1-2**)			
		Perfect	Imperfect I	Imperfect II	Imperfect III
		($\alpha = 0$)	($\alpha = 0.2$)		
0	0.5	3.5588	3.5560	3.5574	3.5575
	1	3.6229	3.6229	3.6229	3.6229
	2	3.6847	3.6872	3.6859	3.6858
0.5	0.5	3.5945	3.5934	3.5939	3.5939
	1	3.6488	3.6499	3.6493	3.6493
	2	3.7013	3.7044	3.7028	3.7028
2	0.5	3.6644	3.6661	3.6652	3.6651

	1	3.6997	3.7028	3.7012	3.7012
	2	3.7343	3.7387>	3.7365	3.7364

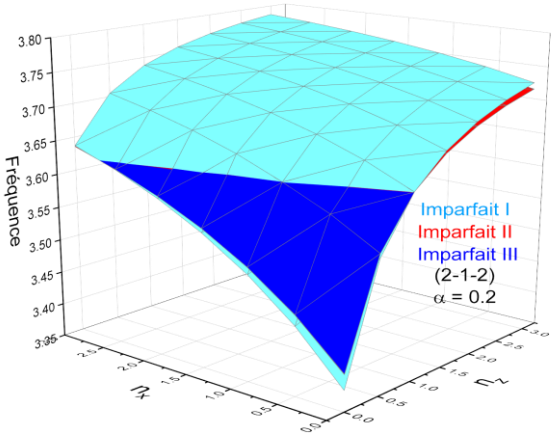

Figure V.14. Variation of frequency as a function of nx and nz and ($\alpha = 0.2$) for model 4 (2.1.2), for the different imperfections (cumulated) of the FGM plate, (Type B).

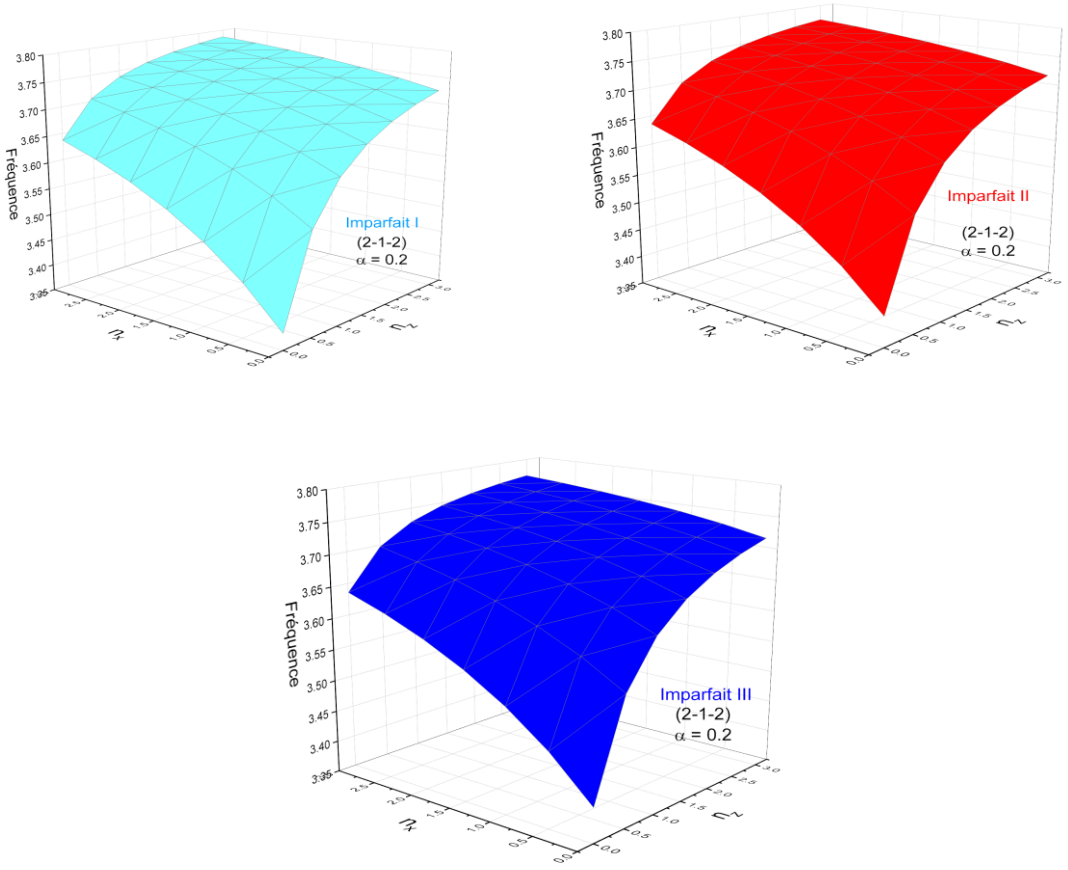

Figure V.15. Variation of frequency as a function of nx and nz and ($\alpha = 0.2$) for model 4 (2.1.2), for the different imperfections of the FGM plate, (Type B).

Table V. 12. Variation of frequency parameter of imperfect multi-directional FGM sandwich of model 5($\alpha = 0.2$ and a=5h).

n_x	n_z	FGM Multidirectionnel M5 (**2-2-1**)			
		Perfect	Imperfect I	Imperfect II	Imperfect III
		($\alpha = 0$)	($\alpha = 0.2$)		
0	0.5	3.6847	3.6899	3.6872	3.6870
	1	3.8012	3.8157	3.8082	3.8078
	2	3.9095	3.9321	3.9204	3.9198
0.5	0.5	3.7501	3.7607	3.7552	3.7549
	1	3.8469	3.8650	3.8556	3.8552
	2	3.9381	3.9627	3.9499	3.9493
2	0.5	3.8742	3.8943	3.8839	3.8834
	1	3.9354	3.9598	3.9471	3.9466
	2	3.9942	4.0226	4.0079	4.0072

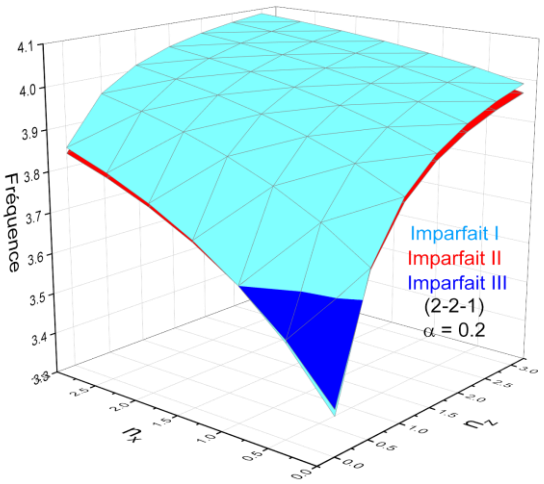

Figure V.16. Variation of frequency as a function of nx and nz and ($\alpha = 0.2$) for model 5 (2.2.1), for the different imperfections (cumulated) of the FGM plate, (Type B).

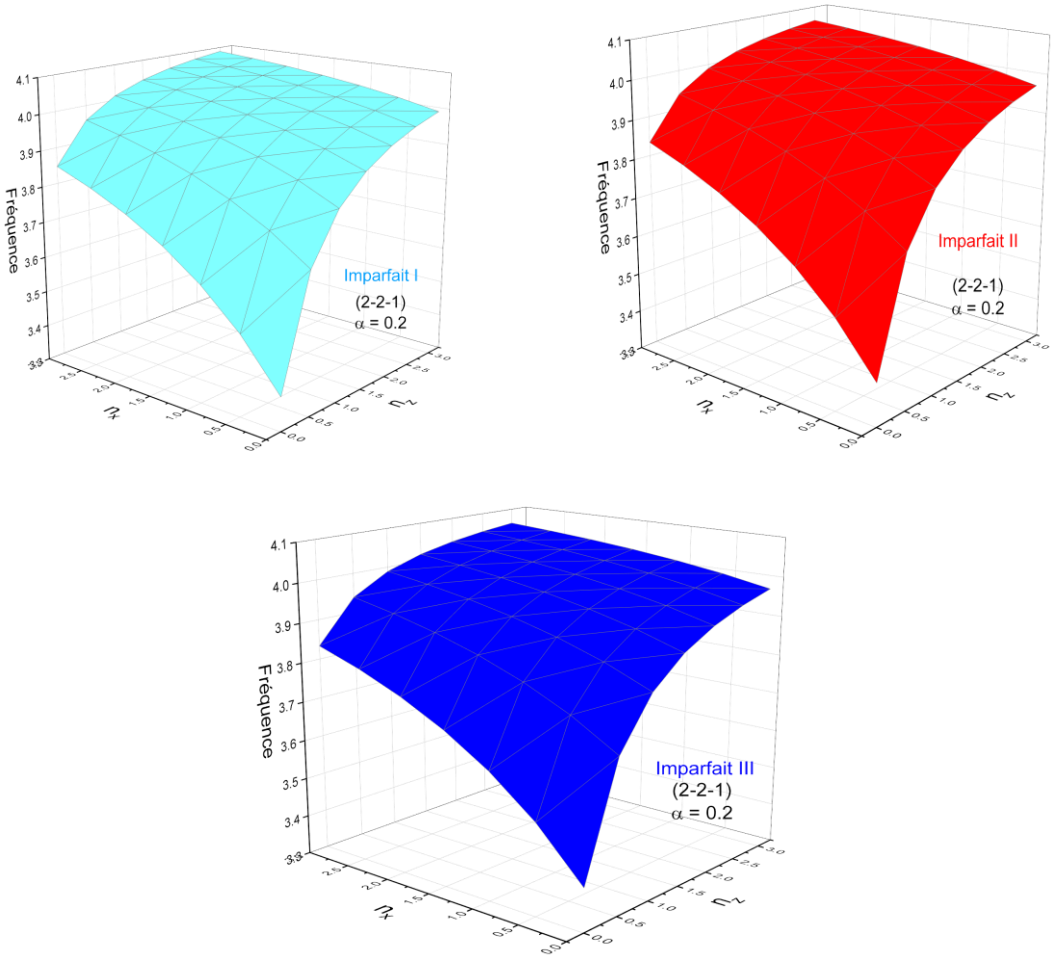

Figure V.17. Variation of frequency as a function of nx and nz and ($\alpha = 0.2$) for model 5 (2.2.1), for the different imperfections of the FGM plate, (Type B).

Figures V.10 to V.17 represent the comparison of the frequency parameters for the three imperfect I.II.III (cumulative and dispersed) of imperfect multidirectional FGM sandwich plate, (type B FGM core FGM and homogeneous skins). Can see from these figures that the frequency decreases with increasing porosity coefficients for nx and nz less than 0.5.

Similarly, the frequency increases with increasing porosity coefficient for nx and nz greater than 0.5. We also note that for nx and nz less than 0.5, the frequency in the case of FGM sandwich plates of imperfections II and III is the highest while the lowest for imperfection I.

Similarly, for nx and nz greater than 0.5, the frequency of the multidirectional FGM sandwich plate type B is the highest while the lowest for imperfections II and III.V.4.

Conclusion

Certainly, here's a rephrased version:

This study demonstrates that producing an FGM (Functionally Graded Material) skin with a uniform core offers more benefits compared to creating an FGM core with a uniform skin, primarily because the former achieves a higher natural frequency.

Across all models, it is advantageous to manufacture an FGM skin with a consistent porosity distribution, except for model 2-1-2, where a logarithmic porosity is necessary. Conversely, manufacturing an FGM core with uneven logarithmic porosity generally yields satisfactory results, except for model 2-2-1, which requires uneven porosity.

Increasing both material parameters nx and nz, which represent the ceramic composition within the FGM, leads to a higher natural frequency in the system. In perfect sandwich plate scenarios, the parameter nz is more critical than nx.

When imperfections are considered, the granulometric parameter nz has a more significant impact than nx on the natural frequency of imperfect plates.

Introducing porosity in FGM skins with a homogeneous core enhances the natural frequency, while in cases where the core consists of FGM with a homogeneous skin material, the natural frequency decreases. Notably, porosity in FGM face skins significantly affects frequency, whereas porosity in FGM cores has a minimal impact on natural frequency.

General conclusion and perspectives

At the conclusion of our work within the civil Engineering Department at the University of Tiaret, focusing on determining the vibrational characteristics of multidirectional composite structures in graded materials (FGM), we devised a direct analytical method. This method allows for the determination of vibration frequencies using two types of sandwich plates: one with FGM porous skins and a homogeneous core, and another with an FGM porous core and homogeneous skins.

Given the limited exact solutions for plate problems dependent on the warping function, we sought to assess a new model in comparison to existing analytical models, which rely on approximations of the displacement field. Our new approach is based on a novel shear deformation theory.

We've developed closed-form solutions for the free vibration analysis of multidirectional sandwich plates in graded materials (FGM). Our methodology assumes that transverse shear displacements vary parabolically throughout the plate thickness. For rectangular plates in P-FGM, we derived equilibrium equations and associated boundary conditions using the Hamilton principle. Analytical solutions for the FGM sandwich plate with simply supported boundary conditions on all sides were obtained using the Navier method. Comparison with existing literature has yielded several insights:

Manufacturing an FGM skin with a homogeneous core yields higher natural frequencies compared to producing an FGM core with a homogeneous skin.

- A uniform porosity distribution in FGM skins is generally advantageous, except for specific configurations that require logarithmic porosity. Similarly, uneven logarithmic porosity in FGM cores produces satisfactory results for most models.
- Increasing both material parameters nx and nz enhances the ceramic composition in FGM, consequently increasing the natural frequency of the system. In imperfect plates, the material parameter nz significantly influences the natural frequency more than nx.
- Introducing porosity increases the natural frequency when the skin consists of FGM with a homogeneous core. Conversely, when the core is FGM with a homogeneous skin, the natural frequency decreases. The effect of porosity on frequency is significant in FGM face skins but negligible in FGM cores.

In conclusion, our refined four-variable theory proves accurate and straightforward for analyzing the free vibration behavior of multidirectional FGM sandwich plates. Nevertheless, further refinement is necessary, particularly when applying the theory to layered structures to ensure continuity of transverse shear stresses between layers. Additionally, we plan to explore applications of our methodology in temperature-dependent vibration studies, buckling

problems, and various support configurations. Lastly, we acknowledge the importance of employing finite element methods for tackling more complex problems beyond the scope of analytical approaches.

References Bibliography

A

(Ait Atmane and al., 2010). Ait Atmane.H, Tounsi. A, Mechab. I, Adda Bedia. E.A, «Free vibration analysis of functionally graded plates resting on Winkler- Pasternak elastic foundations using a new shear deformation theory». Int. J. Mech. Mater. esign; 6 (2): 113-121, 2010.

(Ait Yahia and al., 2015). Ait Atmane, H., Houari, M.S.A. and Tounsi, A. (2015), "Wave propagation in functionally graded plates with porosities using various higher-order shear deformation plate theories", Struct. Eng. Mech., 53(6), 1143-1165.

(Ansari *and* al., 2010). Ansari A, Alhoshan M, Alsalhi M, Aldwayyan A (2010) Prospects of nanotechnology in clinical immunodiagnostics. Sensors 10:6535–6581. https://doi.org/10.3390/s100706535.

(Avila and *al.*, 2007). Avila A. F., composite structuresv, //steel and composite structuresv// 81: 323-330, 2007.

(Amira S, 2022). "A Review on Functionally Graded Materials and Their Applications"

(Adelina M, 2022). Adelina Miteva1, Anna Bouzekova-Penkova1 "Some Aerospace Application of Functionally Graded Materials".

(Arbaoui J., 2009) " ÉTUDE COMPARATIVE ET CARACTÉRISATIONS MÉCANIQUES DES STRUCTURES SANDWICHS MULTICOUCHES"

B

(Belouettar and al., 2009). Belouettar S, Abbadi A, Azari Z, Belouettar R, Freres P., Composites structures, 87 : 265-273, 2009.

(Berthelot and al., 1996). Berthelot J. M., "Matériaux composites : Comportement mécanique et analyse des structures", 4 éme édition, 1996.

C

(Chatin and al., 2000). A. Chatin. Analyse des efforts à l'interface entre les couches des matériaux composites à l'aide de modèles multi particulaires de matériaux multicouches. PhD thesis, ENPC, 2000.

(Chen and al., 2019). Chen F, Zhang C, Chen F, Huang Z, Jia M, Chen G, Ye Y, Lin Y, Liu W, Chen B, Shen Q, Zhang L, Lavernia EJ (2019) Additive manufacturing of functionally graded materials: a review. Mater Sci Eng A 764:138209. https://doi.org/10.1016/j.msea.2019.138209.

(CHEDAD A, 2023)" Etude du phénomène d'instabilité thermomécanique des structures élaborées avec de nouveaux matériaux sous l'effet de la porosité"

(Chi and al., 2003). Chi. Shyang-ho., Chung Yen-Ling. (2003), Cracking in coating-substrate composites of multi-layered and sigmoid FGM coatings. Engineering Fracture Mechanics; 70 (10), 1227–1243.

D

(Delale and al., 1983). F. Delale, F. Erdogan. The crack problem for a non homogeneous plane. ASME Journal of Applied Mechanics 50(3), 609 –614, 1983.

E

(El Meiche and al, 2011). El Meiche, N., Tounsi, A., Ziane, N., Mechab, I. and Adda Bedia, E.A. (2011), "A new hyperbolic shear deformation theory for buckling and vibration of functionally graded sandwich plate", Int. J. Mech. Sci., 53(4), 237-247. https://doi.org/10.1016/j.ijmecsci.2011.01.004.

G

(Gognard and al., 2000). Gognard," collage des métaux généralités et caractéristiques ", Techniques de l'ingénieur BT4, 2000.

H

(Hafizpour and al., 2008). Hafizpour, H.R. and Simchi, A. (2008), "Investigation on compressibility of Al–SiC;composite,powders",Powder,Metallurgy,vol.51No(3),pp217-223.https://doi.org/10.1179/174329007X22250.

(Hexcel and al., 2004). Hexcel Composite. HexWeb tm honeycomb sandwich design technology. http/ /: www. Hexcel composite.com, 2004.

(Jin Dai, 2003). Jin Dai, H.Hahn, 2003/ Composite Structure, 61: 247-253, 2003.

K

(Keddouri and al., 2021). Analyse et modélisation du comportement mécanique des structures sandwich en matériaux à gradient de propretés

(Kamrani and al., 2010). Kamrani, S., Riedel, R., Seyed Reihani, S.M. and Kleebe, H.J. (2010), "Effect of reinforcement volume fraction on the mechanical properties of Al—SiC nanocomposites produced by mechanical alloying and consolidation", J. Composite Materials, vol.44, No. (3), p313-326. https://doi.org/10.1177/0021998309347570.

(Kumar and al., 2022). Kumar Sah, S. and Ghosh, A. (2022), "Influence of porosity distribution on free vibration and buckling analysis of multidirectional functionally graded

sandwich plates", Composite. Structure, Vol 279, p 114795, https://doi.org/10.1016/j.compstruct.2021.114795.

L

(LAGGOUN O., 2022) "LAGGOUN OUALID BADRE MADANI COMPORTEMENT MECANIQUE DES PANNEAUX SANDWICHS AVEC AME EN NID D'ABEILLE"

(Leu and al., 2012). Leu MC, Deuser BK, Tang L, Landers RG, Hilmas GE, Watts JL (2012) Freeze->form extrusion fabrication of functionally graded materials. CIRP Ann Manuf Technol 61:223–226. https://doi. org/10.1016/j.cirp.2012.03.050.

M

(Madan and al, 2022). Madan, R. and Bhowmick, S. (2022), "Fabrication and microstructural characterization of Al-SiC based functionally graded disk", Aircraft Eng. Aeros. Technol., https://doi.org/10.1108/AEAT-03-2022-0096.

(Malandrino and al., 2009). Malandrino G (2009) Chemical vapour deposition. In: Jones C, Hitchman M (eds) Precursors, processes and applications. Angewandte Chemie International Edition, 48, pp 7478–7479.

(Meksi and al., 2016). Meksi abdeljalil. Benyoucef S. Tounsi A (Comportement Mécanique des Plaques Sandwiches sur Fondations Elastiques) USBA.2016.

(Mindlin and al., 1951). Mindlin.R. D «Influence of rotary inertia and shear on flexural motions of isotropic, elastic plates., » Journal of Applied Mechanics, vol. 18, pp. 31-38.

(Manish B and al., 2015) Manish Bhandari1 and Kamlesh Purohit2 Response of Functionally Graded Material Plate under Thermomechanical Load Subjected to Various Boundary Conditions

N

(Nguyen and al., 2004). Viet.Tung. Nguyen. « Modélisation globale et locale des structures multicouches par éléments finis de plaques ». Thèse de doctorat de l'"école nationale des ponts et chaussées ,2004.

. **(Noor and al., 1989).** A. K. Noor & W. S. Burton. Assesment of shear deformation theories for multilayered composite plates. Appl Mech Rev, vol. 42, no. 1, pages 1,12, 1989.

(Rasheedat M, 2017) Rasheedat Modupe Mahamood andEsther Titilayo Akinlabi, Functionally

Graded Materials, Nigeria

(Reddy. J.N and al., 1997). Levinson Murthy. Mechanics of Laminated Composites Plates: Theory and Analysis‖, CRC Press, Boca Raton. Theories de deformation exponentielle des plaques1997.

(Reddy and al., 1997et1999).(Reddy, J.N 1997,1999). Theory and analysis of elastic plates and shells.1997; 1999: CRC press.

(Reddy and al., 2004). Reddy, J.N. Mechanics of Laminated Composite Plates and Shells (2nd Edition). Boca Raton FL: CRC Press, LLC, 2004.

(Redddy B and al. 2014) B. Sidda Redddya, J. Suresh Kumarb, C. Eswara Reddyc, and K. Vijaya Kumar Reddyb " Static Analysis of Functionally Graded Plates Using Higher-Order Shear Deformation Theory"

(Reissner and al., 1945). E Reissner. The e_ect of transverse shear deformation on the bending of elastic plates. J. Appl. Mech., vol. 12, pages 69, 77, 1945.

S

(Seol and al., 2012). Seol Y, Kang T, Cho D (2012) Solid freeform fabrication technology applied to tissue engineering with various biomaterials. Soft Matter View 8:1730–1735. https://doi.org/10.1039/c1sm06863f.

(shear Behnam S, 2014). Vibration and Thermal Stress Analyses of Functionally Graded Materials

(Sallai B and al, 2022). Sallai Ben-Oumrane, Tounsi Abedlouahed , Mechab Ismail, Bachir Bouiadjra Mohamed,Meradjah Mustapha, Adda Bedia El Abbas . A theoretical analysis of flexional bending of Al/Al2O3 S-FGM thick beams

(Sedjrari A. 2018). " Étude du comportement statique des plaques fonctionnellement graduée reposant sur des fondations élastique".

.(Zemani KADA. 2015) Etude des vibrations libres des plaques épaisses en matériaux à gradient fonctionnel (FGM) reposant sur un support élastique de Winkler-Pasternak

[Timoshenko,., 1959]. Theory of plates and Shells. McGraw-Hill, NewYork. Commun. Appl. Numer. Methods, vol. 3, pages 173,180, 1987.